INFORMATION TO USERS

This manuscript has been reproduced from the microfilm master. UMI films the text directly from the original or copy submitted. Thus, some thesis and dissertation copies are in typewriter face, while others may be from any type of computer printer.

The quality of this reproduction is dependent upon the quality of the copy submitted. Broken or indistinct print, colored or poor quality illustrations and photographs, print bleedthrough, substandard margins, and improper alignment can adversely affect reproduction.

In the unlikely event that the author did not send UMI a complete manuscript and there are missing pages, these will be noted. Also, if unauthorized copyright material had to be removed, a note will indicate the deletion.

Oversize materials (e.g., maps, drawings, charts) are reproduced by sectioning the original, beginning at the upper left-hand corner and continuing from left to right in equal sections with small overlaps.

Photographs included in the original manuscript have been reproduced xerographically in this copy. Higher quality 6" x 9" black and white photographic prints are available for any photographs or illustrations appearing in this copy for an additional charge. Contact UMI directly to order.

Bell & Howell Information and Learning
300 North Zeeb Road, Ann Arbor, MI 48106-1346 USA
800-521-0600

Syntheses and Conformational Analysis of Peptide Pheromones and Receptor Fragments

by

HAIBO XIE

A dissertation submitted to the Graduate faculty in Chemistry in partial fulfillment of the requirements for the degree of Doctor of Philosophy, The City University of New York.

2001

This manuscript has been read and accepted for the Graduate faculty in Chemistry in satisfaction of the dissertation requirement for the degree of Doctor of Philosophy.

Jan 20, 2001 — Fred Naider

Date — Chair of Examining committee

Jan. 25, 2001 — Gerald Kaufman

Date — Executive Officer

Howard Hochenstein

Ruth E. Stark

Robert Bittman

Supervisory Committee

The City University of New York

Abstract

Synthesis and Conformational Analysis of Peptide Pheromones and Receptor Fragments

by

Haibo Xie

Adviser: Professor Fred Naider

Part I: Structure-Activity Relationships in the *Saccharomyces cerevisiae* **a**-Factor

To investigate structure-activity relationships in the *Saccharomyces cerevisiae* **a**-factor, we have synthesized 5 analogs of **a**-factor, in which residues at positions 4 and 5 were replaced with Pro-containing conformation constricting sequences (compound I-V). We also prepared 3 **a**-factor analogs with stereoisomeric farnesyl group (compound VI-VIII with *trans/cis, cis/trans and cis/cis* farnesyl configurations, respectively). All analogs were purified to >99% homogeneity as evidenced by HPLC and TLC and were characterized by mass spectrometry and amino acid analysis. A growth arrest assay was employed to determine the bioactivities of the synthetic **a**-factor analogs. CD and NMR techniques were used to explore their secondary structures. In addition, fluorescence spectroscopy was applied to measure the partitioning coefficients of the analogs into synthetic vesicles. The results indicated that appropriate biological conformation and partitioning are both important for high activity, and they affect the activity in different ways.

Part II: Syntheses and Biophysical Characterization of Transmembrane Domains of α-factor Receptor

The Ste2p receptor for α-factor, the mating pheromone of yeast *Saccharomyces cerevisiae*, belongs to the largest known family of cell surface receptors termed as G protein-coupled receptors (GPCRs). In this report we present the synthesis of peptides corresponding to 4 of the seven transmembrane domains (M1-M4) and 2 homologs of the sixth domain (M6). The secondary structures of all seven transmembrane peptides were assessed using a detailed CD analysis in trifluoroethanol, trifluoroethanol-water mixtures, sodium dodecyl sulfate micelles and dimyristoyl phosphatidyl choline bilayers. Tryptophan fluorescence quenching experiments were used to assess the penetration of the membrane peptides into lipid bilayers. Polyacrylamide gel electrophoresis was utilized to study the oligomeric state of the 7 fragments. Our results have implications for the folding of this membrane protein and suggest that the possible functional role of M6 is manifested through a shift in secondary structure. The aggregation of particular transmembrane domains may also reflect a tendency for intermolecular interactions that occur in the membrane environment facilitating formation of receptor dimers or multimers

This thesis is dedicated to my mother Pan Xiuzhu, my father Hong-En Xie, and my wife Annie Xiaodan Wang

Acknowledgments

I would like to thank Dr. Fred Naider, my advisor, for being a teacher and role model. Words cannot fully express my gratitudes for all the help he has given me. It has truly been a pleasure to work in his lab during my graduate studies.

I would also like to thank two collaborators of our group, Dr. Jeffery M. Becker for his endless support in bioassay and helpful advice, and Dr. Richard A. Gibbs, for providing me steroisomers of farnesylated dipeptides.

Thanks also go to my committee, Dr. Ruth E. Stark, Professor Howard Haubenstock, and Dr. Robert Bittman, for their helpful instruction.

I'd like thank my friend Dr. Shifeng Liu. We have had a seemingly never ending discussion about the synthesis of membrane peptides. I'd also like to thank the whole group. Dr. Boris Arshava provided me with endlessly technical support and taught me NMR techniques. Dr. Fa-Xiang Ding helped me in fluorescence quenching experiments. Mr. Enrique Arévalo Perea taught me gel electrophoresis, and David Schriber helped me in the synthesis of M2-35.

I'd also like to thank Dr. Xin Wang teaching me NMR techniques and also for many thoughtful discussions.

This list comprises only a small group of the many people who have been instrumental in helping me attain my goals. I apologize that I cannot mention them all and I wish to express my sincere thanks.

TABLE OF CONTENTS

LIST OF ABBREVIATIONS

Å	Angstrom
A	alanine
Boc	*tert*-butoxycarbonyl
BOP	benzotriazol-1-yloxy-tris(dimethylamino) phosphonium hexafluoro-phosphate
Bu^t	tertiary-butyl
C	cysteine
CD	circular dichroism
COSY	correlation spectroscopy
D	aspartic acid
DCC	dicyclohexylcarbodiimide
DCM	dichloromethane
DIEA	diisopropylethylamine
DIPC	diisopropylcarbodiimide
DMAP	*N,N'*-dimethylaminopyridine
DMF	*N,N'*-dimethylformamide
DMPC	1,2-dimyristoyl-*sn*-glycero-3-phosphocholine
DMS	dimethyl sulfide
DMSO	dimethyl sulfoxide
DMSO-d_6	dimethylsulfoxide-d_6
EDT	1,2-ethanedithiol
ES-MS	electrospray mass spectrometry

EtOAc	ethyl acetate
F	phenylalanine
Farn	farnesyl
Fmoc	9-fluorenylmethoxycarbonyl
For	formyl
G	glycine
H	histidine
HBTU	*O*-benzotriazolyl-*N,N,N',N'*-tetramethyluronium hexafluorophosphate
HOAt	1-hydroxy-7-azabenzotriazole
HOBt	1-hydroxybenzotriazole
HPLC	high performance liquid chromatography
I	isoleucine
J	spin-spin coupling constant
K	lysine
Kp	partitioning coefficient
MES	2-(N-morpholino)ethanesulfonic acid
MS	mass spectroscopy
MWCO	molecular weight cut-off
NMP	*N*-methyl pyrrolidinone
NMR	nuclear magnetic resonance
Nle	norleucine
NOE	nuclear overhauser effect

NOESY	nuclear overhauser enhanced spectroscopy
OMe	methyl ester
Pam	phenylacetamidomethyl
PE	phosphatidylethanolamine
ppm	parts per million
PyBOP	benzotriazolyl)-*N*-oxy-pyrrolidinium phosphonium hexafluorophosphate
RP-HPLC	reverse phase high performance liquid chromatography
SDS	sodium dodecylsulfate
SPPS	solid-phase peptide synthesis
TFA	trifluoroacetic acid
TFE	2,2,2-trifluoroethanol
THF	tetrahydrofuran
TLC	thin-layer chromatography
TMS	trimethylsilyl
TOCSY	total correlation spectroscopy
UV	ultraviolet
V	valine
Val	valine
W	tryptophan
w/v	ratio of weight to volume
Y	tyrosine
ε	extinction coefficient

LIST OF TABLES

LIST OF FIGURES

PART I: STRUCTURE-ACTIVITY RELATIONSHIPS IN THE *SACCHAROMYCES CEREVISIAE* A-FACTOR

CHAPTER I INTRODUCTION

BACKGROUND

Mating in a number of fungi is controlled by diffusible pheromones, which are biosynthesized by one mating type and elicit a specific cellular response from the opposite mating type. In the yeast *Saccharomyces cerevisiae* the mating pheromones are α-factor, Trp-His-Trp-Leu-Gln-Leu-Lys-Pro-Gly-Gln-Pro-Met-Tyr (Stotzler, *et al.,* 1976) and **a**-factor, Tyr-Ile-Ile-Lys-Gly-Val-Phe-Trp-Asp-Pro-Ala-Cys(*S*-farnesyl)-OCH_3 (Anderegg, *et al.,* 1988). The α-factor is secreted by α-cells and is responsible for eliciting the mating response from the target **a**-cell via the Ste2p receptor (Jenness, *et al.,* 1983; Burkholder & Hartwell, 1985; Nakayama *et al.,* 1985), while the **a**-factor is secreted by **a**-cells and its target is Ste3p, a receptor located on the surface of the α-cells (Bender & Sprague, 1986; Hagen & Sprague, 1984). In the case of both pheromones, binding to the receptor results in the transmission of an intracellular G-protein-mediated signal, and subsequent physiological changes, preparing cells of opposite mating type for conjugation and production of diploid progeny (Oehlen & Cross, 1994; Bardwell *et al.,* 1994).

Studies of farnesylated pheromones such as **a**-factor are of general interest because of the need to understand the interaction between lipopeptides/lipoproteins and membranes. Isoprenylation has been recognized as a common post-translational modification of proteins (Zhang & Casey, 1996). Farnesylation of the Ras oncogene product was shown to be a requirement for its ability to localize to the membrane and to transform cells to a cancerous state. Mutant forms of the Ras protein are found in ~30% of human cancers, and this has led to intense interest in inhibitors of protein farnesylation as potential anticancer agents and in the fundamental biochemistry of protein farnesylation (Gibbs & Oliff, 1997). The farnesylated *C*-terminal Cys-sulfhydryl is an important structural feature of **a**-factor distinguishing it from most peptide hormones. Despite this difference **a**-factor appears to be functionally equivalent to α-factor in its role as a ligand for their respective G protein-coupled receptors. As modified analogs of **a**-factor can be prepared by chemical synthesis (Xue, *et al.,* 1989,1990,1991; Naider & Becker, 1997), this pheromone provides a simple model system to provide information about prenyl-membrane and prenyl-protein interactions.

REVIEW OF PREVIOUS WORK

Marcus *et al.* used synthetic methods to demonstrate the requirement for both the C-terminal methyl ester and the lipophilic farnesyl moieties of **a**-factor for high biological activity (Marcus, *et al.,* 1991). Nonmethylated or nonfarnesylated versions had activities of 1.5% and 0.1% of wild type, respectively, while unmodified **a**-factor dodecapeptide was virtually inactive. Caldwell *et al.* noted

that a geranylgeranylated **a**-factor had an activity of 25% of wild type in growth assays (Caldwell, *et al.,* 1994a). Analysis on truncated **a**-factors suggested that sequential removal of NH_2-terminal residues lead to a gradient of potency loss, with some amino acids exhibiting a slightly greater contribution to bioactivity than others (Caldwell, *et al.,* 1994b). In order to assess the importance of the farnesyl moiety of the lipopeptide for biological activity, Dawe *et al.* prepared novel analogs in which the 3-methyl group of the farnesyl chain was replaced, giving analogs containing ethyl, vinyl, *tert*-butyl, and phenyl moieties at the 3-position (Dawe, *et al.,* 1997). The bioassay results these analogs are clearly inconsistent with a simple hydrophobic role for the isoprenoid and instead illustrate that this hydrocarbon chain plays an active role in mediating optimal **a**-factor/receptor interaction.

OBJECTIVE

Compared to extensive studies that have been performed on the structural aspects of α-factor bioactivity and receptor binding, relatively few studies on **a**-factor bioactivity have appeared. Furthermore, little information is available on the conformation-activity and structure-function relationships of this lipopeptide. Therefore the goal of this section of the dissertation is to provide additional insights into the relationship between the biological activity of the **a**-factor and its primary and secondary structure. The β-turn conformation is a well-defined 2^0 structure which contributes significantly to the bioactivity of polypeptides and proteins. In principle, if a turn is a structural requirement of the bioactive

conformation of the **a**-factor, restriction in the pheromone by means of reducing conformational flexibility at the turn region should lead to an enhanced biological activity. In our laboratory, two attempts have been made to constrain the turn region of **a**-factor. By replacing Gly^5 with a *D*-Ala residue, Caldwell *et al* obtained the first agonist with 4-6 fold higher activity compared to wild type **a**-factor (Caldwell, *et al.,* 1993). In a follow up study, Zhang *et al.* incorporated the (*R*)-3-amino-2-oxo-1-pyrrolidineacetic acid in place of Lys^4Gly^5 and obtained a potent agonist with 32-fold higher bioactivity (Zhang, *et al.,* 1996).

In this work, we attempt to investigate further the degree of importance of the β-turn structure involving residues 4 and 5. A Pro-Gly or Pro-*D*-Ala sequence favors a type II β-turn, while a *D*-Pro-Gly or *D*-Pro-Ala sequence favors a type II' β-turn (Yan *et al.,* 1995). A series of position 4,5 analogs of **a**-factor (I-V) in which Lys^4Gly^5 is replaced with the following dipeptide sequences: *D/L*-Pro^4-*L/D*-Ala^5 or *D/L*-Pro^4-Gly^5 (Table 1, Figure 1) were designed and synthesized to analyze the importance of the Lys ε-NH_2 for bioactivity and to study whether replacement of Lys^4Gly^5 by conformationally constrained sequences would alter activity of the pheromone. Results these analogs will help to determine whether the **a**-factor adopts a reverse turn as its bioactive conformation. As a continuation of studies with novel farnesyl analogs, the effect of geometrical isomerism of the farnesyl group on the bioactivity has been studied by comparing the bioactivities of geometrical isomers of **a**-factor (compounds VI through VIII) with that of wild-type, compound I' (Table 1 and Figure 1).

Table 1 Synthetic **a**-factor and its analogs

No.	Peptides
I'	**a**-factor: YIIKGVFWDPAC(Far)OMe
I	[*L*-Pro^4]**a**-factor: YIIPGVFWDPAC(Far)OMe
II	[*D*-Pro^4]**a**-factor: YII*d*PGVFWDPAC(Far)OMe
III	[*L*-Pro^4, *D*-Ala^5]**a**-factor: YIIP*d*AVFWDPAC(Far)OMe
IV	[*D*-Pro^4, *L*-Ala^5]**a**-factor: YII*d*PAVFWDPAC(Far)OMe
V	[*L*-Nle^4]**a**-factor: YIINleGVFWDPAC(Far)OMe
VI	*cis, trans*-farnesylated **a**-factor
VII	*trans, cis*-farnesylated **a**-factor
VIII	*cis, cis*-farnesylated **a**-factor

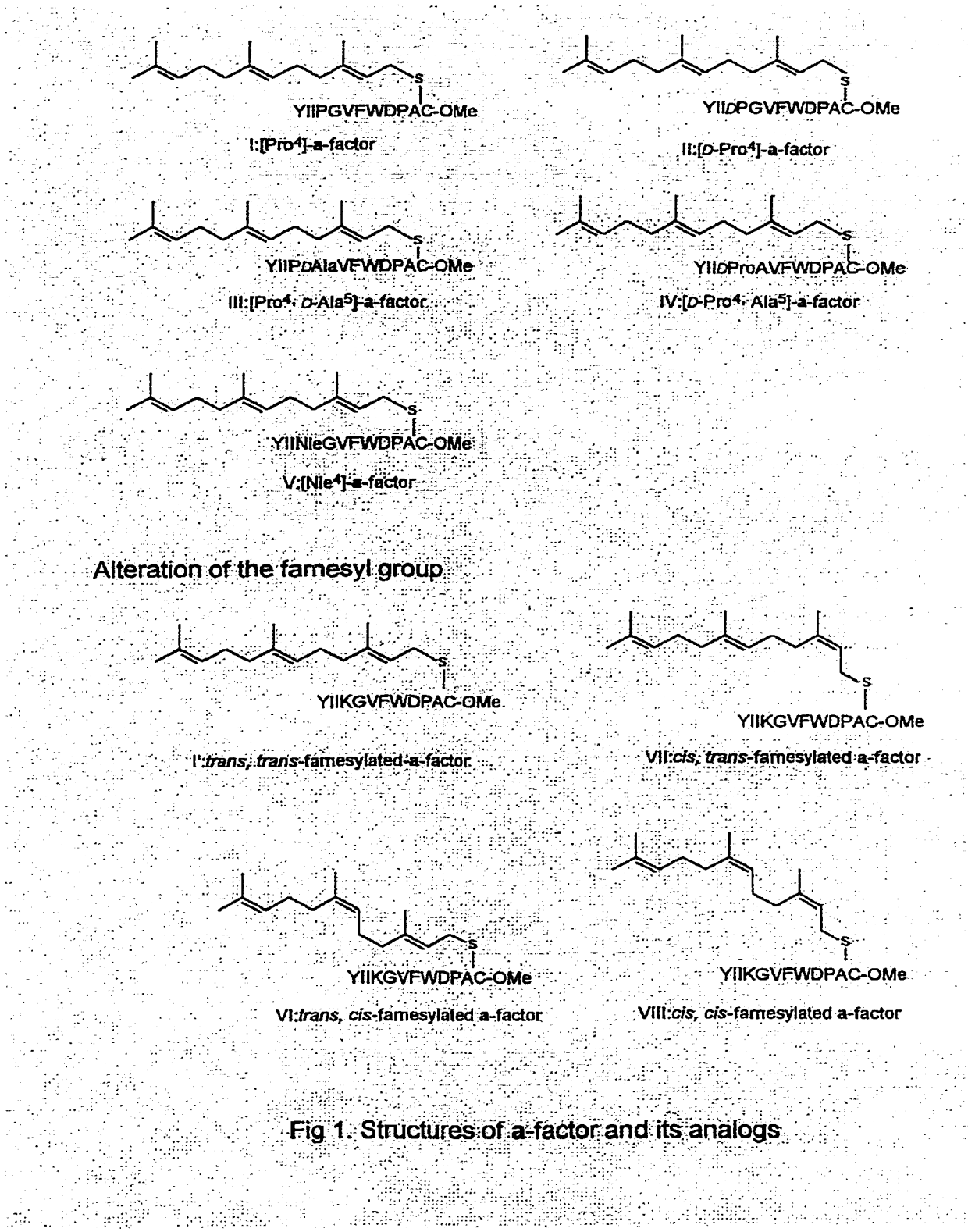

Fig 1. Structures of a-factor and its analogs

In addition to relating bioactivity to primary structure I also determined the conformation-function and structure-function relationships of **a**-factor through spectroscopic methods such as circular dichroism (CD), NMR, and fluorescence-enhancement assay. CD studies were carried out to see if changes in primary sequence could be related to a change in secondary structure, which might be correlated with biological activity. Previous CD and 2D-NMR studies have shown that **a**-factor in DMSO or in presence of DMPC (1,2-dimyristoyl-*sn*-glycero-3-phosphocholine) or lyso-PC (1-palmitoyl-lysophosphatidylcholine) is largely disordered (Epand, *et al.,* 1993; Gounarides, *et al.,* 1991). However, this doesn't preclude the existence of a transient β-turn structure. The advantages of CD spectroscopy are the simplicity of the measurement and the unique conformational sensitivity of the method. During the past three decades peptide chemistry has witnessed the synthesis and chiroptical characterization of thousands of linear and cyclic model peptides of β and γ turns, which demonstrate that CD spectroscopy can detect β-turns and distinguish between their two major families, type I(III) and II, in small (up to ten residues) protected and unprotected peptides. The standard values of ϕ, ψ angles for the different β-turn types are summarized in Table 2 (Perczel, and Hollosi, 1996; Perczel, *et al.,* 1993). Perczel *et al.* summarized the classes of CD spectra observed for linear peptides in Table 3 (Perczel and Hollosi. 1996). For comparison, we also ran the CD spectra of [(*R*)-γ-lactam^{4,5}]-**a**-factor and [(S)-γ-lactam^{5,6}]-**a**-factor (Figure 2), which contain Freidinger's γ-lactams (Freidinger, *et al.,* 1980) that are reported to mimic a type II β-turn or a type II' β-turn, in 90% TFE (Zhang, *et al.,* 1996). We

that CD studies on these **a**-factor analogs can provide qualitative conformational information concerning the presence or absence of various turn structures.

The use of multi-dimensional NMR methods for structure elucidation of small and midsize peptides has increased enormously in recent years (Chiou, *et al.,* 1996; Bradley, *et al.,* 1994; Bechinger, *et al.,* 1999; Moy, *et al.,* 2000). The most definitive information about the structure of a molecule comes from nuclear Overhauser experiments (NOE). NOE is a particularly powerful means of differentiating between types I and type II β-turns, in which the distance between the $C^{\alpha}H$ and NH protons of residue at *i*+1, *i*+2, and *i*+3 is significantly different. Finally, the partitioning into the lipid of the positions 4,5 **a**-factor analogs (compounds I-IV and IX) as well as three farnesyl modified a-factor analogs (compounds X-XII, synthesized by Dawe *et al.,* 1997, Figure 2) was assessed using fluorescence spectroscopy in the presence of lipid vesicles. The results of this investigation provide further evidence concerning the structure-activity relationships of **a**-factor and allow us to comment on the role of secondary structure and membrane partitioning in the biology of this pheromone.

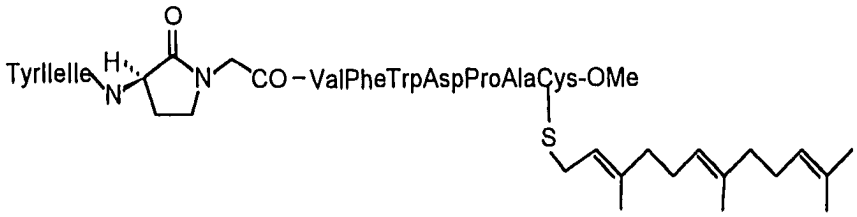

[(*R*)γ--lactam^{4,5}] **a**-factor

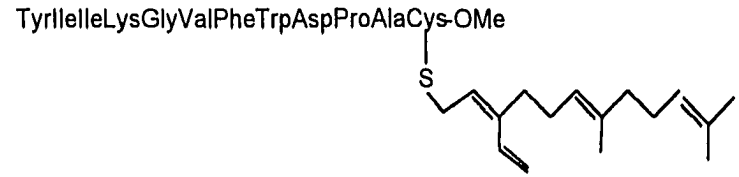

X:[3-vinyl-farnesyl] **a** -factor

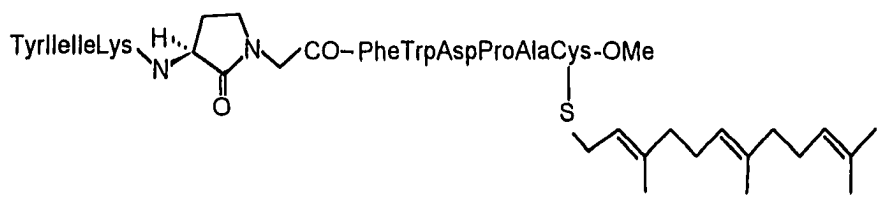

[(*S*)γ--lactam^{5,6}] **a** -factor

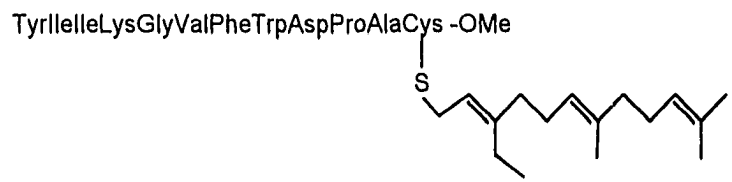

XI:[3-ethyl-farnesyl] **a** -factor

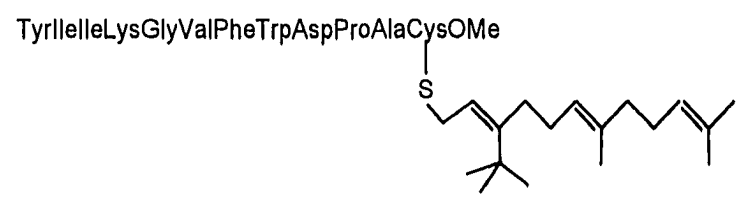

XII:[3- *tert*-butyl-farnesyl]**a** -factor

Figure 2 Structures of previously synthesized **a**-factor analogs

Table 2. The Four Successive Backbone Torsional Angle Values Associated with Residue i+1 and i+2 That Identify the "Ideal" Form of β-turn Types (Perczel, A. and Hollosi, M. 1996)

β-turn type	Back bone torsional angle values				
	ϕ_{i+1}	ψ_{i+1}	ϕ_{i+2}	ψ_{i+2}	τ^a
I	-60	-30	-90	0	45
I'	60	30	90	0	-45
II	-60	120	80	0	1
II'	60	-120	-80	0	-1
III	-60	-30	-60	-30	65
III'	60	30	60	30	-65
VIa[b]	60	120	-90	0	-4
VIb[b]	-120	120	-60	0	-7
VIII	-60	-30	-120	120	46

[a] Defined by the relative orientation of the $C^{\alpha}_{i}, C^{\alpha}_{i+1}, C^{\alpha}_{i+2}, C^{\alpha}_{i+3}$ peptide backbone atoms (Perczel, *et al.*,. 1993)

[b] With a *cis* peptide bond between residue i+1 and i+2

Table 3 Classes of CD Spectra Observed for Linear Peptides (Perczel, A. and Hollosi, M. 1996)

Class of CD Spectrum	Definition	Conformation
A	Negative band near 216 nm, stronger positive band between 195 and 200 nm, negative band near 175 nm	β Sheet
B	Weak negative band between 220 and 230 nm, stronger positive band between 200 and 210 nm, and a strong negative band predicted between 180 and 190 nm	β turn type II
C	α-Helix-like CD spectrum	β turns type I, III, and II'
	α-Helix-like CD spectrum with low-intensity, blue-shifted bands	β turns type I, III
C'	Positive shoulder above 220 nm, positive band at ~200 nm, and negative band below 190 nm	Xxx-D-Yyy or Xxx-Gly type II turns
D	Low-intensity, redshifted Class B spectrum	β turns
U	Weak negative or shoulder band between 215 and 230 nm, strong negative near or below 200 nm	aperiodic (unordered, random coil, or irregular)
U(PPII)	Weak positive band near 220 nm and a strong negative band between 195 and 200 nm	PPII (extended or left-handed extended helix)

Chapter II Experimental Procedures

Materials

N-α-Boc-Pro-OCH_2-PAM-resin was supplied by Applied Biosystems. Protected amino acids were purchased from Bachem Inc. (Torrance, CA) and Advanced ChemTech (Louisville, KY). 1-Hydroxybenzotriazole (HOBt) was purchased from Advanced ChemTech. 1-Hydroxy-7-azabenzotriazole (HOAt) was purchased from PerSeptive Biosystems (Framingham, MA). Diisopropylethylamine (DIEA), dicyclohexylcarbodiimide (DCC), diisopropylcarbodiimide (DIPC), trifluoroacetic acid (TFA), anisole, dimethyl sulfide (DMS), benzotriazol-1-yloxy-tris(dimethylamino) phosphonium hexafluorophosphate (BOP), *N,N'*-dimethylaminopyridine (DMAP), 2-(*N*-morpholino) ethanesulfonic acid (MES), and all other reagents were purchased from Aldrich Chemical Co. (Milwaukee, WI). Solvents used for synthesis were purchased from VWR Scientific (Piscataway, NJ) and Fisher Scientific (Pittsburgh, PA). HPLC grade acetonitrile (MeCN), *N, N'*-dimethylformamide (DMF), dichloromethane (DCM), and methanol (MeOH) were all purchased from VWR Scientific. 1,2-dimyristoyl-sn-glycero-3-phosphocholine (DMPC) was purchased from Avanti Polar Lipids (Birminham, AL).

*Synthesis of **a**-factor analogs*

The synthesis of farnesylated peptides is complicated in comparison to normal peptides because the farnesyl group is very hydrophobic and acid labile.

In general, we undertook a strategy which involved the condensation of the amine terminal protected decapeptide (Fmoc-YIIX$_1$X$_2$VFW(formyl)D(OFm)P-OH, X$_1$ =*D/L*-Pro or Nle or Lys, X$_2$ =*D/L* Ala or Gly) with the carboxylic terminal S-farnesylated dipeptide [NH_2-Ala-Cys(Far)OMe], i.e. 10+2 coupling. This avoided the exposure of the farnesyl moiety to acid and eliminated low yields at the latter stages of the synthesis (Xue, *et al.,* 1989).

(1) Solid-phase Synthesis of Protected Decapeptides

In the synthesis of the amine terminal protected decapeptides, we utilized Boc as the temporary protecting group for all α-amines except that of Tyr. Fmoc and OFm groups were used for the permanent protection of the Tyr α-amine, the Lys ε-amine and the Asp β-carboxyl, because these protecting groups are stable to acid but can be removed by base (e.g., piperidine) without damage to the farnesyl side chain. *tert*-Butyl was used to protect the phenolic hydroxyl of Tyr. This group was removed before HF cleavage in order to avoid side reactions from *tert*-butyl carbocations. A preloaded Boc-Pro-OCH_2-PAM resin was employed as the support. All decapeptides were synthesized using either an automated solid-phase protocol on an Applied Biosystem Model 433A peptide synthesizer or manually. To ensure a high degree of coupling efficiency, all amino acids were double coupled using 10 eq. of amino acid and DCC/HOBt in the automated protocol, and 4 eq. of amino acid and DIPC/HOBt or DIPC/HOAt in the manual protocol as coupling agents, respectively. The HOAt activation was used mainly for incorporation of Tyr and both Ile residues. After 9 cycles and

removal of the *tert*-butyl group of Tyr, the partially protected decapeptide-resin was dried completely in vacuum and subjected to HF treatment as previously described (Xue, *et al.,* 1989). The protected decapeptides were recovered as white powders in about 70-80% yield (based on the starting amine content on the resin). Since the protected decapeptides are very hydrophobic, the direct evaluation of their purity by reverse phase HPLC was complicated because of precipitation in the tubing and on the column. After removal of all protecting groups with 10% piperidine in DMF, the crude deprotected decapeptides were found to be over 85% homogeneous on HPLC (Figure 3). They were used for 10+2 couplings without purification.

(2) Synthesis of Farnesylated Dipeptide Fmoc-Ala-Cys(*t,t*-Far)OMe

To a solution of [Fmoc-Ala-Cys-OMe]$_2$ (0.5 mmol) in 10 ml HOAc/water (9:1), zinc powder (500 mg) was added with stirring. After 1 h, the zinc powder was filtered off and the solution was dried by speed-vac to give 470 mg of crude product. This crude product was dissolved in 40 ml of DMF /CH_3CN (v:v=2:1, with 0.025% aqueous TFA), and cooled in an ice bath. *trans,trans*-Farnesyl bromide (1.5 mmol) was added dropwise to the stirred solution. Stirring was continued for 2 h wherein HPLC and TLC indicated the completion of reaction. The solution was diluted with EtOAc and washed with brine two times (Xue, *et al.,* 1992). The organic layer was dried over $MgSO_4$ for 2 h, and concentrated to give crude product, which had >90% purity as indicated by HPLC.

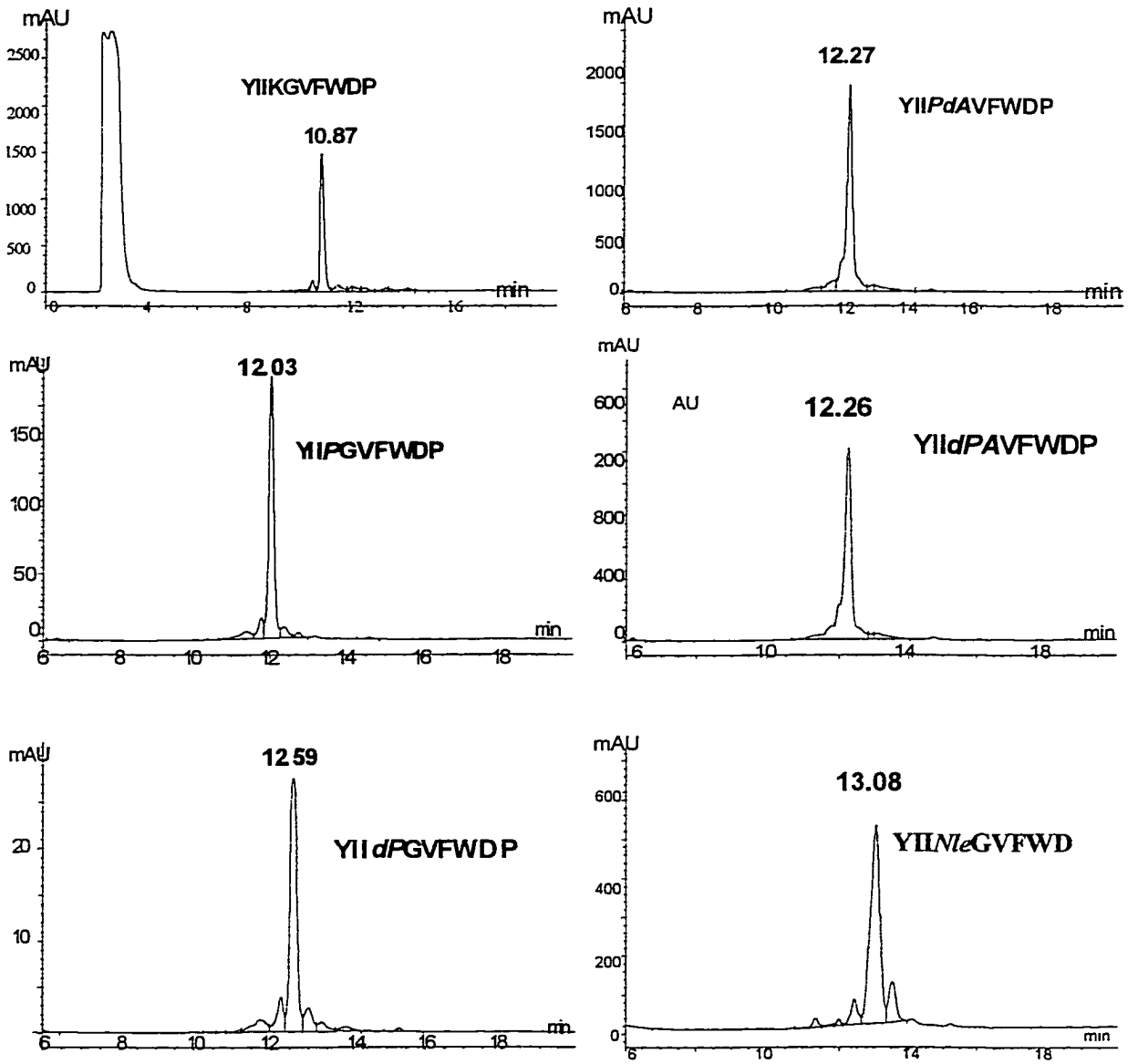

Figure 3 High performance liquid chromatography of crude decapeptides after deprotection with 20% piperidine. The peptides were eluted from a C_{18} reversed phase column using water(0.025% TFA)/acetonitrile(0.025% TFA) with a linear gradient from 10% acetonitrile to 100% acetronitrile in 30 minutes.

After being washed with cooled petroleum ether, the final product was >96% pure by HPLC (80% overall yield), mp 79-81^{0}C. ^{1}H NMR (600 MHz, $CDCl_3$) δ(ppm) 1.408 (d, 3H), 1.565 (d, 6H), 1.616 (s, 3H), 1.652 (s, 3H), 1.92-2.08 (m, 8H), 2.82-2.98 (m, 2H), 3.04-3.18 (m, 2H), 3.736 (s, 3H), 4.207 (t, 1H), 4.288 (narrow m, 1H), 4.379 (narrow, m, 3H), 4.741 (m, 1H), 5.057 (m, 2H), 5.147 (t, 1H), 5.340 (d, 1H), 6.646 (d, 1H), 7.291 (t, 2H), 7.375 (t, 2H), 7.563 (narrow m, 2H), 7.739 (d, 2H).

(3) Synthesis of Fmoc-Ala-Cys(*t,c*-Far)OMe, Fmoc-Ala-Cys(c,t-Far)OMe, and Fmoc-Ala-Cys(c,c-Far)OMe

(These compounds were synthesized in Dr. Gibbs's laboratory, Wayne State University.) The purities of these compounds were identified by analytical HPLC and the structures were confirmed by ^{1}H NMR.

trans,cis- dipeptide:

^{1}H NMR (600 MHz, $CDCl_3$) δ (ppm) 1.416 (d, 3H), 1.576 (s, 3H), 1.619 (s, 3H), 1.657 (s, 6H), 1.92-2.09 (m, 8H), 2.80-2.99 (m, 2H), 3.04-3.19 (m, 2H), 3.724 (s, 3H), 4.212 (t, 1H), 4.306 (narrow m, 1H), 4.372 (narrow m, 2H), 4.749 (m, 1H), 5.063 (m, 2H), 5.151 (t, 1H), 5.340 (d, Cys NH), 6.775 (d, Ala NH), 7.295 (t, 2H), 7.380 (t, 2H), 7.574 (d, 2H), 7.743 (d, 2H).

cis,trans- dipeptide:

^{1}H NMR (600 MHz, $CDCl_3$) δ (ppm) 1.416 (d, 3H), 1.571 (d, 6H), 1.657 (s, 3H), 1.709 (s, 3H), 1.92-2.09 (m, 8H), 2.81-2.99 (m, 2H), 3.06-3.20 (m, 2H), 3.758 (s, 3H), 4.279 (t, 1H), 4.316 (narrow m, 1H), 4.397 (narrow m, 2H), 4.749 (m, 1H),

5.079 (nm, 2H), 5.177 (t, 1H), 5.360 (d, Cys NH), 6.771 (d, Ala NH), 7.314 (t, 2H), 7.391 (t, 2H), 7.574 (d, 2H), 7.745 (d, 2H).

cis,cis- dipeptide:

^{1}H NMR (600 MHz, $CDCl_3$) δ (ppm) 1.416 (d, 3H), 1.570 (s, 3H), 1.657 (d, 6H), 1.69 (s, 3H), 1.92-2.09 (m, 8H), 2.80-2.99 (m, 2H), 3.04-3.19 (m, 2H), 3.731 (s, 3H), 4.210 (t, 1H), 4.309 (narrow m, 1H), 4.376 (narrow m, 2H), 4.749 (m, 1H), 5.060 (nm, 2H), 5.155 (t, 1H), 5.307 (d, Cys NH), 6.605 (d, Ala NH), 7.304 (t, 2H), 7.398 (t, 2H), 7.594 (d, 2H), 7.753 (d, 2H).

(4) Syntheses of a-factor analogs (Compounds I -VIII)

The final **a**-factor analogs (compounds I-VIII, Table 1) were synthesized by condensing the appropriate protected decapeptide with the farnesylated dipeptide as previously performed in this laboratory (Xue, *et. al.* 1989, 1990). Fmoc-Ala-Cys(Far)-OMe (17 mg, 27 μmol) was dissolved in 1 ml of DMF, and 100 mg of DMAP was added. After stirring at room temperature overnight, when HPLC indicated the complete deprotection of the Fmoc group, the solution was added to a solution of protected decapeptide (27 μmol) in 2 ml of DMF at 0^0C followed by BOP reagent (12 mg, 27 μmol). After stirring at 0^0C for 1 h, HPLC showed that the decapeptide had disappeared. The reaction was terminated by and the Fmoc/OFm groups were removed by adding 0.5 ml of piperidine. After stirring for 1 h, the solution was added to 50 ml of precooled ethyl ether and the precipitate was washed with 10 ml of ethyl ether. The solid was dissolved in 2.5

ml of MeOH and acidified with 1% aqueous TFA and applied to a Waters μ-Bondapak column (19×150 mm or 19×300 mm) for purification.

*Purification and Characterization of **a**-factor analogs*

Reversed phase HPLC (RP-HPLC) was performed on a Waters system. Analytical HPLC was run on a Waters μ-Bondapak-C_{18} column (3.9×300 mm), and all peptides were eluted with either a water/acetonitrile (both containing 0.025%TFA) or a water/methanol (both containing 0.025%TFA) linear gradient. Preparative HPLC was run on a Waters μ-Bondapak-C_{18} column (19×300 mm or 19×150 mm) using a linear gradient of water (0.025%TFA) and acetonitrile (0.025%TFA) from 10% to 100% over 120 min. Detection was at 220 nm and/or 275 nm. All peptides were purified to over 99% homogeneity as judged by RP-HPLC except for compound V, whose purity was 97% (Figure 4). Electrospray mass spectrometry was carried out at PeptidoGenics Inc. Amino acid analyses were performed by the Biopolymers Laboratory at the Brigham and Women's Hospital (Cambridge, MA).

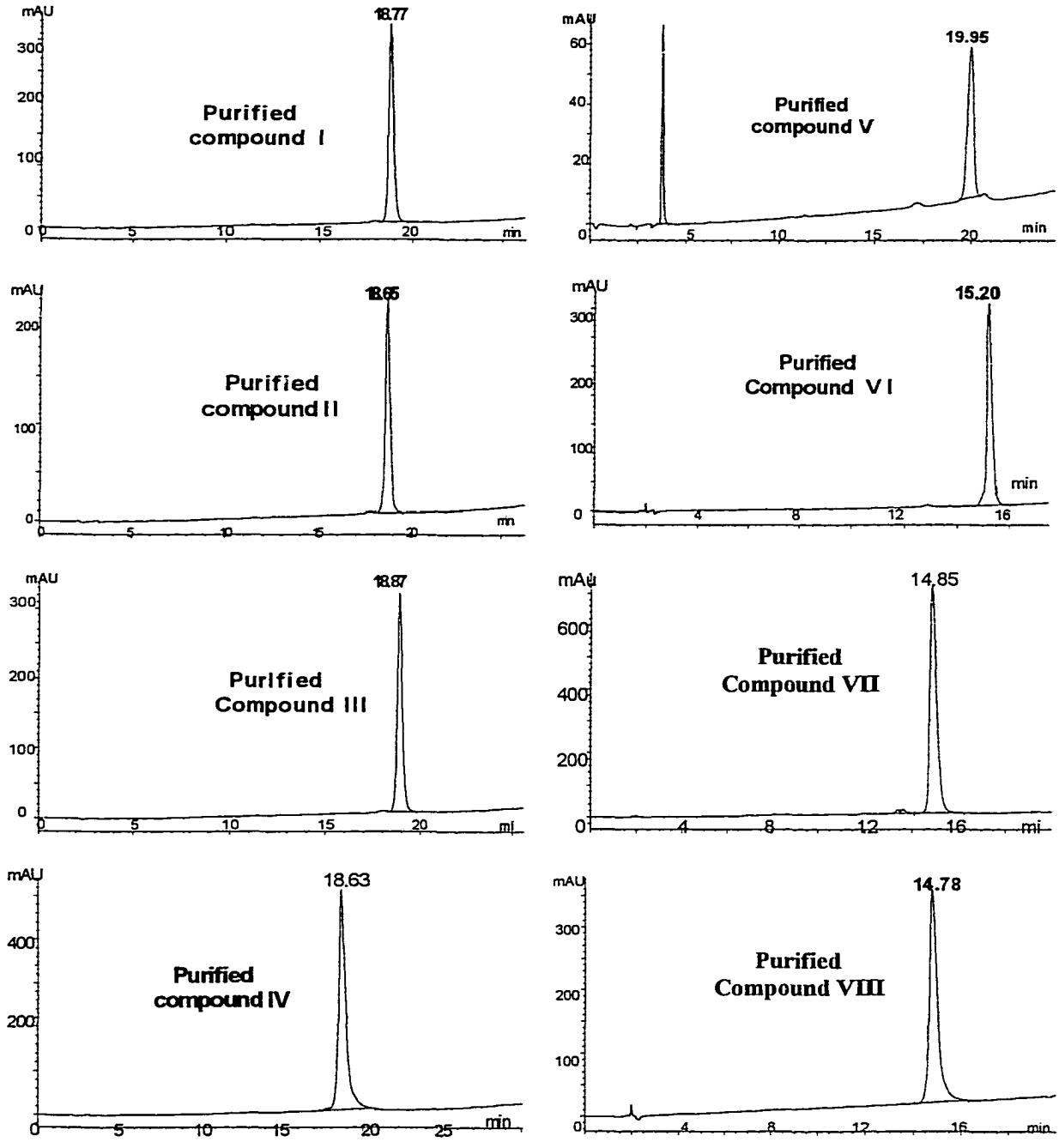

Figure 4 High performance liquid chromatography of purified peptides I through VIII. The peptides were eluted from a C_{18} reversed phase column using a linear water(0.025% TFA)/acetonitrile(0.025% TFA) gradient.

Growth Arrest Assay of Compounds I through VIII

(This work was done by Dr. Becker's Laboratory, University of Tennessee.) *Saccharomyces cerevisiae strain RC757 [MATα sst2-1 rme1 his6 met1 can1 cyh2], a gift from Russell Chan (University of Cincinnati), was used for measurement of the biological activity of various* **a***-factor peptides.* The ability of pheromone analogs to elicit growth arrest was measured by examining induction of a halo of growth arrest when spotted onto a lawn of RC757 cells, a strain supersensitive to **a**-factor. No activity was observed when pheromones were tested against an isogenic *MAT***a** strain indicating specific activity toward RC757 cells and not nonspecific growth arrest. The end point of activity is defined as the minimum quantity of peptide resulting in the formation of an observed halo as described previously (Marcus, *et al.,* 1991). The tests of biological activity were repeated at least four times, and the end point of activity did not vary more than two-fold among the experiments. The concentrations of the peptides in solution were determined by absorbance measurements at 280 nm (ε = 7000 M^{-1} cm^{-1}).

Preparation of DMPC Vesicles

A solution of DMPC in chloroform was transferred to a 7 ml vial. The solvent was removed by rotary evaporation under a stream of nitrogen, and then placed in a vacuum desiccator for several hours to eliminate traces of solvent. The dried film was kept in the freezer until ready for use. For CD studies, the lipid was hydrated with 10 mM pH 7.4 phosphate buffered saline. For binding assay, the

lipid was hydrated with buffered solution that contained 10 mM 2-(*N*-morpholino)ethanesulfonic acid (MES), adjusted to pH 6.4 with KOH. The stock suspension with concentration of 4 mM was vortexed for 1 min. and sonicated at 40 ^{0}C until homogeneity and transparency were obtained.

Circular Dichroism Spectroscopy

It is vital to know the concentrations used so that $\Delta\varepsilon$ can be determined accurately. Dry weight is the least accurate method for measuring the concentration of a peptide in the mg/ml range. Errors of up to 20% may result because of salt or water contamination. For proteins that contain Tyr or Trp, the molar extinction coefficient at 280 nm for normal absorption is closely approximated as the sum of the extinction coefficients for all Trp (5690 $M^{-1}cm^{-1}$), Tyr (1280 $M^{-1}cm^{-1}$), and cysteine (120 $M^{-1}cm^{-1}$) residues (Elwell & Schellman, 1977). If the protein contains no Tyr or Trp, an alternative is quantitative amino acid analysis with ±10% accuracy. Lowry or Biuret analysis is not an accurate measure of protein concentration; they are often in error by as much as a factor of two.

The CD spectra of the peptides were recorded on an AVIV model 62 DS CD instrument (AVIV Associates, Lakewood, NJ), which was interfaced with a computer used for all mathematical calculations. A 1 mm sample cell with a thermostated cell holder was used for all spectral studies. The bandwidth was 1 nm, and the averaging time was 0.5 sec. Each scanning was repeated 3 times. Peptide concentrations in solution were determined from the UV absorption at

280 nm, with the molar absorptivity = 7,000 $M^{-1}cm^{-1}$. Prior to calculation of the final ellipticity, all spectra were corrected by subtracting the reference spectrum. CD intensities are expressed as mean residue ellipticities ($deg \cdot cm^2/dmol$).

NMR Spectroscopy of [D-Ala^5]a-factor and [Pro^4, D-Ala^5]a-factor

1H-NMR spectra were recorded on a UNITY INOVA 600 Varian spectrometer. **a**-Factor samples were approximately 3 mM peptide in 0.5 ml DMSO-d_6 (99.9%, Aldrich Chemical Co., Milwaukee, WI), and farnesylated dipeptide samples were 3 mM in 0.5 ml of $CDCl_3$. All spectra were accumulated at 25^0C unless noted otherwise. Chemical shifts are reported relative to the residual proton resonance of DMSO at 2.50 ppm, or of chloroform at 7.24 ppm, respectively. Phase-sensitive COSY, TOCSY, and NOESY spectra were collected with 1024 complex points in t_2, 512 t_1 increments, 16 acquisitions per t_1 increment, and relaxation delay (d_1) of 2 s. The spectral width in each dimension was 7017.5 Hz. The mixing time in the TOCSY experiment was 70 ms. NOESY spectra were obtained at a mixing time of 200 ms and processed with a 90^0 shifted squared sine bell weighting function in both the t_2 and t_1 dimensions. Gradient HMQC data were collected at 150.87 MHz for ^{13}C NMR, 599.94 MHz for ^{1}H NMR, 1024×256 complex points, 4 scans per t_1, and d_1 of 1 s. The spectral widths in t_1 and t_2 dimensions were 6062.9 and 30173 Hz, respectively. Signal assignments were made using total correlation spectroscopy (TOCSY) spectra and sequential connectivities were determined from NOESY spectra.

Fluorescent Binding assays

In our study, the intrinsic fluorescence of tryptophan was used to measure the partitioning of **a**-factor derivatives into lipid vesicles. The partitioning of the peptides into the apolar environment of the lipid bilayer results in an increase of the quantum yield of the tryptophan residue and a blue shift of emission wavelength (Figure 5). Stepwise addition of the peptide to DMPC vesicles resulted in an enhanced fluorescence signal (Khouri, *et al.,* 1996). The enhancement of fluorescence in the presence of vesicles was calculated as the ratio of the extrapolated molar fluorescence of the pheromone in the presence of lipid (F) to the molar fluorescence in the absence of lipid (F_0) and then plotted according to equation 1 (Khouri, *et al.,* 1996)

$$(F-F_0)^{-1} = (F_{max}-F_0)^{-1} (M_{50}/[M]+ 1) \qquad (1)$$

where [M] is the concentration of the accessible lipid in the outer leaflet of the vesicle bilayer and is assumed to be 2/3 the total concentration of lipid, F_{max} is a constant corresponding to the fluorescence of the bound pheromone, and M_{50} is a constant corresponding to the concentration of lipid at which the enhancement is half-maximal. The factor of 2/3 was based on previous ^{31}P NMR evaluations of DPPC vesicles prepared in a manner similar to that used for the DMPC vesicles we studied. The NMR investigation quantitated the relative number of lipid head groups in the outer and inner leaflet of the vesicles (Naider, *et al.,* 1989). The parameter M_{50} reflects the concentration of lipid at which 50% of pheromone is bound and half the pheromone is free. A low value of M_{50} means a high affinity

and a high M_{50} corresponds to a low affinity. The affinity of a peptide for a membrane can also be represented as a partitioning coefficient:

$$K_p = (C_b[H_2O]) / ([M]C_f) = [H_2O] / M_{50} \quad (2)$$

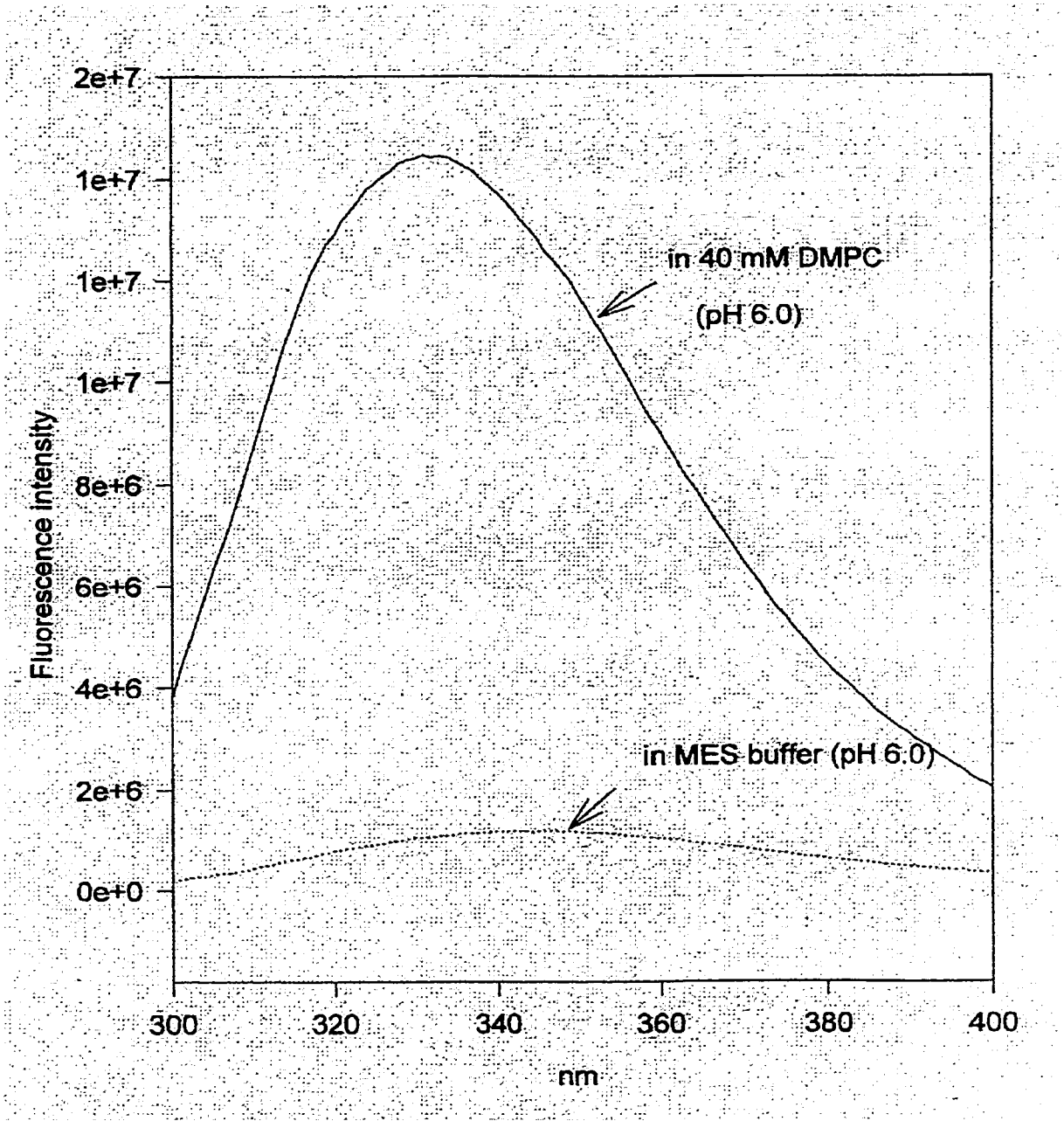

Figure 5 Emission spectra of a-factor in buffer and lipid (30 ^{0}C)

where K_p is the partitioning coefficient corresponding to the ratio of the mole fraction of peptide in the membrane phase to that in the aqueous phase, C_f is the concentration of free pheromone, and C_b is the concentration of bound pheromone.

(2) Fluorescence measurements

The stock lipid vesicles were diluted into a solution of 10 mM MES/KOH buffer, pH 6.4, in a 3 ml quartz cuvette at 30°C. The final lipid concentration ranged from 40 μm to 1 mM. The **a**-factor analogs were each dissolved in methanol and heated at 30 °C for 10 min, and 5μl of the concentrated stock solution was added sequentially to each dilution of lipid vesicles. After addition of the peptide the solution was allowed to equilibrate for 5 to 10 minutes and the fluorescence was measured. The final concentration of the peptides ranged from 0.4 to 3 μM. The experiments were performed in a total volume of 3 ml with constant stirring of the solution using a Teflon coated stir bar. The fluorescence was measured using a RF-5000U fluorometer. The sample was excited at a wavelength of 280 nm (3 nm bandwidth), and the emission was measured at 350 nm (3 nm bandwidth). Each measurement was repeated three times and the data were collected for a minimum of 30 s and averaged. The signal was stable over the time measured.

CHAPTER III EXPERIMENTAL RESULTS

*Synthesis and Characterization of **a**-factor analogs*

The synthesis of the **a**-factor pheromones was carried out by a combination of solid phase synthesis and coupling in solution (Xue, *et al.,* 1990). Fmoc-Ala-Cys(Far)OMe was made by reaction of Fmoc-Ala-CysOMe with *trans, trans*-farnesyl bromide using $Zn(OAc)_2$ as catalyst. Previously, farnesylation of the dipeptide was carried out under basic conditions or using KF as a catalyst (Xue, *et al.,* 1990). Careful HPLC analysis revealed several by-products under these conditions. In contrast, using $Zn(OAc)_2$ as catalyst under weakly acidic aqueous conditions (pH= 5-6), fewer side products were noted and the crude product had over 88% purity. Final purification of the farnesylated dipeptide was carried out by washing with petroleum ether or recrystallization instead of using flash chromatography on silica gel. This method gave the product in good yield (80%) and high purity (>96%).

During synthesis of protected decapeptides difficulty resulted from the highly hydrophobic sequences (*e.g.* YIIPA) at the amino terminus. Using a manual protocol it was very difficult to couple the last three amino acids. Usually HOBt was replaced with HOAt in the activation step and the last coupling was carried out overnight. This change yielded better coupling results and a purer protected decapeptide. It was critical to prevent aggregation of the protected decapeptides, as aggregation proved to be highly deleterious during the final 10 +2 coupling step. The observed aggregation of these peptides occurred most

likely during the ether precipitation or washing steps and was most likely a result of self-association. Fortunately, the aggregation of almost all of the protected decapeptides was not irreversible and could be eliminated using strongly polar solvents like DMF or DMSO and gently heating of the solution (~ 40^0C). Total solubilization of peptides to give a clear solution with decreased viscosity indicated the recovery of unaggregated materials as confirmed by analytical HPLC (see chapter II experimental procedures). Aggregation during synthesis has also been observed in the synthesis of membrane-spanning peptides (Tomicil, *et al.,* 1988). Although the final 10+2 reaction was efficient as judged by HPLC, low yields of the final product (4-43%) were obtained (Table 4). These yields reflect the low solubility of the products in aqueous media, which resulted in significant problems with precipitation on the column during HPLC purification. Compound V was especially problematic. The YII(Nle)GVFWDP sequence contains a long hydrophobic domain which increased the tendency for aggregation, made chain assembly difficult, led to poor solubility and precipitation on the column, and resulted in only 5% yield. In another proposed analog YII(Nle)*D*-Ala-VFWDP these problems were so severe that the protected peptide could not be prepared and the synthesis was abandoned.

Analogs were purified by reverse-phase C_{18} preparative HPLC as evidenced by analytical HPLC (see Figure 4 in Chapter II). Peptides were also homogeneous on silica gel thin layers developed in two different solvent systems

Table 4. Chemical Characterization of **a**-factor Analogs

Compound	Yield[a] (%)	MS[b] ($M+H^+$)	K'[c]	R_f [d]	R_f[e]	Amino acid analysis[f]
I	19	1599.9 (1599.8)	9.1	0.16	0.69	A(1)1.02; D(1)1.02; F(1)0.95;G(1)1.01; I(2)1.60; P(2)2.43; V(1)1.00; Y(1)0.95
II	43	1599.0 (1599.8)	9.5	0.15	0.70	A(1)1.02; D(1)1.05 F(1)0.99;G(1)1.02; I(2)1.62; P(2)2.33; V(1)1.00; Y(1)0.96
III	28	1613.8 (1613.8)	9.3	0.16	0.70	A(2)2.00; D(1)1.00; F(1)1.01;I (2)1.62; P(2)2.37; V(1)1.01; Y(1) 0.99
IV	35	1613.7 (1613.8)	9.7	0.17	0.71	A(2)2.01; D(1)0.99; F(1)0.98; I(2)1.60; P(2)2.40; V(1)0.99 Y(1)0.96
V	5	1615.9 (1616.1)	10.1	0.18	0.67	A(1)1.00;D(1)1.01; F(1)0.99; G(1)1.02; I(2)1.60; Nle(1)1.25;P(1)1.26;V(1)1.00; Y(1)0.88
VI	19	1629.1(1628.9)	7.9	0.16	0.66	A(1)1.05; D(1)1.05; F(1)1.04 G(1)1.06 ;I(2)1.73 K(1)1.05; P(1)1.08 V(1)1.04; Y(1)0.98
VII	27	1626.3(1628.9)	7.9	0.16	0.66	A(1)1.05; D(1)1.04; F(1)1.04; G(1)1.06; I(2)1.73; K(1)1.03; P(1)1.08,V(1)1.05; Y(1)1.01
VIII	4	1629.4(1628.9)	7.9	0.16	0.66	A(1)1.14; D(1)1.08; F(1)0.98; G(1)1.20;I(2)1.78; K(1)1.10; P(1)1.11; V(1)1.11; Y(1)1.01

a. Yield is for the 10+2 coupling, deprotection and purification steps

b. Values in parentheses are calculated ones. Experimental values were from electron spray mass spectroscopy

c. K' is defined as $(V_p-V_f)/V_f$, where V_p is the elution volume for the peptide and V_f is the breakthrough volume. HPLC was performed on a Waters μ-Bondapak-C_{18} column (3.9×300 mm) using a linear gradient of water (0.025%TFA) and MeCN (0.025%TFA) with water from 20% to 80% over 30 minutes.

d. Eluent: 1-butanol:acetic acid:water(4:1:1)

e. Eluent: 1-butanol: acetic acid:water:pyridine(5:1:3:3)

f. Not determined for Trp and Cys.

using UV light (254 nm) and ninhydrin visualization, and gave the molecular weights within one Dalton of calculated values as judged by electron spray mass spectrometry (Table 4). Amino acid ratios were within 10% of theoretical confirming the composition of these peptides, and the presence of intact Trp was verified by absorption measurements.

Biological Activity of Compounds I through VIII

We have employed the halo or growth arrest assay, which serves to determine the minimum quantity of peptide required to induce growth arrest of α-cells, to measure the bioactivities of **a**-factor analogs. As summarized in Table 5 analogs I and III were approximately equally active to **a**-factor whereas II and IV had about 2% of the activity of the wild type **a**-factor. The substitution of Nle for Lys^4 resulted in a nearly inactive pheromone. Geometric isomers VI through VIII exhibited 50% to 100% of the activity of the wild type **a**-factor.

Table 5. Biological activity of **a**-factor and its analogs

Compound No.	Sequence	Bioactivity[a] (%)
a-factor	YIIKGVFWDPAC(Far)OMe	100
I	[*L*-Pro^4]**a**-factor	100
II	[*D*-Pro^4]**a**-factor	2
III	[*L*-Pro^4, *D*-Ala^5]**a**-factor	100
IV	[*D*-Pro^4, *L*-Ala^5]**a**-factor	2
V	[*L*-Nle^4]**a**-factor	0.5
VI	*cis, trans*-farnesylated-**a**-factor	100
VII	*trans,cis*-farnesylated-**a**-factor	50
VIII	*cis, cis*-farnesylated-**a**-factor	100

a. The biological activity of **a**-factor was set at 100% at 60 pg peptide, the lowest concentration of pheromone eliciting growth arrest on a lawn of responding cells. All peptides were diluted serially two-fold, and the resulting solutions spotted on cell lawns. The biological activities of the analogs are expressed as a percent of activity, in comparison to **a**-factor, corresponding to the lowest amount of peptide inducing growth arrest. Each test was done independently at least four times. The end point for each peptide did not vary in more than one dilution among the four assays.

*Determination of Secondary Structures of **a**-Factor Analogs by CD*

In order to see if we could relate changes in 1^0 structure to a change in 2^0 structure we examined CD spectral features of compounds I through V and [*D*-Ala^5]**a**-factor(IX). Since these analogs are virtually insoluble in water we ran CD spectra in an organic/aqueous solvent system, 90% aqueous TFE, and in the presence of DMPC vesicles which mimic the environment of the cell membrane. For comparison, we also ran the CD spectra of [(*R*)-γ-lactam^{4,5}]-**a**-factor and [(S)-γ-lactam^{5,6}]**a**-factor, which contain Freidinger's γ-lactams that are reported to mimic a type II β-turn or a type II' β-turn, in 90% TFE (Zhang, *et al.,* 1996). Due to the relatively low ellipticity of these peptides and the strong absorption of solvent or phosphate ions at lower wavelength (<195 nm), the CD signals below 195 nm were unstable and not reliable. Therefore the following discussion will focus on the wavelength range from 195 to 260 nm.

The CD data for these pheromones are shown in Figure 6. All spectra were measured at pheromone concentrations of 0.1 - 0.25 mM as determined using absorbance measurements at 280 nm. The CD spectra of compounds I-IV in TFE are characterized by a weak minimum at around 215 nm with a mean residue ellipticity of approximately –5000-6000 deg·cm^2·decimol^{-1}. The profiles of these compounds are quite similar for peptides containing *D* or *L* proline(Figure 6A-D). Comparison with the spectra for **a**-factor or compound V (Figure 6F) reveals that these latter compounds do not exhibit a distinct minimum in the

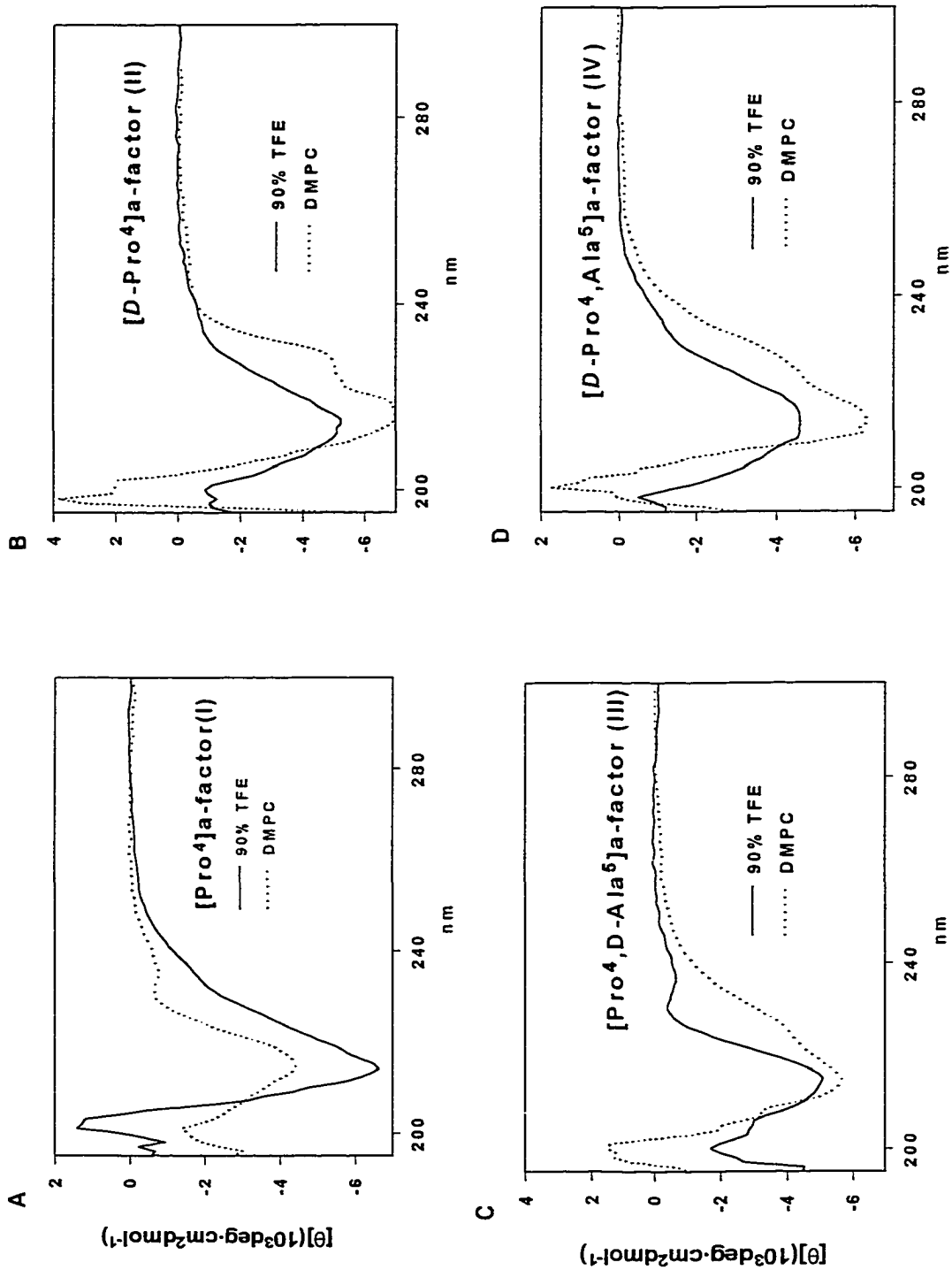

Figure 6 CD of a-factor and its analogs in 90% TFE and DMPC vesicles

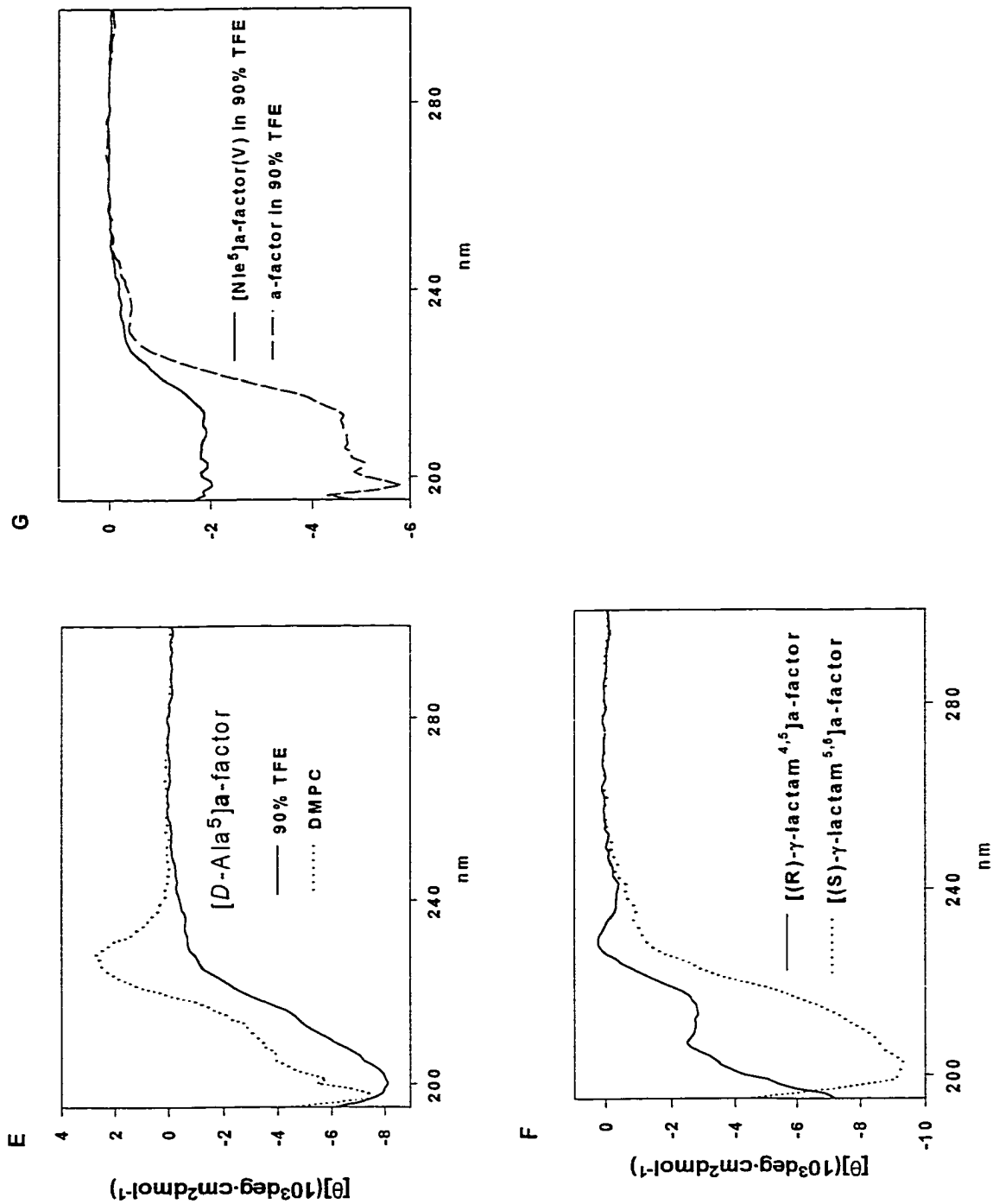

Figure 6 (Continued)

210-220 nm wavelength range. In addition two conformationally constrained analogs containing the Freidinger γ-lactam ([(*R*)-γ-lactam^{4,5}]**a**-factor and [(S)-γ-lactam^{5,6}]**a**-factor) also have CD profiles with low ellipticities in the far UV region (see Figure 2 for structures). In general, the CD profiles of both **a**-factor and its analogs in 90% TFE are not typical of peptides in either an α-helical or a β-sheet conformation, and the CD results indicate that these peptides assume predominantly disordered structures. This result is consistent with previous 2D NMR studies, which indicated that the **a**-factor in DMSO is largely structureless and S-prenylation of the Cys^{12} does not induce folding (Gounarides, *et al.,* 1991).

As will be shown below, **a**-factor peptides partition into lipid bilayers. CD spectra for compounds I-IV in the presence of DMPC vesicles in approximately a 7-18 fold molar excess (lipid/peptide) were similar to those measured in 90% aqueous TFE. In the case of the *D*-Pro containing peptides (compounds II & IV) distinct shoulders were observed at 223-227 nm. All of these peptides showed minima near 215 nm and positive ellipticity at or below 200 nm. In contrast the spectra of [*D*-Ala^5] **a**-factor in the presence of lipid (Figure 6E) exhibited a weak maximum at 227 nm and a minimum below 200 nm. This result is similar to what has been previously reported for **a**-factor in the presence of vesicles (Epand, *et al.,* 1993). Again the spectra for the **a**-factor analogs in the presence of lipid are not indicative of highly ordered pheromones. However, it is clear that the distribution of dihedral angles differs substantially in the proline peptides from those which contain the wild type Lys^4 residue.

Conformational analysis of [D-Ala^5]a-factor and [Pro^4, D-Ala^5]a-factor

Based on CD data, all these analogs are predominantly disordered in both aqueous solution and in the presence of bilayers prepared from synthetic lipids. To gain insights into the detailed conformation of the position 4,5 a-factor analogs, two dimensional NMR analyses were carried out on two model compounds [*D*-Ala^5]a-factor and [Pro^4, *D*-Ala^5]a-factor, which are expected to assume a type II β-turn structure.

1. Assignments

Proton assignments (Table 6,7) were made by identification of amino acid spin systems in the TOCSY spectra and were aided by analysis of 1D spectra. Figure 7 and 8 show the 25 ^{0}C, one dimensional 600 MHz ^{1}H spectra of [*D*-Ala^5]a-factor and [Pro^4, *D*-Ala^5]a-factor, respectively. Figures 9 and10 show the 25 ^{0}C, two dimensional 600 MHz TOCSY spectra of [*D*-Ala^5]a-factor and [Pro^4, *D*-Ala^5]a-factor, respectively. Sequential NOEs were used to discriminate between spin systems (Wüthrich, K. 1986). Table 6 and 7 show that chemical shifts of residues 1,2 and 7 through 12 in both pheromones are within 0.05 ppm of the corresponding resonances in the a-factor (Gounarides, *et al.,* 1991). In contrast, those of residues 3 through 6 showed a greater variation.

Table 6 ^{1}H Assignments for [*D*-Ala^{5}]-**a**-factor in DMSO-d_6 at 25 ^{0}C

Residue	NH	αCH	βCH	γCH	δCH	εCH	Other
Tyr^{1}	-----	4.01	2.94 2.79	----	----	----	NH_2 7.96 OH 9.32 $C_{2,6}H$ 7.02, $C_{3,5}H$ 6.66
Ile^{2}	8.51	4.30	1.68	1.47 1.09 0.82	0.82	----	----
Ile^{3}	8.12	4.19	1.74	1.44 1.05 0.82	0.82	----	----
Lys^{4}	8.04	4.25	1.64 1.47	1.30	1.47	2.71	εNH_2 7.68
D-Ala^{5}	7.89	4.35	1.16	----	----	----	----
Val^{6}	7.79	4.17	1.91	0.72		----	
Phe^{7}	8.09	4.52	2.96 2.75	----	----		Ring Protons: 7.19, 7.18, 7.11
Trp^{8}	8.01	4.54	3.07 2.93	----	-----	----	Ring Protons: 7.54, 6.97, 7.05, 7.32, 7.09 Indole NH: 10.84
Asp^{9}	8.42	4.74	2.70 2.38			----	----
Pro^{10}	------	4.24	1.82	1.72 1.58	3.39 3.17	----	----
Ala^{11}	7.76	4.20	1.19				
Cys^{12}	8.06	4.37	2.80 2.67	----	----	----	Farnesyl: 5.15, 5.06, 5.04, 3.14, 2.04, 2.00, 1.98, 1.92, 1.62, 1.61, 1.54 OCH_3 :3.61

[a] Chemical shifts are given in parts per million relative to the residual proton resonance of DMSO at 2.49 ppm.

Table 7 ^{1}H Assignments for [Pro^{4},*D*-Ala^{5}]-**a**-factor in DMSO-d_6 at 25 ^{0}C

Residue	NH	αCH	βCH	γCH	δCH	Other
Tyr^{1}	-----	4.02	2.93 2.82	----	----	NH_2 8.07/8.03 OH 9.33 $C_{2,6}H$ 7.01, $C_{3,5}H$ 6.67
Ile^{2}	8.47	4.31	1.67	1.44 1.04 0.81	0.80	----
Ile^{3}	8.27	4.35	1.80	1.56 1.10 0.88	0.82	----
Pro^{4}	----	4.29	1.99	193 1.78	3.87 3.64	----
D-Ala^{5}	7.97	4.26	1.17	----	----	----
Val^{6}	7.59	4.13	1.94	0.75 0.72	----	----
Phe^{7}	8.09	4.52	2.96 2.78	----	----	Ring Protons: 7.20, 7.19, 7.15
Trp^{8}	7.97	4.57	3.07 2.94	----	----	Ring Protons: 7.55, 6.97, 7.05, 7.31, 7.12 Indole NH: 10.82
Asp^{9}	8.42	4.76	2.70 2.39	----	----	----
Pro^{10}	------	4.25	1.83	1.74 1.58	3.38 3.20	----
Ala^{11}	7.77	4.23	1.20	---	---	
Cys^{12}	8.07	4.40	2.80 2.68	----	----	Farnesyl: 5.15, 5.08, 5.07, 3.15, 2.04, 2.00, 1.92, 1.63, 1.62, 1.56 OCH_3 : 3.61

[a] Chemical shifts are given in parts per million relative to the residual proton resonance of DMSO at 2.49 ppm.

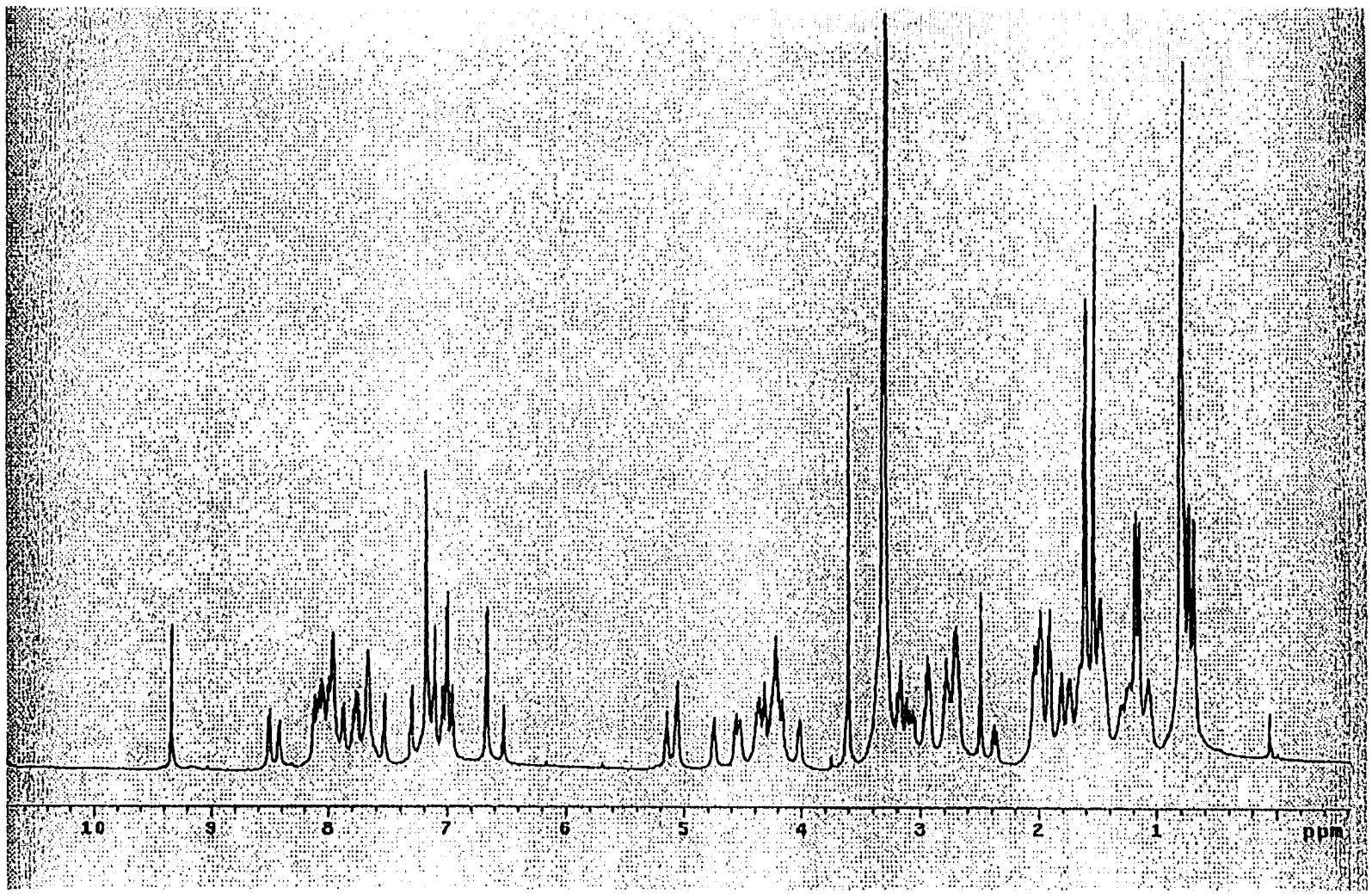

Figure 7. The 600 MHz ^{1}H NMR of [*D*-Ala^{5}] **a**-factor in DMSO-d_6 at 25 ^{0}C. The spectrum was collected with 64 scans, and relaxation delay (d_1) of 3 sec. The spectral width was 12001.2 Hz.

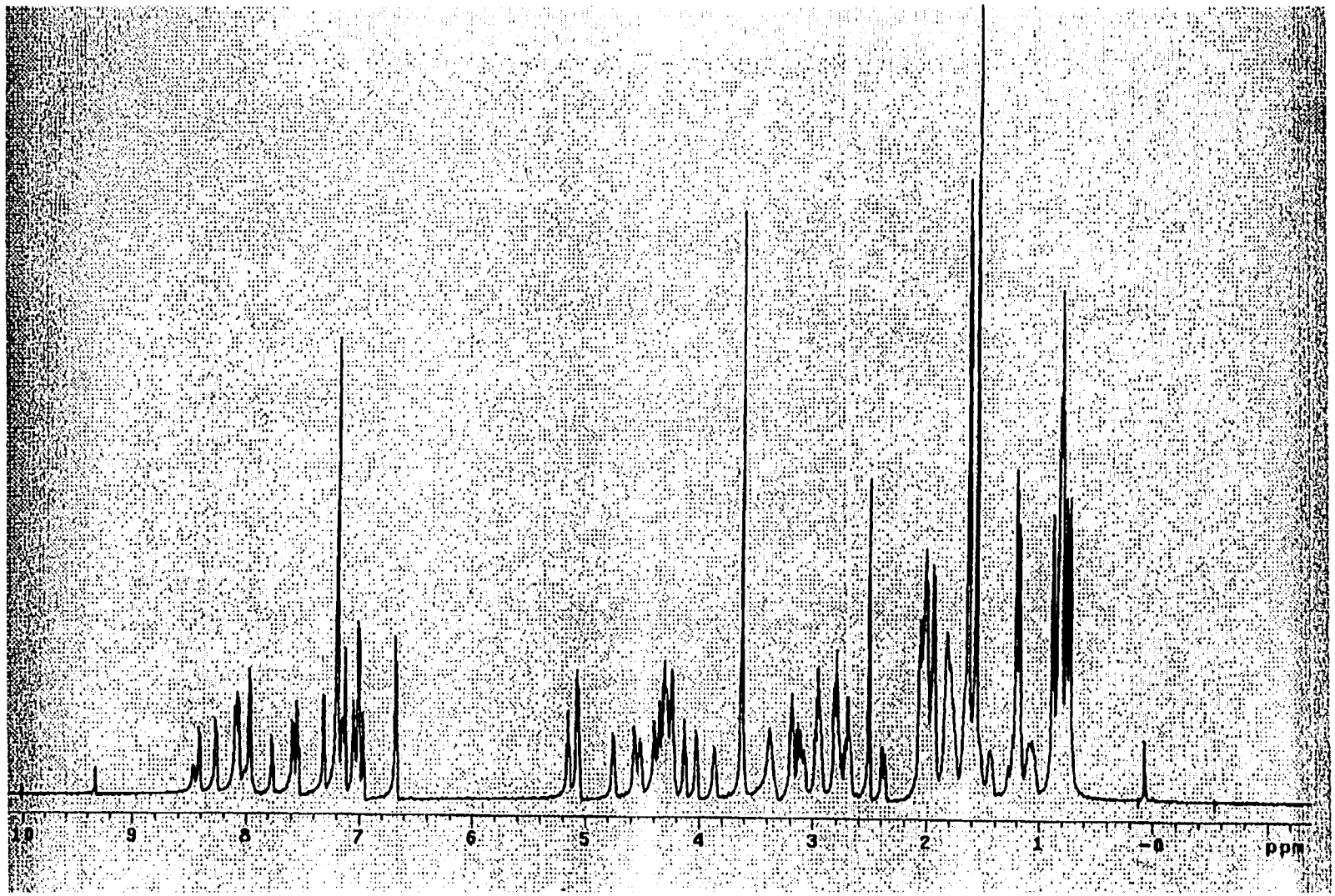

Figure 8. The 600 MHz ^{1}H NMR of [Pro^{4},*D*-Ala^{5}] **a**-factor in DMSO-d_6 at 25 ^{0}C The spectrum was collected with 64 scans per t_1, and relaxation delay (d_1) of 3 sec. The spectral width was 10000.0 Hz.

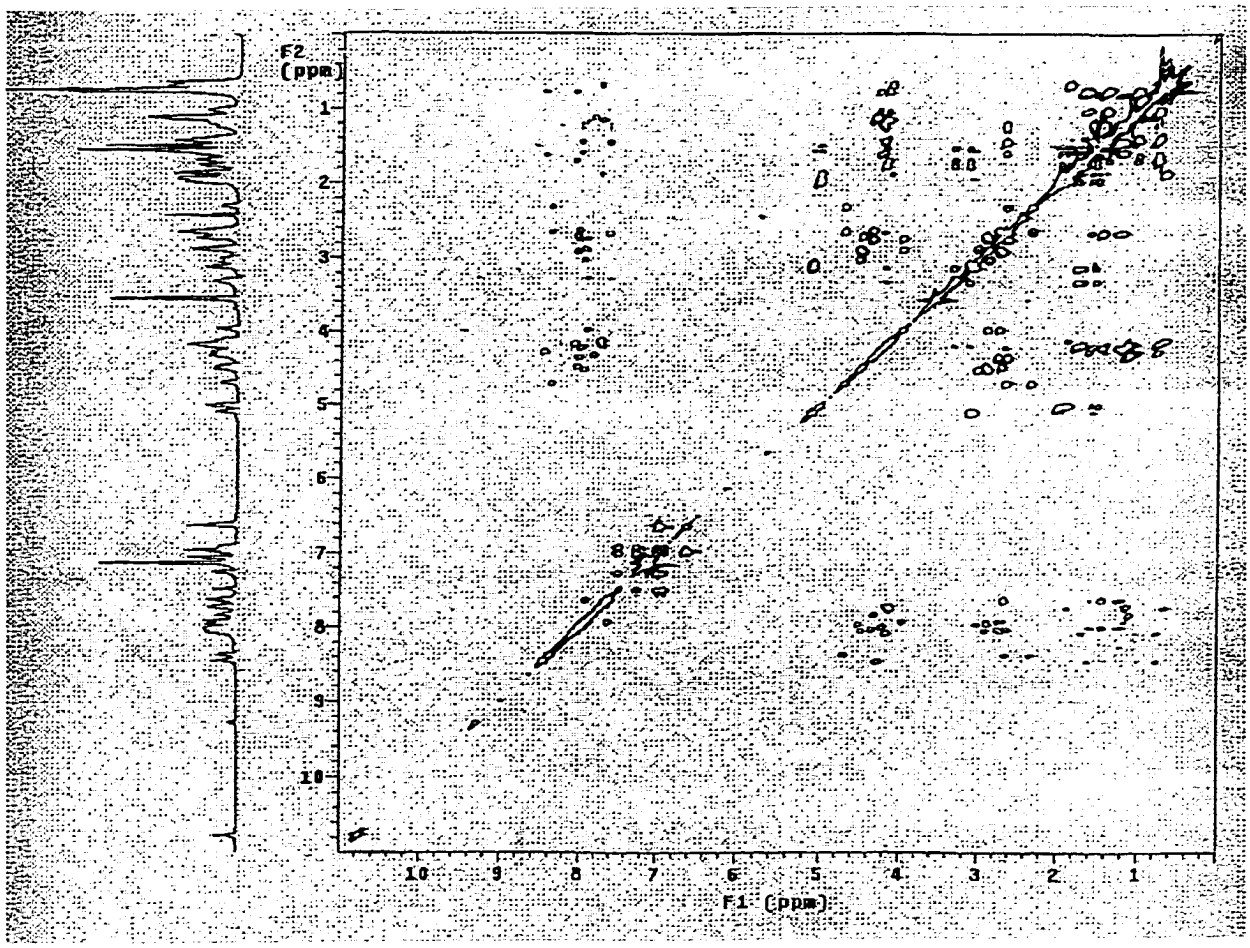

Figure 9. The 600 MHz TOCSY of [*D*-Ala^5] **a**-factor in DMSO-d_6 at 25 ^{0}C. Phase sensitive TOCSY was collected with 1024x512 complex points, 16 scans per t_1, and relaxation delay (d_1) of 2 sec. The spectral width in each dimension was 7017.5 Hz.

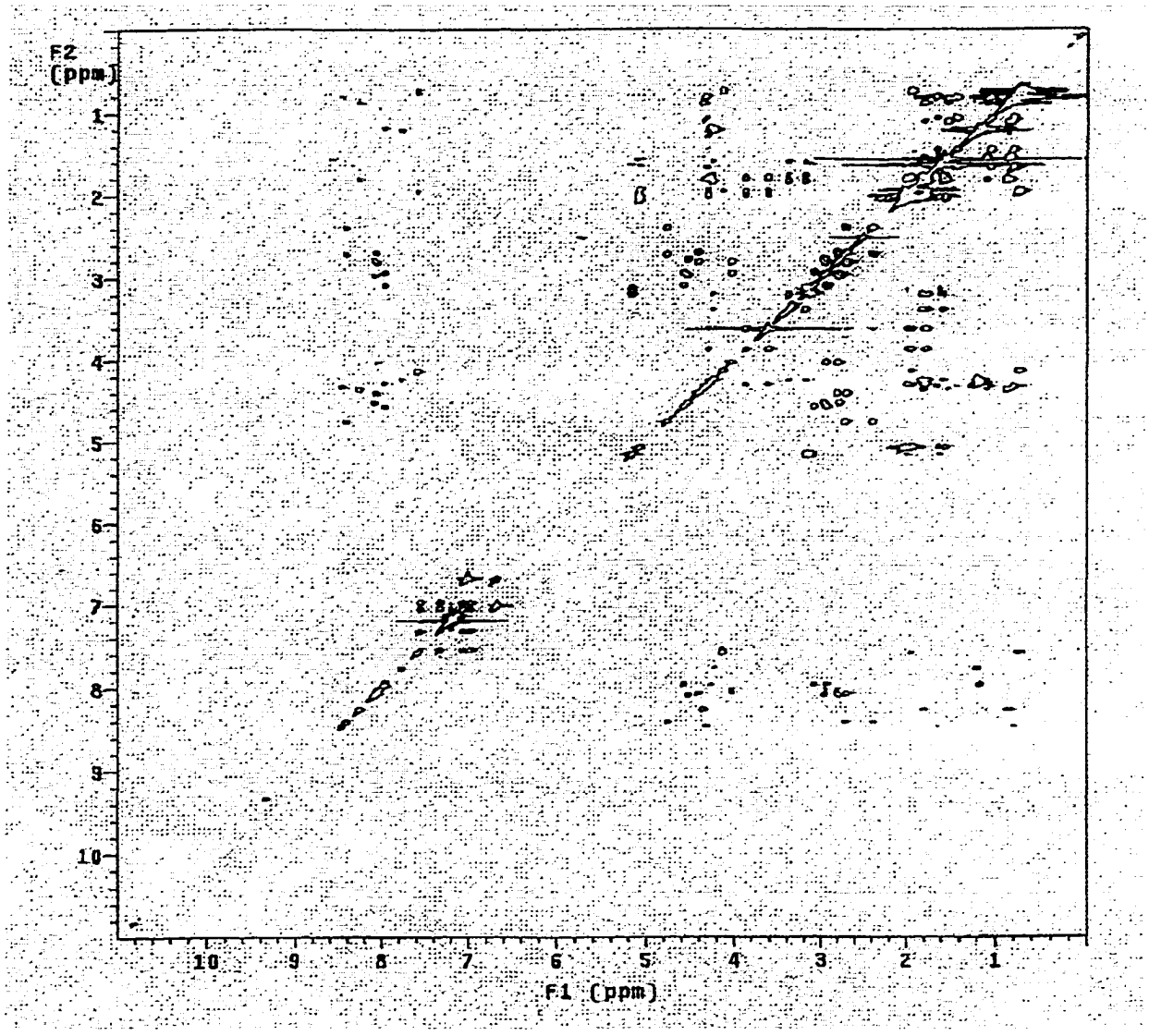

Figure 10 The 600 MHz TOCSY of [Pro^4, *D*-Ala^5] **a**-factor in DMSO-d_6 at 25 ^{0}C. Phase sensitive TOCSY was collected with 1024x512 complex points, 16 scans per t_1, $d_1$of 2 sec and a mixing time of 70 ms. The spectral width in each dimension was 7017.5 Hz.

2. Conformational analysis

In the NOESY spectra of [*D*-Ala^5]**a**-factor and [Pro^4, *D*-Ala^5]**a**-factor, αCH_i-NH_{i+1} cross-peaks were observed between all residues except I^3-P^4 in [Pro^4, *D*-Ala^5]**a**-factor and D^9- P^{10} in both pheromones; numerous NH_i-NH_{i+1} connectivities were also observed (Figure 11,12). However, the absence of non-sequential NOEs and the comparatively strong intensities of the αCH_i-NH_{i+1} cross peaks preclude the identification of an α-helical structure and suggest that the NH-NH connectivities observed are associated with a predominantly disordered peptide. The similar chemical shifts for residues 1, 2 and 7 through 12 also indicated their conformational similarity to disordered **a**-factor. The variation in the chemical shifts of residues 3 through 6 is likely due to the sequence variation rather than a change in conformation. In addition, a nonsequential αCH_{i+1}-NH_{i+3} connectivity between Pro^4 and Val^6 that would be expected for a β-turn structure (Wüthrich, 1986; Dyson, *et al.* 1988) was not observed.

Neither the NH temperature coefficients nor the $^3J_{\alpha NH}$ coupling constants reflect the presence of a long-lived secondary structure (Table 8). The temperature dependence of the amide proton chemical shifts (NH $\Delta\delta/T$) was determined over the ranges 19-39^{0}C with an interval of 2^{0}C. For both pheromones the NH temperature coefficient values of all amide NH's were greater than 2 ppb/K, indicating the absence of strong intramolecular hydrogen bonds (Balaram, 1985). The high temperature coefficient value (4.7 ppb/k) of

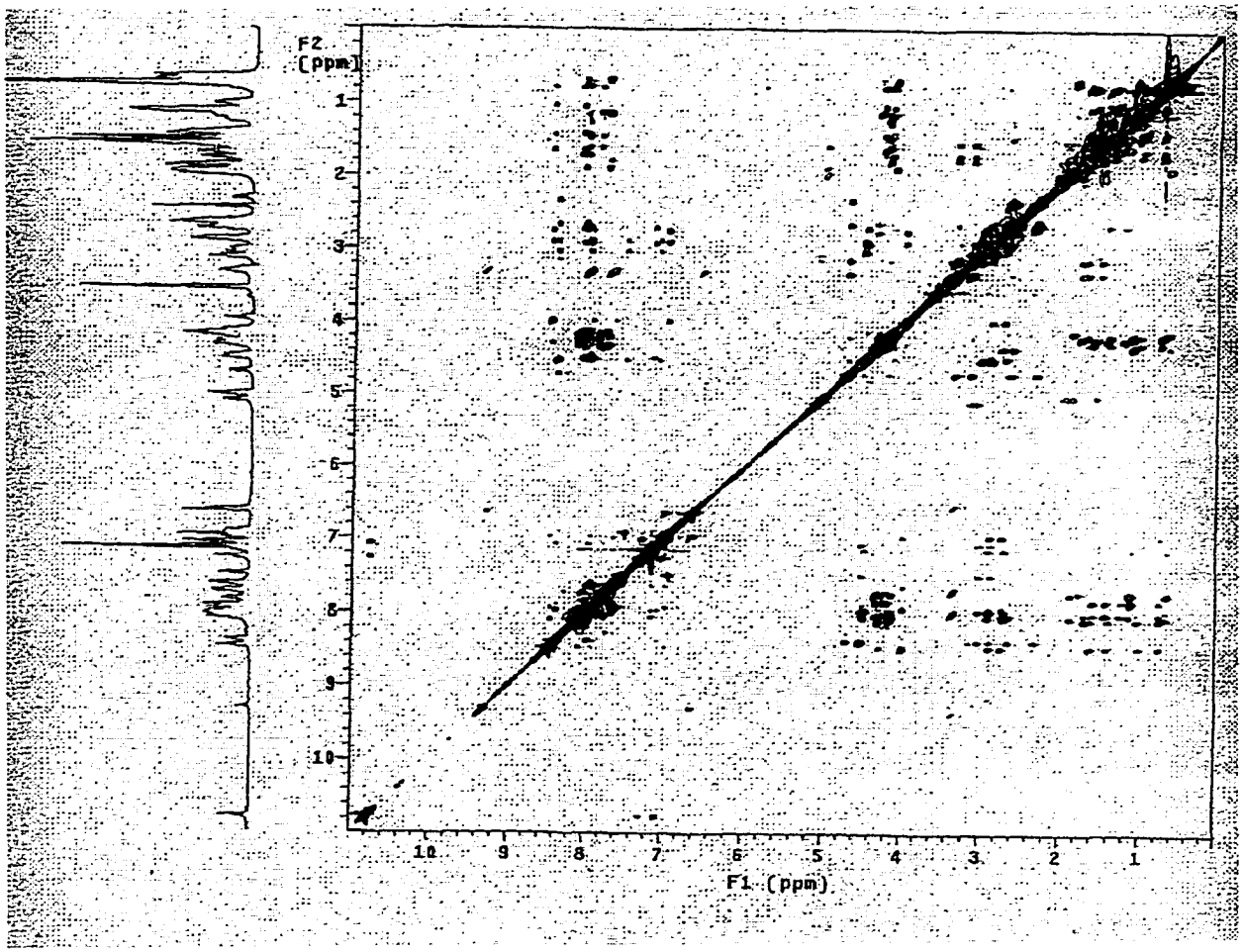

Figure 11. The 600 MHz NOESY of [*D*-Ala^5] **a**-factor in DMSO-d_6 at 25^{0}C. Phase-sensitive NOESY was collected with 1024x512 complex points, 16 scans per t_1, d_1 of 2 s, and a mixing time of 200 ms. The spectral width in each dimension was 7017.5 Hz.

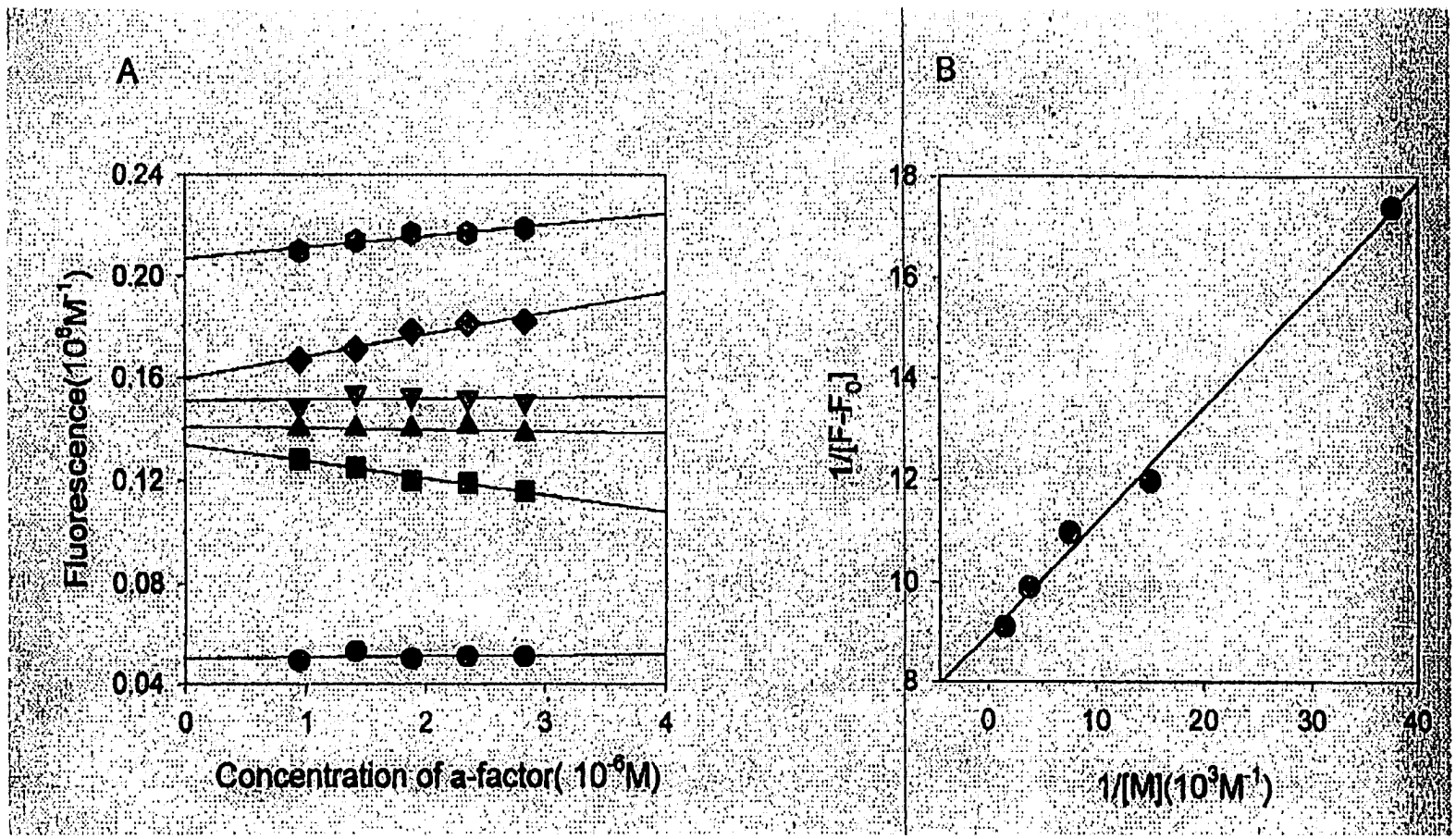

Figure 15 Fluorescence measurements on **a**-factor in the presence of DMPC vesicles. (A) Change of **a**-factor fluorescence as a function of concentration of pheromone. For experiments with **a**-factor, the total concentrations of DMPC vesicles are: O 0 mM; □ 0.040 mM; Δ 0.100 mM; ∇ 0.200 mM; ◊ 0.400 mM; ⬡ 1 mM. All data points are averages of three measurements. (B) Plot of 1/[F-F_0] vs. 1/[M]. Concentrations of DMPC vesicles are given in terms of the accessible lipid and are 2/3 of the total concentration of lipid.

Table 8. Amide Proton Temperature Coefficients and Coupling Constants for [*D*-Ala^5]**a**-factor in DMSO-d_6

NH	[*D*-Ala^5]**a**-factor	
	NH $\Delta\delta$/T(ppb/K)	$^3J_{\alpha NH}$ (Hz)
Ile^2	3.7	8.43
Ile^3	4.7	8.70
Lys^4	3.9	7.59
D-Ala^5	2.9	7.33
Val^6	4.7	8.80
Phe^7	4.1	8.33
Trp^8	5.4	7.59
Asp^9	5.4	7.92
Ala^{11}	4.6	7.56
Cys^{12}	4.7	7.79

amide NH of V^6 further precluded the existence of a type II β-turn involving residues 3 through 6.All $^3J_{\alpha NH}$ coupling constants of of [*D*-Ala^5]**a**-factor were in the range of 7-9 Hz expected for rapid conformational averaging (Wüthrich, 1986; Balaram, 1985).

The NMR results lead us to conclude that all of these position 4,5 **a**-factor analogs assume predominantly disordered structures in DMSO.

Stereochemical Assignments of a-Factor Analogs VI-VIII

Several studies on lipid-modified analogues of **a**-factor have indicated that the farnesyl moiety does not simply enhance hydrophobicity, but also plays a more active role in the biological actions of this pheromone. Recently, Dawe *et al.* (1997) prepared novel analogs in which the 3-methyl group of the farnesyl chain was replaced with ethyl, vinyl, *tert*-butyl, and phenyl groups. The results observed with the two phenyl isomers provided the impetus to further explore the effects of double bond isomerization of the farnesyl moiety on **a**-factor biological activity (Dawe *et al.*, 1997). Therefore, we wished to prepare compounds VI, VII, and VIII, the three geometric farnesylated stereoisomers of **a**-factor (Figure 1).

One particular concern in the preparation of the isomeric farnesylated peptides was to ensure that the double bond geometry had been maintained at the C_2-C_3 double bond. I had thought that simple 1D NOE experiments would provide evidence supporting the geometry of these isomers. However, these experiments were inconclusive due to the fact that H6 and H10 vinylic proton signals overlap and both appear at about 5.05 ppm. Thus, I tried to use the chemical shift values of the four methyl groups in these isomers to make the stereochemical assignments. Considering the structural similarity of these isomers, I assumed that all vinylic protons (H_2, H_6, and H_{10}) should show a similar shielding effect on chemical shift values of the methyl groups at position 3, 7 and 11 (C_3 Me, C_7 Me, and C_{11} Me), respectively (Burrell, *et al.*, 1966). Therefore, the chemical shift values of C_3 Me should be the same in the natural *trans,trans*-dipeptide and *trans,cis* -isomer, and in the *cis,trans* -isomer and the *cis,cis* -

isomer. However, this chemical shift should differ between the *trans,cis*-isomer and the *cis,cis*-isomer, thus allowing one to determine if isomerization of the C_2-C_3 double bond had occurred during the synthesis of either isomer. Similarly, the chemical shift values of C_7 Me should be the same between the natural *trans,trans*-dipeptide and the *cis,trans*-isomer, and in the *trans,cis*-isomer and the *cis,cis*-isomer. Assuming that the shielding effect is about 0.07-0.09 ppm, I assigned chemical shift values for the 4 methyl groups of 4 dipeptide stereoisomers as shown in Table 9. Note that the signal of C_7 Me always overlaps with one of C_{11} Me signals, which is due to the fact that with the same chemical shift values of the H_6 and H_{10} vinylic protons, they should shield to a similar extent the C_7 Me and one of C_{11} Me groups (the one with the same configuration as the C_7 Me).

Table 9 600 MHz ^{1}H Chemical shift assignments for the farnesyl methyl groups of isomeric dipeptides (Solvent: $CDCl_3$)

Fmoc-Ala-Cys(Far)-OMe	C_3 Me	C_7 Me	C_{11} Me
trans, trans	1.62 ppm	1.57 ppm	1.57 ppm, 1.66ppm
trans, cis	1.62 ppm	1.66 ppm	1.57 ppm, 1.66 ppm
cis, trans	1.70 ppm	1.57 ppm	1.57 ppm, 1.66 ppm
cis, cis	1.69 ppm	1.66 ppm	1.57 ppm, 1.66 ppm

Likewise, the ^{13}C chemical shift values for 4 methyl groups of dipeptide stereoisomers were assigned (Table 10) by the aid of HMQC spectroscopy

(Figure 13 illustrates HMQC spectrum of *cis, trans*-farnesylated dipeptide as a representative example). Each peak was simply assigned by recognizing its corresponding proton resonance. Compared to the small shielding effect(~0.07-0.09 ppm) in the proton NMR spectrum, Figure 13 shows a significant carbon shielding effect. In the natural *trans, trans*-dipeptide the C1 carbon shields the C3 methyl carbon, which appears at 16.0 ppm, and the C5 carbon shields the C7 methyl carbon, which appears at 16.0 ppm. In comparison, the C3 Me carbon appears at 23.43 ppm in the *cis, trans*-isomer because the C1 carbon shields the C4 methylene carbon, and C7 Me carbon appears at 16.0 ppm since the C5 carbon shields the C7 methyl carbon. As with the ^{1}H chemical shifts, the ^{13}C chemical shift values of the C_3 Me are almost identical in *trans*, *trans* and *trans*, *cis* isomers, and in *cis*, *trans* and *cis, cis* isomers, but different in *trans*, *trans* and *cis*, *trans* isomers. Also, the ^{13}C chemical shift values of C7 Me are almost the same in *trans*, *trans* and *cis*, *trans* isomers, and in *cis*, *cis* and *trans, cis* isomers, but different in *cis*, *trans* and *cis*, *cis* isomers. From Table 10, one can calculate the shielding effect, i.e. 23.1-16.0 = 25.6-17.5 = ~8 ppm.

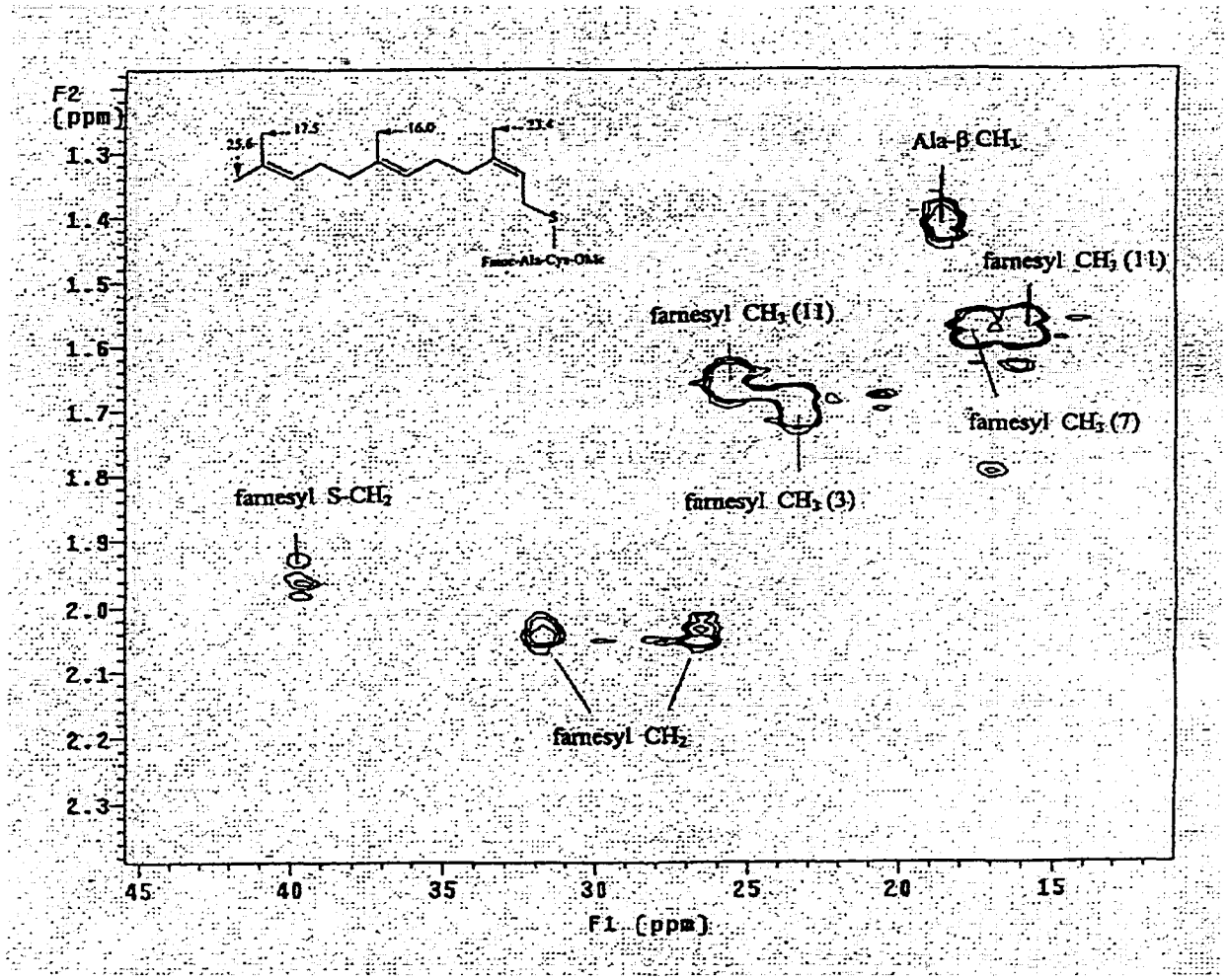

Figure 13 The 600 MHz HMQC spectrum of *cis,trans*-farnesylated dipeptide in $CDCl_3$. Gradient HMQC was collected at 150.87 MHz for ^{13}C, 599.94 MHz for ^{1}H, 1024x256 complex points, 4 scans per t_1, and d_1 of 1 s. The spectral widths in t_1 and t_2 dimensions were 6062.9 and 30173 Hz, respectively.

Table 10. 600 MHz ^{13}C Chemical shift assignments for the farnesyl methyl groups of the isomeric dipeptides (Solvent: $CDCl_3$)

Fmoc-Ala-Cys(Far)-OMe	C_3 Me	C_7 Me	C_{11} Me*
trans, trans	16.0 ppm	16.0 ppm	17.4 ppm, 25.5 ppm
trans, cis	15.8 ppm	23.1 ppm	17.4 ppm, 25.4 ppm
cis, trans	23.4 ppm	16.0 ppm	17.5 ppm, 25.6 ppm
cis, cis	23.1 ppm	23.1 ppm	17.5 ppm, 25.6 ppm

Figure 14 shows ^1H Chemical shift assignments for the farnesyl methyl groups of isomeric **a**-factor pheromones. Note that the proton shielding effect in isomeric **a**-factor pheromones is close to that in isomeric dipeptides (Table 9), i.e. 0.07-0.09 ppm. From these results, we can conclude that isomerization of the C_2-C_3 double bond did not occur during the synthesis of the various dodecapeptides.

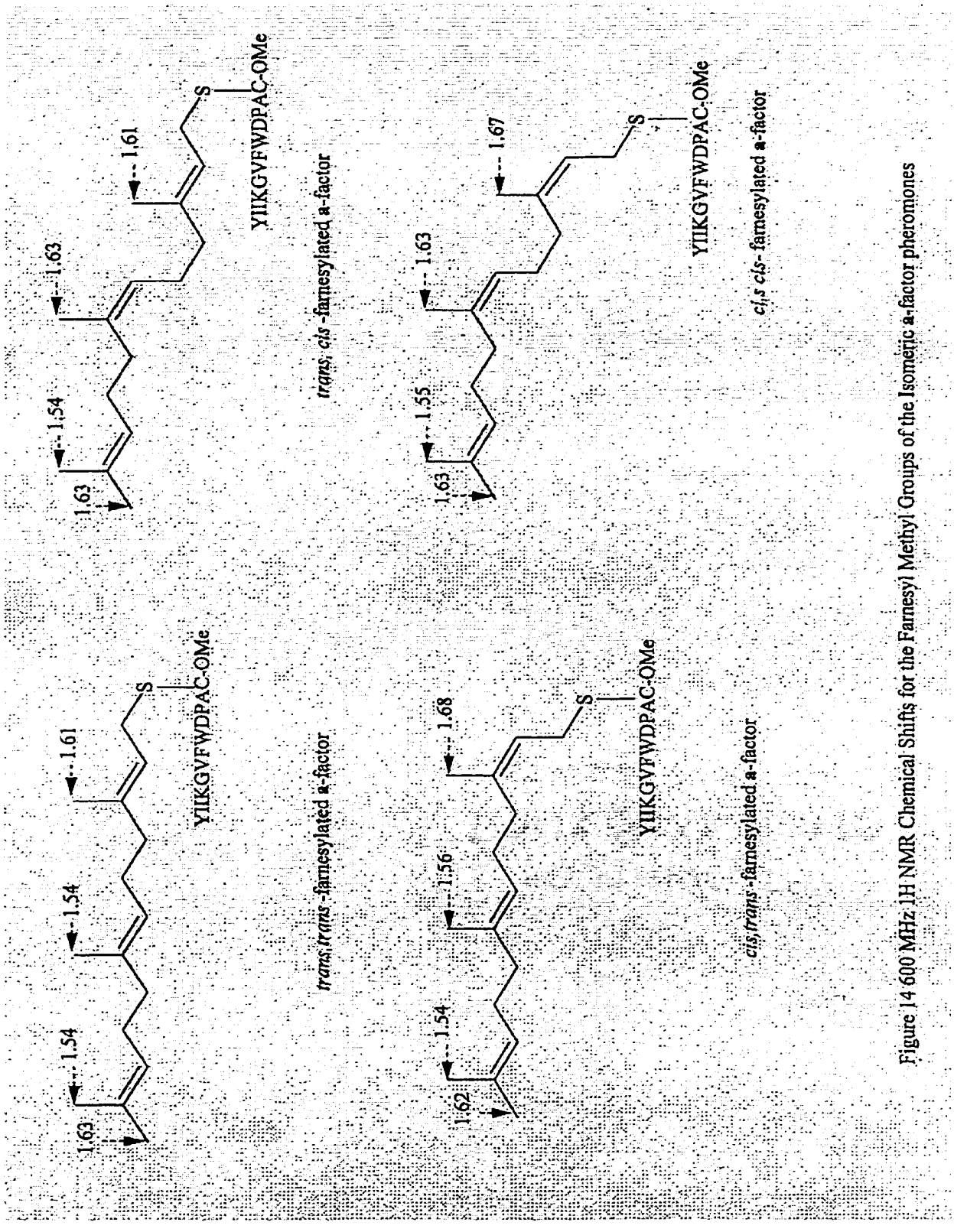

Figure 14 600 MHz 1H NMR Chemical Shifts for the Farnesyl Methyl Groups of the Isomeric a-factor pheromones

*Determination of Membrane Partitioning Coefficients of Position 4,5 **a**-Factor Analogs and Three Farnesyl Modified **a**-factor Analogs*

An important objective of this work was to determine how peptide sequence and the nature of the lipid moiety affect interaction of the **a**-factor pheromone with membranes. To this end, we used the fluorescence of Trp^8 to measure the partitioning coefficients of **a**-factor, position 4 and 5 analogs (compounds I through IV and X) and three farnesyl-modified analogs (compound X through XII synthesized by Dawe *et al.,* 1997) into synthetic vesicles. The structures of pheromones examined in these binding assays are illustrated in Figures 1 and 2.

The partitioning of the peptides into the apolar environment of the lipid bilayer results in an increase in the quantum yield of the tryptophan residue and stepwise addition of the peptide to DMPC vesicles resulted in an enhanced fluorescence signal (Khouri, *et al.,* 1996). In the absence of vesicles, the molar fluorescence remained constant as the pheromone concentration was increased. In the presence of low concentrations of lipid (0.04 mM - 0.2 mM) the molar fluorescence decreased in a linear manner as the concentration of peptide was increased. At higher lipid concentrations (0.4 mM - 1.0 mM) the molar fluorescence increased as the concentration of peptide was increased (Figure 15A). The effect of pheromone concentration was corrected by linear extrapolation of the molar fluorescence values to zero peptide concentration so

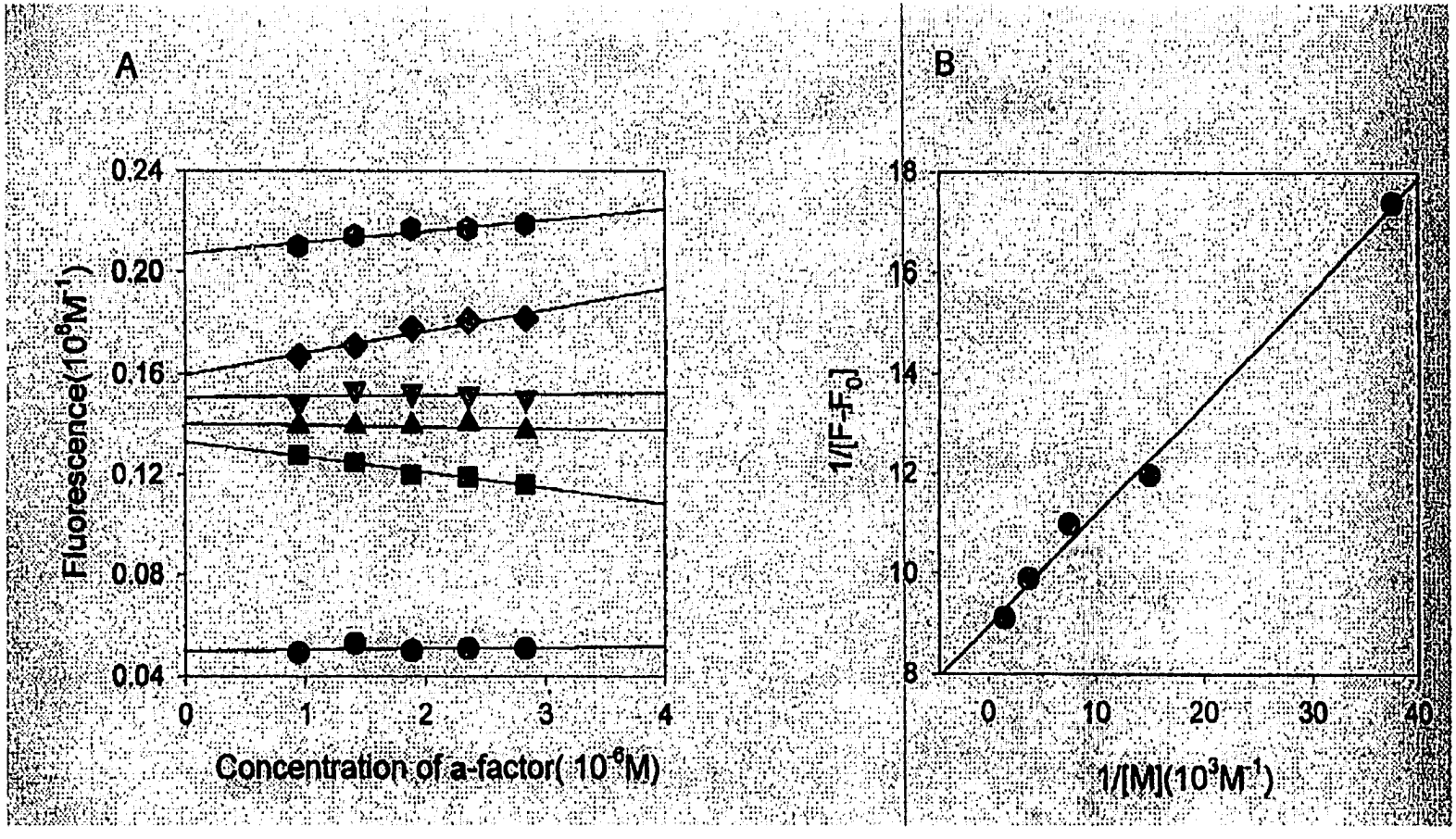

Figure 15 Fluorescence measurements on **a**-factor in the presence of DMPC vesicles. (A) Change of **a**-factor fluorescence as a function of concentration of pheromone. For experiments with **a**-factor, the total concentrations of DMPC vesicles are: O 0 mM; □ 0.040 mM; Δ 0.100 mM; ∇ 0.200 mM; ◊ 0.400 mM; ⬡ 1 mM. All data points are averages of three measurements. (B) Plot of $1/[F-F_0]$ vs. 1/[M]. Concentrations of DMPC vesicles are given in terms of the accessible lipid and are 2/3 of the total concentration of lipid.

so that both the inner-filter effect and saturation of binding sites are eliminated. The binding of **a**-factor analogs to DMPC vesicles was well described by equation (1) (Figure 15B). The values of M_{50} and K_p of the pheromones we examined are summarized in Table 11.

Table 11 Binding Affinities of **a**-Factor Analogs for Uncharged DMPC vesicles

Pheromone	Relative bioactivity[a]	$M_{50}(\mu M)$[b]	$K_p(\times 10^5)$[c]
a-factor	1	24.8±2.4	22.4±2.1
I: [Pro^4]**a**-factor	1	32.7±2.4	17.0±1.2
II: [*D*-Pro^4]**a**-factor	0.02	30.3±2.2	18.3±1.3
III: [Pro^4, *D*-Ala^5]**a**-factor	1	28.7±2.2	19.4±1.5
IV: [*D*-Pro^4, Ala^5]**a**-factor	0.02	30.5±2.8	18.2±1.7
IX: [*D*-Ala^5]**a**-factor	4-6	43.7±4.5	12.7±1.3
X: [3-vinyl-farnesyl]**a**-factor	8	66.5±6.9	8.35±0.87
XI: [3-ethyl-farnesyl]**a**-factor	4	48.9±5.1	11.4±1.2
XII: [3-*tert*-butyl-farnesyl]**a**-factor	2	17.9±1.8	31.0±3.1

[a] Growth arrest (halo)assay

[b] Values of M_{50} were determined by fitting data from binding experiments to equation 1. All data are averages of three measurements.

[c] Values of Kp were calculated from the values of M_{50} using equation 2.

The results indicate that **a**-factor partitions strongly into DMPC vesicles with a $K_p = 2.2 \times 10^{-4}$. The partitioning coefficients for the Pro^4 containing **a**-factor analogs were all approximately equal and were slightly lower than that of **a**-factor. [*D*-Ala^5]**a**-factor had approximately one half the membrane affinity of **a**-

factor for the artificial membranes. The membrane affinities of the farnesyl analogs where the position 3 is varied from methyl, ethyl, vinyl to *tert*-butyl were 2.2×10^{-4}, 1.1×10^{-4}, 0.84×10^{-4} and 3.1×10^{-4}, respectively. These results suggest that the affinities of these molecules do not correlate with their hydrophobicities.

CHAPTER IV DISCUSSION

Except for studies on pheromones from filamentous fungi (Fujino *et al.,* 1980; Koppitz *et al.,* 1996), almost no reports on structure-activity relationships between the secondary structure of farnesylated peptides and their biological activities have been published. The results reported here provide insights into both the relationship of the conformation of the peptide portion of **a**-factor and bioactivity, and also address the influence of the farnesyl moiety on biological activity and membrane partitioning, and the correlation of partitioning with biological activity.

The β-turn conformation has been reported to contribute significantly to the secondary structure of proteins and is often found in the biologically relevant structure of small peptides (Hruby, 1982). In our laboratory, two previous attempts have been made to constrain the turn region of **a**-factor. Replacement of Gly^5 with a *D*-Ala residue resulted in an agonist with 4-6 fold higher activity compared to wild type **a**-factor (Caldwell *et al.,* 1993). Incorporation of a (*R*)-γ-lactam in place of Lys^4Gly^5 led to a hyperactive agonist with 32-fold higher bioactivity (Zhang *et al.,* 1996). To further study the importance of Lys^4 Gly^5 we here present data on constrained analogs in which this sequence was replaced with *DIL* Pro^4-*LID*-Ala^5 or *DIL* Pro^4-Gly^5.

Based on a free energy analysis (Yan *et al.,* 1995), a *L*-Pro^4-*D*-Ala^5 or *L*-Pro^4-Gly^5 sequence may assume a type II β-turn, while a *D*-Pro^4-*L*-Ala^5 or *D*-Pro^4-Gly^5 sequence favors a type II' β-turn. As a control and to directly assess

the importance of the Lys^4 ε-amino group I also prepared [Nle^4]**a**-factor (Nle = norleucine which contains a side chain that is nearly isosteric to that of lysine but lacks the ε-amine). The results show that [Pro^4]**a**-factor and [Pro^4,*D*-Ala^5]**a**-factor both have the same activity as **a**-factor in a growth arrest assay, whereas the [*D*-Pro^4]**a**-factor and [*D*-Pro^4,Ala^5]**a**-factor have about 2% of the wild-type activity (Table 5). The [Nle^4]**a**-factor is nearly inactive. The very low activity of this nearly isosteric Lys replacement suggests that the Lys ε-NH_2 contributes significantly to the biological activity of the pheromone. Given this conclusion the high biological activities of [Pro^4]**a**-factor and [Pro^4, *D*-Ala^5]**a**-factor are striking as both lack the Lys side chain. It appears that the incorporation of sequences expected to favor a Type II β-turn can compensate for loss of the interaction between Lys and the pheromone receptor. In contrast similar sequences which would favor Type II' β turn cannot restore bioactivity. This result provides additional evidence that a Type II β turn near the center of **a**-factor is likely a structural requirement of the bioactive conformation of the pheromone. Interestingly, the more rigid β turn in [(*R*)-γ-lactam^{4,5}]**a**-factor results in a 32-fold increase in activity while the more flexible Pro-Gly and Pro-*D*-Ala sequences in compounds I and III just compensate for the loss of the ε-NH_2 group.

The CD analysis of the position 4,5 a-factor analogs in membrane mimetic environments (TFE/H_2O and DMPC vesicles) indicates that these peptides are predominantly disordered in both environments. Although weak minima are observed near 215 nm none of the patterns fit into any of the turn classes designated by Woody (Woody, R.W. 1974). In addition there is no clear

correlation between CD peak shape and biological activity since spectra were similar for compounds I-IV and different from those of **a**-factor and [*D*-Ala^5]**a**-factor. A shape analysis of the spectra for compounds I-IV is most consistent with type I(III) and II' turns which fall into a class C spectrum using the definitions of Woody (Woody, R.W. 1974). However, severe deviations from the standard spectra are found in the 195 to 210 nm range, and the ellipticities are much lower than expected. The presence of Tyr, Phe, and Trp residues in the peptides and the high flexibility of most residues in these molecules complicate spectral analysis. Prudence would suggest that the CD analysis does not distinguish important elements of the secondary structure which relate to biological activity. However it is clear that the distribution of Φ,Ψ angles sampled by peptides I-IV are different from those in the native **a**-factor. NOESY spectra of two model **a**-factor analog pheromones with conformational restraints in the center of the peptide are also indicative of the predominance of a structureless conformation of these position 4,5 a-factor analogs. Apparently the interaction with the receptor plays a very important role in selecting the biologically relevant structure of these pheromones.

The purpose of isoprenoid modifications is a basic question in the field of protein prenylation. Whether these additions serve to locate an attached peptide to membranes via lipid-lipid interactions, or bind to proteins through lipid-protein interactions has been a contentious issue (Zhang *et al.,* 1996; Marshall, 1993; Parish *et al.,* 1996; Schafer, *et al.,* 1992), and evidence to support several models can be found in the literature. To this end, I have also synthesized three

geometric isomers of the farnesyl moiety and examined the biological activities of the corresponding **a**-factor analogs in a well-characterized assay system. In comparison, the almost identical activity of geometrical isomers VI-VIII indicated that the geometry of the farnesyl group has little effect on the biological activity and is less important than the conformation of the peptide portion of this pheromone. Considering our previous results that subtle modifications of the 3-position of the farnesyl moiety significantly affected the bioactivity of the pheromone (Table 11), this result was unexpected, and inconsistent with a traditional tight ligand-receptor interaction. Instead, it indicates that the isomeric farnesyl moieties could adopt conformations that allow them to mimic the natural *trans,trans*-farnesyl moiety in the protein binding site. As an aside during this study it was demonstrated that ^{1}H NMR and HMQC experiments were useful methods for determination of the assignment of the geometry of the farnesyl group.

A previous fluorescence analysis of **a**-factor and **a**-factor analogs concluded that the role of the farnesyl was simply to partition the peptide into the membrane (Khouri, *et al.,* 1996). Similarly, a study of analogs of *Ustilago maydis* pheromones concluded that lipid modification increases the effective concentration of the pheromone in the target cell membrane without additional structure-inducing or receptor-binding effects (Koppitz, *et al.,* 1996). The data in Table 11 showed that the biological activities of a series of **a**-factor analogs in which the 3 methyl group of the farnesyl side chain was replaced with various groups (Dawe *et al.,* 1997). The biological activities of these analogs did not

correlate with their hydrophobicities. In the present chapter of this dissertation, in order to further assess the effect of these modifications on membrane affinity I used the fluorescence of Trp^8 to measure the partitioning into DMPC vesicles of compounds IX-XI (Figure 2) in which the methyl is replaced with vinyl, ethyl and *tert*-butyl. Concurrently we also determined whether constraint of the center of the peptide would influence membrane partitioning.

Based on the values of M_{50} and K_p determined by fluorescent spectroscopy, subtle modifications on the farnesyl moiety significantly affected the membrane binding: the more hydrophobic 3-*tert*-butyl derivative had a higher partitioning coefficient than the smaller 3-ethyl and 3-vinyl derivatives. Interestingly, **a**-factor with a 3-methyl farnesyl group also exhibited a higher partitioning coefficient than either the 3-ethyl or the 3-vinyl derivatives. Apparently modification of farnesyl affects the partitioning of the pheromone in a complex way. Perhaps there is a general effect of the overall lipid side chain and more localized effects that reflect not only the hydrophobicity of the 3 position substituent but also its size.

As judged by fluorescence techniques, the effect of peptide sequence modification on partitioning of **a**-factor into lipid vesicles is also complex. Replacement of Gly with *D*-Ala^5 results in a pheromone which exhibits nearly two-fold lower partitioning than the wild-type **a**-factor. Compounds I through IV show almost the same values of K_p, which are only slightly lower than that of **a**-factor. The partitioning coefficients do not correlate with bioactivities: compounds I through IV exhibit almost the same partitioning coefficient but very different

bioactivities, I and III have almost 100% of the activity of the wild type pheromone, while compounds II and IV have only 2% activity. The discrepancy between our findings and those previously reported (Khouri *et al.,* 1996) could reflect the different lipids used in the two studies. Nevertheless, our results indicate that simple partitioning into the membrane cannot explain the bioactivities of **a**-factor analogs. Other factors, such as specific lipid-lipid or lipid-protein interactions or stabilization of a specific pheromone conformation, may be important.

The isoprenylated cysteine residue has been suggested as an important potential mediator of protein-protein as well as protein-lipid interactions as various proteins shuttle between membrane and cytoplasmic compartments. One role of isoprenylation is to anchor proteins to membranes by hydrophobic interactions (Casey *et al.,* 1989; Nial, 1982; Schafer *et al.,* 1989). However, there are a number of reasons for thinking that lipid association may be only part of the way in which prenylated proteins bind to membranes. Several studies have demonstrated that the farnesyl group of Ras is required for its proper interaction with other proteins in the signal transduction pathway (Bhattacharya, *et al.,* 1995; McGeady, *et al.,* 1995), implying the involvement of prenyl-protein binding sites. In addition, the fact that prenyl cysteine analogs can block certain signal transduction pathways has been taken as evidence for prenyl binding sites on intracellular proteins (Ma, *et al.,* 1994; Niv, *et al.,* 1999; Scheer & Gierschik 1995;). Moreover, the determined structure of the rhoGDI protein clearly indicates an isoprene-binding site on this protein that interacts with the prenyl

group of the Rho protein (Gosser *et al.,* 1997; Keep *et al.,* 1997). More recently, Prendergast and co-workers have demonstrated that the biological activity of geranylgeranylated RhoB is significantly different from that of farnesylated RhoB, consistent with an active role for the prenyl group of this protein (Du *et al.,* 1999). Even in the absence of direct prenyl-protein binding (Siddiqui *et al.,* 1998), it appears that the prenyl group can direct an attached protein to a specific membrane type (Niv *et al.,* 1999), or even a specific location in the membrane (Melkonian, 1999).

CHAPTER V CONCLUSION

In conclusion, we successfully synthesized eight new **a**-factor analogs, purified them to homogeneity, characterized their structure, and used these analogs for bioassays and several spectroscopic methods to study the relationship of structure-activity and the interaction between pheromone and lipid vesicle. The results indicated that appropriate biological conformation and partitioning are both important for high activity, and they affect the activity in different ways. Moreover, the geometry of farnesyl group exhibits little effect on the bioactivity of **a**-factor suggesting that the isomeric farnesyl moieties may adopt conformations that allow them to mimic the natural *trans,trans*-farnesyl moiety in protein binding site. In addition, our results demonstrate for the first time an inverse relationship between the bioactivities and the partitioning coefficients for various **a**-factor analogs. These results are clearly incompatible with a simple hydrophobic model for isoprenoid function. Instead, they support an active involvement of the pheromone isoprenyl group in peptide-protein or peptide-lipid interaction that influences pheromone bioactivity.

The work outlined in this part of my thesis has resulted in the following publications:

a) Xie, H., Becker, J.M., Gibbs, R. A., and Naider, F. (2000) Structure, biological activity and membrane partitioning of analogs of the isoprenylated a-factor mating peptide of *Saccharomyces cerevisiae*. *J. Pep. Res. 55*, 372-383;

b) Xie, H., Becker, J.M., and Naider, F. (2000) The **a**-factor lipopeptide pheromone of *Saccharomyces cerevisiae:* Synthesis, bioactivity and biophysical analyses of positions 4,5 analogs. *Peptides: Proceedings of the 16th American Peptide Symposium.* pp 330-331.

c) Xie, H., Shao, Y., Becker, J.M., Naider, F. and Gibbs, R. A. (2000) Synthesis and preliminary biological evaluation of the geometric farnesylated analogs of the **a**-factor mating peptide of *Saccharomyces cerevisiae. J. Org. Chem.* In press.

PART II: SYNTHESIS AND BIOPHYSICAL CHARACTERIZATION OF DOMAINS OF α-FACTOR RECEPTOR

CHAPTER I INTRODUCTION

Background

All cells respond in a specific and highly regulated manner to signals from the external environment. One communication strategy involves signal transduction pathways which are cascades of highly regulated protein phosphorylations. In these elaborate sets of intracellular proteins interact and relay most signals from the cell surface to the nucleus where they alter gene expression and hence cell behavior. The first step is the detection of the signal molecule by a cell surface receptor, which is an integral membrane protein.

The largest family of these cell surface receptors is known as G protein (guanyl-nucleotide binding protein)-coupled-receptors (***GPCRs***). It is estimated that approximately 1000 ***GPCRs*** exist in mammals (Wess 1997). They receive and mediate the responses to a diversity of signals which include hormones such as epinephrine, glucagon and parathroid hormone, neurotransmitters such as acetylcholine and serotonin, light and olfactants (Wess 1997). This super-family of receptors transduces particular signals by coupling physically to their cognate hetero-trimetric G-proteins at the cytoplasmic face of the membrane. The protein-protein interaction activates the G-protein to commence intracellular signal transduction.

Although remarkably diverse in primary amino acid sequence, all ***GPCRs*** are characterized by a common molecular motif consisting of seven transmembrane domains (M1-M7) linked by alternating intracellular (I1-I3) and extracellular (E1-E3) loops (Dohlman *et al.,* 1991). The predicted topology is based on data from hydropathy analyses which have proven to be a very useful tool for obtaining tentative topological information on many transmembrane proteins hence revealing clues about their structure (Lehninger *et al.,* 1992). Based on a detailed analysis of sequence data of various G protein-coupled receptors, the arrangement of the seven transmembrane helices has been predicted to be counterclockwise beginning from helix one near the amino terminus and proceeding to the carboxyl terminus (Baldwin 1993). The structural model proposed by Baldwin is used by many workers as a point of reference in model building for particular ***GPCR*** structures and ligand binding sites. This novel study leads to a tentative three dimensional structure for the membrane embedded portion of all ***GPCRs***. The predicted conformation has a closely packed structure near the intracellular surface and a more open structure at the extracellular surface (presumably forming a ligand binding pocket). The helix-helix interactions and relative orientations predicted by this model have been supported by additional biochemical and genetic studies (Suryanarayana *et al.,* 1992; Lui *et al.,* 1995; Mizobe et al., 1995).

All transmembrane domains are believed to assume an α-helical secondary structure roughly perpendicular to the membrane, which is the most physically stable structure in the hydrophobic environment of the membrane

because of the extensive intra-helical hydrogen bonding. Direct biophysical evidence for this secondary structure comes from studies with rhodopsin, a G-protein coupled photoreceptor (Schertler *et al.,* 1993; Urger and Schertler 1995). Recently, detailed information on the 3D structure of an integral membrane protein was obtained from X-ray and electron microscopy analysis on bacteriorhodopsin. This protein has been crystallized and its structure is available at a resolution of 3Å (Pebay-Peyroula *et al.,* 1997; Grigorieff *et al.*, 1996, Kimura *et al.,* 1997). The analysis indicated that the protein has seven transmembrane domains, which are primarily α-helical and which are arranged in a compact, roughly elliptical, structure when viewed from above the plane of the membrane. Very recently, the structure of the ***GPCR*** rhodopsin was solved at 2.8Å resolution (Palczewski *et al.,* 2000).

The Ste2p receptor for α-factor, the mating pheromone of yeast *Saccharomyces cerevisiae*, belongs to the super family of ***GPCRs***, and also shares the hepta-helical structural theme (Burkholder and Hartwell, 1985; Nakayama *et al.,* 1985). Ste2p has a molecular weight of approximately 48-53 kD (431 residues plus some glycosylations within the first extracellular domains). It binds the pheromone α-factor, a 13-amino acid peptide of sequence WHWLQLKPGQPMY which is produced and secreted by the haploid α cell mating type of *Saccharomyces cerevisiae* (Blumer *et al.,* 1988). Ste2p is located on the surface of the haploid **a** cell mating type. When α-factor binds to Ste2p it induces a conformational change in the receptor that is required for G-protein coupling and hence subsequent intracellular signal transduction events. Figure

16 illustrates a cartoon representation of Ste2p. The approximate placement of the seven transmembrane domains (**TMs**) of Ste2p has been experimentally corroborated using gene fusion and protein reporter methodologies (Cartwright, C.P. and Tipper, D.J. 1991; Harley, C.A. and Tipper, D.J. 1996). Therefore, the yeast *Saccharomyces cerevisiae* provides an ideal model system for the study of pheromone-receptor interactions, and studies on the individual receptor should shed light on the structure of its related members of ***GPCR*** family.

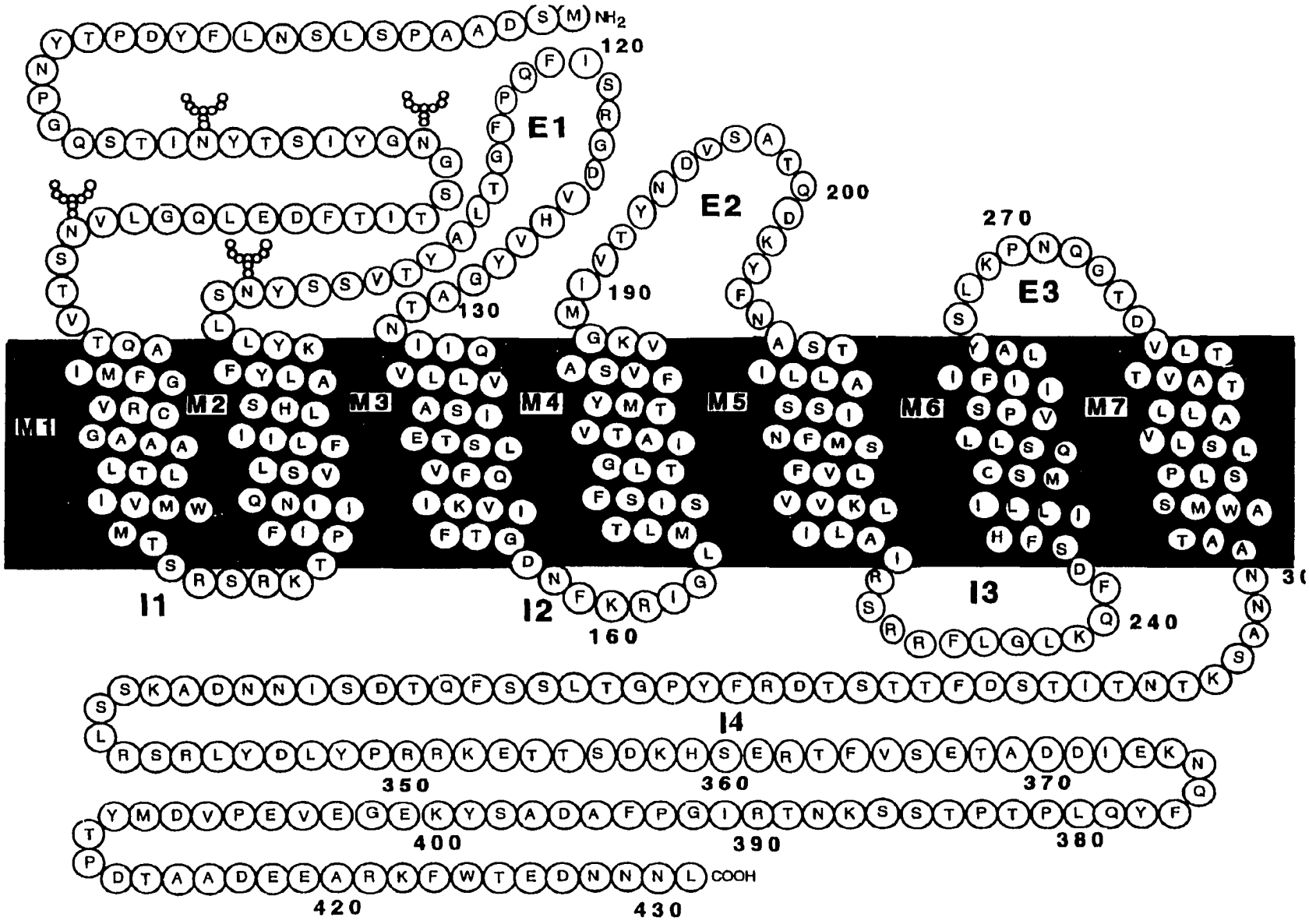

Figure 16. Cartoon representation of the α-factor receptor (Ste2p) Domains are indicated by the following: E: extracellular loops; I: intracellular loops; M: transmembrane domains. Four of the Asn residues are represented as glycosylation positions.

Objective and approach

Despite the elegant studies on bacteriorhodopsin and its G protein-coupled homolog, rhodopsin, very little information is available about the structure of other *GPCRs*. The pathway of folding of these molecules is also relatively virgin territory. Although various hydropathy algorithms are useful in placing putative transmembrane domains within the primary sequence of these receptors, direct evidence for either the authenticity of these placements or the stability of the domains is lacking. The difficulty in generating crystals of *GPCRs* suitable for X-ray crystallography has prevented the shaping of a high-resolution structure of *GPCRs*.

In order to elucidate the structure of *GPCRs*, biochemical and biophysical techniques have been applied to study individual TMs. This approach is based on a two-step model postulating that individual TMs are first inserted in the membrane followed by their association to form the mature tertiary structure (Popot, J.L. and Engelman, D.M. 1990). Recent studies of reconstitution of functional receptors from their noncovalently linked TM fragments in cell membranes strongly supported this model (Martin 1998; Martin *et al.,* 1999; Gudermann *et al.,* 1997; Ridge *et al.,* 1995 &1996; Schoneberg *et al.,* 1995; Lemmon *et al.,* 1994). This model has also been examined in detail with the chemically synthesized seven TMs of bacteriorhodopsin (Hunt *et al.,* 1997a&b). It was shown that five of the seven TMs formed stable α-helices in isolation, but two TMs did not. The authors concluded that the folding of α-helical membrane proteins might proceed spontaneously with the caveat that some TMs might

require external constraints such as links between helices, interactions with the rest of the protein, or involvement of cellular chaperones or translocases.

Experience with individual transmembrane domains suggests that they are highly insoluble and have marked tendencies to form intractable aggregates. Since short fragments of receptors are amenable to biophysical analysis using nuclear magnetic resonance techniques information concerning their structural tendencies and the relevance of these tendencies to the structure and function of the cognate integral membrane protein is highly desirable. An early report provided CD evidence that the sixth and seventh transmembrane domains of the α-factor receptor of *Saccharomyces cerevisiae* formed stable helices in trifluorethanol and trifluorethanol-water mixtures (Reddy *et al.,* 1993). Recently the detailed structure of the sixth domain was determined by NMR to contain a kink at a Pro residue predicted to be in the middle of the membrane (Arshava *et al.,* 1998). A detailed study on peptides representing the seven transmembrane helices of bacteriorhodopsin presented CD, IR, and proton-deuterium exchange data which indicated that the peptides corresponding to helices A-H of this protein had very different biophysical tendencies and structural stabilities (Hunt *et al.,* 1997). NMR studies of several cytoplasmic loops and the carboxyl terminus of rhodopsin suggested that these receptor domains were stabilized by short-range interactions and assumed secondary structures such as β-turns and α-helices (Dorey *et al.,* 1999; Yeagle *et al.,* 1997,1995). Very recently a high-resolution structure of a 15-residue portion of the sixth transmembrane domain of rhodopsin was reported (Chopra *et al.,* 2000)

As part of a continuous attempt to gain insight into the secondary structures of α-factor receptor TMs, Iplanned to carry out syntheses of four transmembrane peptides (M1-M4), which are predicted by hydropathy analysis to be the first through the fourth of seven transmembrane domains: M1 (44-77, C59A), M2 (74-108), M3 (132-160), and M4 (163-190) (Table 12). Unless indicated otherwise, the numbering system used in this thesis assigns the amine terminal residue (Met1) as position 1 and the carboxyl terminal residue (Leu431) as residue 431. The syntheses of M5 (198-235, M218Nle), M6 (239-269, M250Nle, C252A) and M7 (273-302) were previously reported (Xie *et al.,* 2000; Reddy *et al.,* 1994; Arshava *et al.,* 1998). I designed each polypeptide to include the entire transmembrane helix (Cartwright & Tipper, 1991) plus some portion of the flanking sequences (Figure 17). On the basis of our previous experience with polypeptides M5 and M6, I believed that the charge density of the transmembrane sequences is a crucial factor in determining the overall solubility properties of the highly hydrophobic polypeptides. To this end, most of the residues in the inter-helix loops on both sides of a given helix are included in the synthetic polypeptides in order to improve the solubility. For M3 and M4, the difficulty of solubility was so serious that I was unable to carry out efficient HPLC purification. Therefore, several artificial lysines with positive-charged side chain were added to both termini (Table 12). I reasoned that these would increase the solubility and decrease the aggregation of peptide chains. I started the synthesis with Fmoc-Gly-Wang resin, which is available with low loading. In the case of

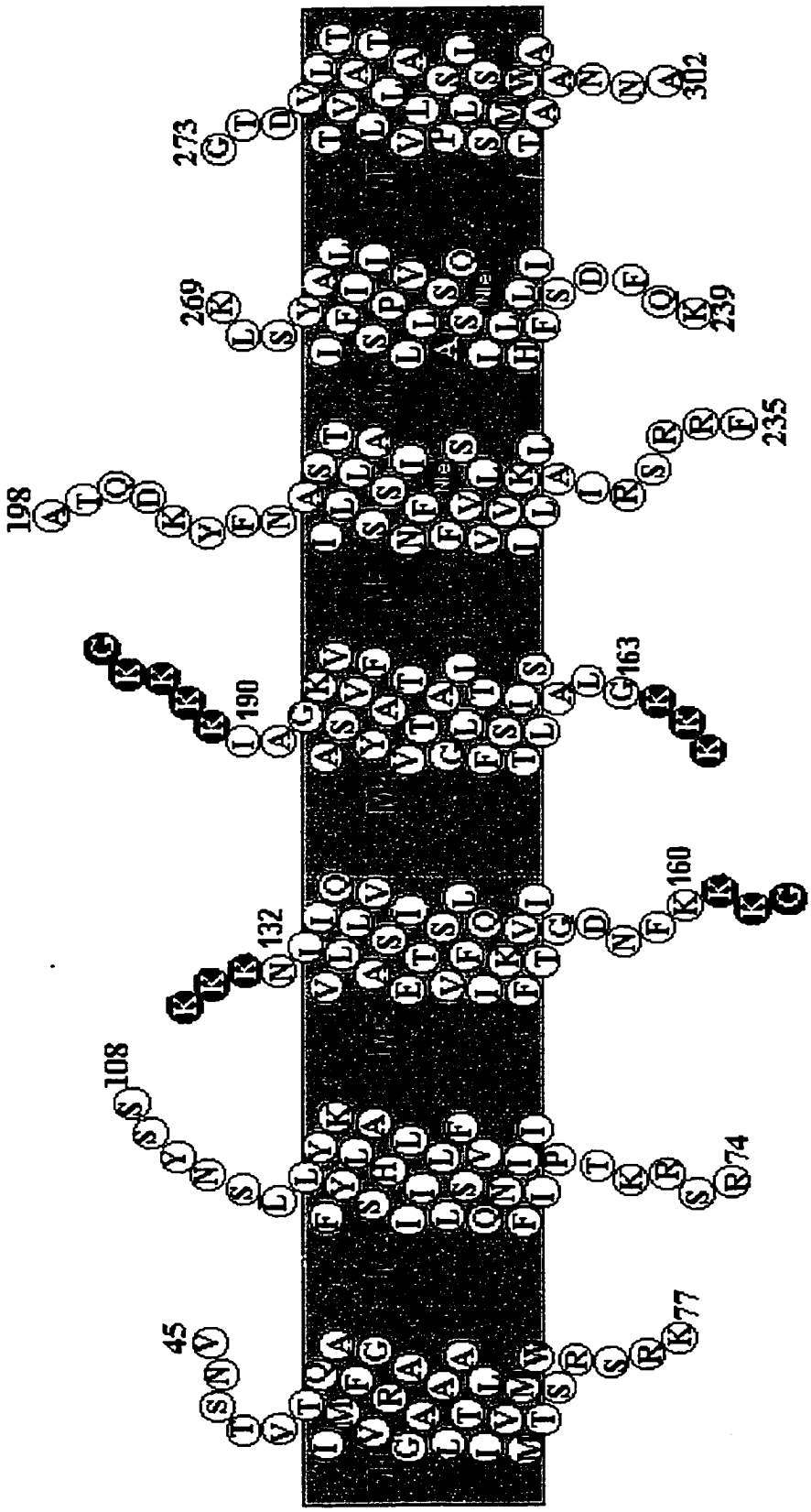

Figure 17 Synthetic fragments of Ste2p.

M1-33, Cys^{59} was replaced with Ala to eliminate synthetic problems from oxidation of Cys. Based on our previous studies on M6 and M7 (Reddy *et al.,* 1994; Arshava *et al.,* 1998), I believe that these mutations will not significantly change the secondary structure of M1. Moreover a mutant receptor with Met218 substituted by Leu had nearly full bioactivity (Arevalo, E., personal communication).

Another intriguing objective in this report is to provide direct biophysical evidence for the activation mechanism of ***GPCRs***. The current model of signal transduction by G protein-coupled receptors involves the isomerization of the receptor from an inactive to an active form (Hibert *et al.,* 1993; Lefkowitz *et al.,* 1993; Zhang and Weinstein, 1993). This model was supported by several elegant mutagenesis studies (Clark *et al.,* 1994; Weiner *et al.,* 1993; Stefan and Blumer, 1994). Support for receptor isomerization was forthcoming from a study which characterized a **mutant** receptor (**P258L**) that caused the receptor to be active in the absence of pheromone (Konopka *et al.,* 1996). It was suggested that the constitutive activity of the receptor might arise from a conformational transition in transmembrane domain 6, which may affect a change in the adjacent sequences in the third intracellular loop (I3 loop) that are thought to interact with the G-protein. Previously we have synthesized a 31-residue peptide, M6-31 (239-269, M250Nle, C252A) corresponding to this domain (Arshava *et al.,* 1998). However, the synthesis of the homolog M6-31L (239-269, M250Nle, C252A, P258L), which I believed could provide comparative information, failed due to

extreme aggregation. Based on the successful synthesis of M3 and M4, I thus designed and synthesized M6-35L (241-269, C252A, P258L) with hydrophilic residues (Lys and Ser) on both termini. To investigate if the additional residues affect the secondary structure of the peptide, a control peptide M6-35P (241-269, C252A) without mutation at position 258 was also prepared (Table 12).

Combined with M5-38, M6-31 and M7-30 (Table 12) previously synthesized in our lab (Xie *et al.,* 2000; Reddy *et al.,* 1994; Arshava *et al.,* 1998), I utilized CD to characterize secondary structures of all the synthetic membrane peptides in TFE/water, DMPC vesicles and SDS micelles. A 25-residue peptide [M2(84-108)] of the second transmembrane domain was selected as a representative segment and detailed NMR analysis was employed to define its secondary structure. In addition, fluorescence measurements were used to study the partitioning of M1 in phospholipid vesicles. Furthermore, I studied their oligomeric state and domain-domain interactions in SDS by Tricine-SDS-polyacrylamide gel (Tricine-SDS-PAGE).

Table 12. Sequences and Names of Transmembrane Peptides of Ste2p

Name[a]	Residue[b]	Sequence[c]
M1-33	45-77, C59A[d]	VNSTVTQAIMFGVR**A**GAAALTLIVMWMTSRSRK
M2-35	74-108	RSRKTPIFIINQVSLFLIILHSALYFKYLLSNYSS
M3-35	132-160	**KKK**NIIQVLLVASIETSLVFQIKVIFTGDNFK**KKG**
M4-36	163-190	**KKK**GLMLTSISFTLGIATVTMYFVSAVKGMI**KKKKG**
M5-38[e]	198-235, M218Nle[d]	ATQDKYFNASTILLASSINF**Nle**SFVLVVKLILAIRSRRF
M6-31[e]	239-269, M250Nle, C252A	KQFDSFHILLI**Nle**S**A**QSLLVPSIIFILAYSLK
M6-35L	241-269, P258L, C252A	**KKK**FDSFHILLIMS**A**QSLLV**L**SIIFILAYSLK**KKS**
M6-35P	241-269, C252A	**KKK**FDSFHILLIMS**A**QSLLVPSIIFILAYSLK**KKS**
M7-30[e]	273-302	GTDVLTTVATLLAVLSLPLSSMWATAANNA

a. M: transmembrane; the first follows the order of the transmembrane domains in the receptor, the second number represents the total number of residues in the peptides.

b. The numbering system assigns the amine terminal residue (Met1) as position 1 and the carboxyl terminal residue (Leu 431) as residue 431.

c. The bold and underlined represent artificial or mutant residues.

d. The letters in front of the number represent original residues, and those behind mutant ones.

e. Previously synthesized compounds (Xie *et al.*, 2000; Reddy *et al.*, 1994; Arshava *et al.*, 1998).

CHAPTER II EXPERIMENTAL PROCEDURES

Materials

Wang resin and Fmoc protected amino acids were purchased from Advanced ChemTech (Louisville, KY) except Fmoc-His (Trt) from Calbiochem-Novabiochem Corp. (San Diego, CA) and Bachem Inc. (Torrance, CA). HBTU, HOBt and NMP were purchased from Advanced ChemTech. SDS was purchased from Aldrich Chemical Co. (Milwaukee, WI).

Synthesis of Membrane Peptides

The peptides synthesized in this report are predicted by hydropathy analysis to be the first through the fourth of seven transmembrane domains: M1(44-77), M2(74-108), M3(132-160), and M4(163-190). The syntheses were carried out using solid-phase procedures as reported previously (Reddy *et al.* 1994). All peptides were synthesized in a stepwise manner on a 0.1 mmol scale using an Applied Biosystems Inc. Model 433A synthesizer. The coupling strategy utilized FastMoc chemistry. Double couplings were carried out for each residue using HBTU/HOBt activation and capping was accomplished with acetic anhydride in presence of DIEA. The Fmoc group was used for protection of all N-α groups, and Boc, Trt, Trt, tBu, tBu, tBu, Pmc were employed for protection of Lys, Gln, His, Ser, Tyr, Asp and Arg respectively. All Fmoc groups were deprotected in 20% piperidine in NMP. After completion of chain assembly the Fmoc group was deprotected and the resin was treated with either a cocktail

composed of 0.75 g phenol, 0.5 ml thioanisole, 0.25 ml EDT, 0.5 ml water and 10 ml TFA when the peptide contained Arg or Met, or a cocktail composed of 9.5 ml TFA, 0.25 ml EDT, and 0.25 ml water when the peptide contained neither Arg nor Met but contained Trt or Trp. The reaction was carried out at room temperature for 1-2 hours, the reaction mixture was filtered and the filtrate was concentrated to a small volume on a rotatory evaporator. The crude peptides were precipitated by addition of anhydrous ether.

Purification of Membrane Peptides

For peptides with less than 20 residues, reversed phase HPLC (RP-HPLC) was performed on a Waters system. Analytical HPLC was run on a Waters μ-Bondapak-C_{18} column (3.9x300 mm) and all peptides were eluted with either a water/acetonitrile (both containing 0.025%TFA) or a water/methanol (both containing 0.025%TFA) linear gradient. Preparative HPLC was run on a Waters μ-Bondapak-C_{18} column (19x300 mm or 19x150 mm) using a linear gradient of water (0.025%TFA) and acetonitrile (0.025%TFA). Detection was at 220 nm and/or 275 nm. All peptides were purified to over 99% homogeneity as judged by RP-HPLC.

For peptides with more than 20 residues, reversed phase HPLC (RP-HPLC) was performed on a Vydac system. Analytical HPLC was run on a Vydac 259VHP54 polymer column (4.6x250 mm) at 80 ^{0}C and all peptides were eluted with either a water/acetonitrile or a water/methanol (all containing 0.1%TFA) linear gradient. Semipreparative HPLC was run on a Vydac 259VHP510 polymer

column (10×250 mm) with a water jacket, using a linear gradient of either water/acetonitrile or water/methanol (all containing 0.1%TFA) at 55-65^{0}C. Detection was at 220 nm. All peptides were purified to over 95% homogeneity as judged by RP-HPLC. The final products were assessed by electrospray mass spectrometry (ES-MS) and amino acid analysis. The molecular weights were in agreement with the calculated molecular weights for each peptide, and the discrepancies between observed and calculated *m/z* values were usually within +2. ES-MS was performed at Peptido Genic Research & Company, Livermore, CA. Amino acid analyses were performed at the Biopolymer laboratory Brigham and Women's Hospital of Harvard Medical School after acid hydrolysis with 6N HCl for 72 hours at 110°C.

Sample Preparation

Buffers MES buffer contained 10 mM MES, adjusted to pH 6.4 with KOH. SDS buffer contained 0.5% SDS (w/v), 30 mM $NaHPO_4$, 0.025% NaN_3, pH 8.0

(1) In SDS buffer

The lyophilized peptide was dispersed at 2 mg/ml in TFE; this solution was diluted with 9 vol. of 0.5% SDS (w/v) prior to the initiation of dialysis against buffer. Dialysis was performed in Spectrapor 6 dialysis tubing (MWCO 1000). The volume of the dialysis buffer was at least 200-300 times that of the hydro-organic mixture, and the buffer was changed twice during a total period of 48-72 h dialysis. The buffer had a pH =8.0 for the initial round of dialysis and a pH =6.0 for the subsequent two rounds.

(2) In DMPC vesicles

To 100 μl of stock peptide solution (0.6 mg/ml TFE) was added 1.2 mg of DMPC in 300 μl of chloroform. The solvent was removed by rotary evaporation under a stream of nitrogen, and the residue was placed in a vacuum desiccator for several hours to eliminate traces of solvent. The lipid was hydrated with 0.5 ml MES buffer and vortexed for 1 min and sonicated at 30^{0}C until homogeneity and transparency were obtained. In the case of M1, a modified procedure was used because of the failure to obtain a clear suspension: To the hydrated lipid suspension without peptide, 50 μl of TFE was added and the resultant solution was sonicated at 30^{0}C until homogeneity and transparency were obtained. This suspension was finally dialyzed with MES buffer for 3 days. The volume of the dialysis buffer was at least 200-300 times that of the mixture, and the buffer was changed twice.

Circular Dichroism Spectroscopy of Membrane Peptides

(1) Spectroscopic measurements

The CD spectra of the peptides were recorded on an AVIV model 62 DS CD instrument (AVIV Associates, Lakewood, NJ), which was interfaced with a computer used for all mathematical calculations. A 1 mm sample cell with a thermostated cell holder, was used for all spectral studies. Bandwidth: 1nm; Averaging time: 0.5 sec. Repeat 6 times. Peptide concentrations in solution were determined from amino acid analysis. Prior to calculation of the final ellipticity, all

spectra were corrected by subtracting the reference spectrum. CD intensities are expressed as mean residue ellipticities (deg•cm^2/dmol).

(2) Estimation of percent α-helicity

Estimation of percent α-helicity was made using a method initially suggested by Greenfield and Fasman (1969) and later modified by Wu, *et al.* (1981) and Chen *et al.* (1979). These methods use ellipticities at either 208 or 222 nm and calculate fractional helicities as follows:

$$f_h = ([\theta]_{222} - [\theta]^0_{222}) / ([\theta]^{100}_{222} - [\theta]^0_{222}) \quad (A)$$

$$f_h = ([\theta]_{208} - [\theta]^0_{208}) / ([\theta]^{100}_{208} - [\theta]^0_{208}) \quad (B)$$

Where $[\theta]_{222}$ is the experimentally observed mean residue ellipticity at 222 nm, and values for $[\theta]^0_{222}$ and $[\theta]^{100}_{222}$, corresponding to 0 and 100% helical content at 222 nm, were estimated to be 2000 and 30,000 deg•cm^2/dmol, respectively (Wu *et al.,* 1981; Chen *et al.,* 1979). When the wavelength used is 208 nm, the 0 and 100% helicities were 4000 and 33,000 deg•cm^2/dmol, respectively (Greenfield and Fasman, 1969)

(3) Thermal stability studies

Conformational transitions of transmembrane peptides in SDS buffer were followed by CD spectroscopy using stepwise heating from 25 ^{0}C to 85 ^{0}C. During stepwise heating, samples were heated at increments of 10 ^{0}C and were then incubated at constant temperature for 5 min before spectra were recorded.

NMR Spectroscopy of M2-25 in TFE/Water

^{1}H-nmr spectra were recorded on UNITY INOVA 600 Varian spectrometer. 1.9 mg of M2-25 was dissolved in an organic mixture of trifluoroethanol/water[TFE/water, (4:1 v/v)]. The water suppression was achieved with a standard presaturation pulse sequence. Proton signal assignments were made using total correlation spectroscopy (TOCSY) spectra with contact times of 80 ms and aided with sequential connectivities determined from nuclear Overhauser effect spectroscopy (NOESY) spectra. Medium and long-rang interresidue connectivities were found by NOESY spectra at a 300 ms mixing time.

Fluorescence Quenching of M1-33 in vesicle or methanol by KI

(1) Preparation of Lipid-Peptide Vesicles

To 100 μl of M7-30 solution (1 mg /ml TFE) was added a solution of 1 mg of DMPC in 0.5 ml of chloroform. The resulting solution was dried under N_2 flow. Residual traces of organic solvent were removed by placing the dried film under vacuum overnight and the lipid was hydrated in 10 ml MES buffer (10 mM, pH 6.3). The suspension was sonicated at approximately 50°C for 60 min in a Misonix Inc. W-385 sonicator equipped with a cup horn. The resulting vesicles were then passed through a 0.45 μM polycarbonate filter. The molar ratio of peptide was 1:500.

(2) Fluorescence Spectroscopy

Fluorescence measurements were recorded using a Spex Fluoromax (Instrument S.A. Inc., Edison, NJ) with a 1 x 1 cm quartz cuvette. Two ml of sample volume was stirred continuously with a magnetic bar. The emission spectra were scanned between 300 and 420 nm with an excitation wavelength of 280 nm at intervals of 1 nm with 1 s integration time at each wavelength. Both the excitation and emission bandwidths were 3 nm. The fluorescent intensities, calculated by integration within the emission range, minus the intensities of control buffer alone (vesicle or methanol) at appropriate KI and KCl concentrations were used to calculate the quenching constants. Each data point was averaged from three independent measurements.

(3) Collisional Quenching Experiments

The lipid-peptide vesicle solution was stirred in a cuvette for 30 min. Fluorescence collisional quenching experiments with iodide were performed by sequentially adding a 4 M KI solution in 10 mM MES buffer to a final concentration of 56 mM. After addition of the peptide the solution was allowed to equilibrate for 5 to 10 minutes and the fluorescence was measured. Changes in fluorescence due to the addition of quencher were corrected by subtracting the fluorescence measured in the DMPC vesicle control. The quenching constant of the fluorescence emission at the maximum wavelength (342 nm) was calculated with the Stern–Volmer equation:

$$F_0/F = 1 + K_{sv}[I^-] \qquad (1)$$

Where F_0/F is the ratio of fluorescence intensities in the presence of KCl and KI. The Stern-Volmer quenching constant K_{sv} was determined from the slope of F_0/F as a function of the iodide concentration [I^-].

Tricine-SDS Polyacrylamide Gel Electrophoresis

Electrophoresis in polyacrylamide gels in the presence of sodium dodecyl sulfate (SDS), an anionic detergent, is useful for separating protein subunits and determining their molecular weights. The molecular weight of a protein can be determined by comparing its electrophoretic mobility with those known protein markers. An approximately linear relationship is obtained if logarithms of the molecular weights of standard polypeptide chains are plotted against their respective electrophoretic mobilities.

The oligomeric state of synthetic transmembrane peptides and their interactions in SDS were investigated by gel electrophoresis. The buffer system of Schagger and von Jagow (1987), was employed. Briefly, peptides dissolved in 0.5% (17 mM) SDS and 3 mM phosphate buffer (pH 6.0) were diluted 1 fold with 1× SDS loading buffer containing the tracking dye Serva Blue G. Samples were heated at 50°C for 3 min and centrifuged, and then loaded onto a 27.7 % polyacrylamide-Tricine-SDS gel and separated at a constant 120 V. After gel electrophoresis, the gel was placed in the BIO-RAD fixative enhancer solution (containing 50% methanol, 10% acetic acid, 10% fixative enhancer concentrate and 30% distilled water), and fixed with gentle agitation for 20 min. Peptides were visualized by staining with either Commassie blue or silver.

CHAPTER III EXPERIMENTAL RESULTS

Synthesis and Purification of Membrane Peptides

All putative TM peptides examined in this study were prepared using solid phase peptide chemistry. New peptides were synthesized on a Wang resin using α–Fmoc protection strategies and HBTU/HOBT activation. Since membrane peptides usually contain a predominance of hydrophobic amino acid residues, growing peptide chains which are built up on the resin matrix can form secondary structures or aggregate either with other peptide chains or with the polymer support. Also, the formation of certain secondary structures (in particular β-sheets) leads to incomplete solvation and therefore inefficient penetration of the reagents through the resin beads (Kent *et al.,* 1992). Moreover, difficulty is encountered during analytical and preparative HPLC of membrane peptides due to their insolubility in the mobile phases, tendency to precipitate, and irreversible adsorption to the column material. It was found that each transmembrane domain peptide behaved differently, making it difficult to develop a universal approach during purification. Thus different procedures were applied to each individual peptide using some of the approaches described below. In general the syntheses of M1-33, M2-35 and M5-38 were less problematic than those of M3-35 and M4-36. After cleavage from the resin these latter peptides were almost insoluble and several additional flanking lysines had to be added to both termini to achieve dissolution in solvents which were suitable for HPLC purification. In general, the order of synthetic difficulty with the transmembrane domains of Ste2p was M3-35/M4-36 >M1-33/M5-38>>M2-35.

To aid the readers, M2 was chosen as a representative example since the synthetic strategy for these transmembrane peptides is similar. The synthesis of M2 was performed in a stepwise manner. After each synthesis, a small amount of peptide was cleaved from the resin and purified in order to test its purity by HPLC and mass spectrometry. If the results agreed with theoretical calculations, I continued the step-wise manner of the synthesis with 5-10 residues added each time. Table 13 summarized MS results of synthetic fragments of M2-35. Figure 18 illustrates HPLC spectra of these fragments.

Table 13 MS results of synthetic fragments of M2

Symbols	Peptide sequence	ES-MS
M2-10: M2(99-108)	F^{99}KYLLSNYSS^{108}	Found: 1220.84 Calculated: 1220.61
M2-16: M2(93-108)	L^{93}HSALYFKYLLSNYSS^{108}	Found:1906.04 Calculated:1904.97
M2-20: M2(89-108)	F^{89}LIILHSALYFKYLLSNY SS^{108}	Found: 2391.88 Calculated: 2391.29
M2-25: M2(84-108)	N^{84}QVSLFLIILHSALYFK YLLSNYSS^{108}	Found 2933.73 Calculated: 2932.57
M2-35: M2(74-108)	R^{74}SRKTPIFIINQVSLFLIIL HSALYFKYLLSNYSS^{108}	Found :4146.97 Calculated: 4144.22

In the purification step, traditional RP-HPLC based on either a C_{18} or C_4 column doesn't work on peptides with more than 20 residues because of their high hydrophobicity and tendency to aggregate. I chose a novel type of column

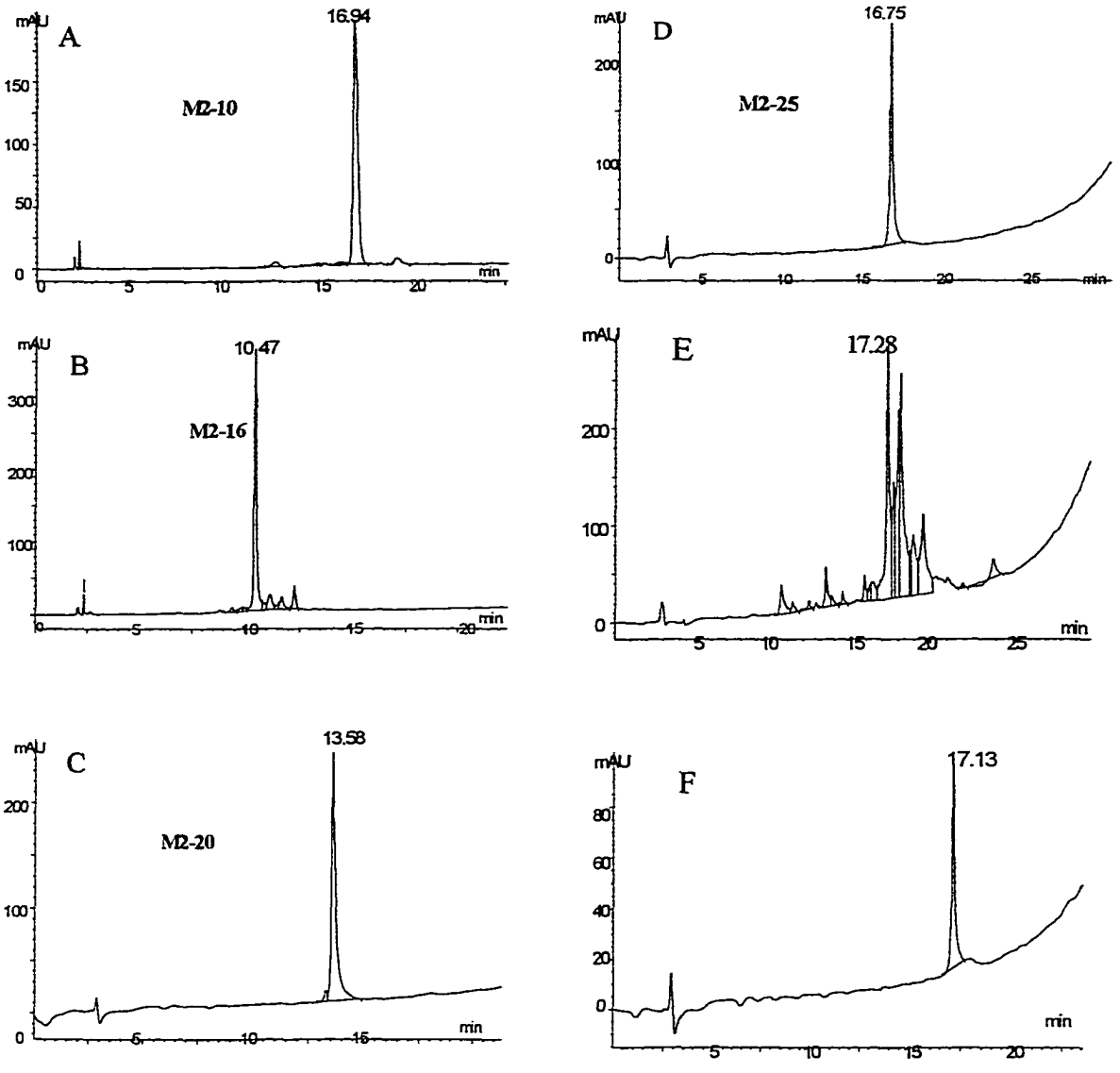

Figure 18 HPLC spectrum of fragments of M2-35. (A) crude M2-10; (B) crude M2-16; (C) purified M2-20; (D) purified M2-25; (E) crude M2-35; (D) purified M2-35. (A)-(C): Waters μ-Bondapak-C_{18} column (3.9x300 mm) at 25 ^{0}C; (D)-(F): 259VHP54 polymer column (4.6x250 mm) at 80 ^{0}C.

from Vydac company, termed Vydac polymer 259VHP RP column. The column material consists of a highly cross-linked polystyrene-divinylbenzene polymer in the form of rigid, porous (300 Å pore diameter) spheres. The 259VHP polymer matrix is chemically resistant to acid and alkali from pH 0 to 14, is heat stable up to 80 ^{0}C, and can be operated at pressures up to 3000 psi. Using this column, the M1–M4 transmembrane domains were purified to >98% homogeneity as evidenced by analytical RP-HPLC (Figure 19). Peptides gave the molecular weights within 0.1% of calculated values as judged by electrospray mass spectrometry (Table 14). The amino acid ratios were also consistent with the composition of the transmembrane peptides except for low Ser and Thr values, which we have observed before and I believe are due to degradation of the extremely hydrophobic peptides (Arshava *et al.,* 1998). The presence of intact Trp was verified by absorption measurements (Table 14).

During the purification of the membrane peptides, I also noted that the purification yields using this novel polymer-based column are dependent on a variety of factors such as temperature, elution solvents, flow rate and gradient. Figure 20 illustrates the effect of temperature on the purification of M1-33: the intensity ratio of the peak at about 10 min to that at about 14 min decreases with the increasing temperature, which indicates that heating can decrease the aggregation and improve the purification recovery (Figure 20). Therefore RP-HPLC was carried out above room temperature, usually at 80 ^{0}C for analysis and 65 ^{0}C for purification.

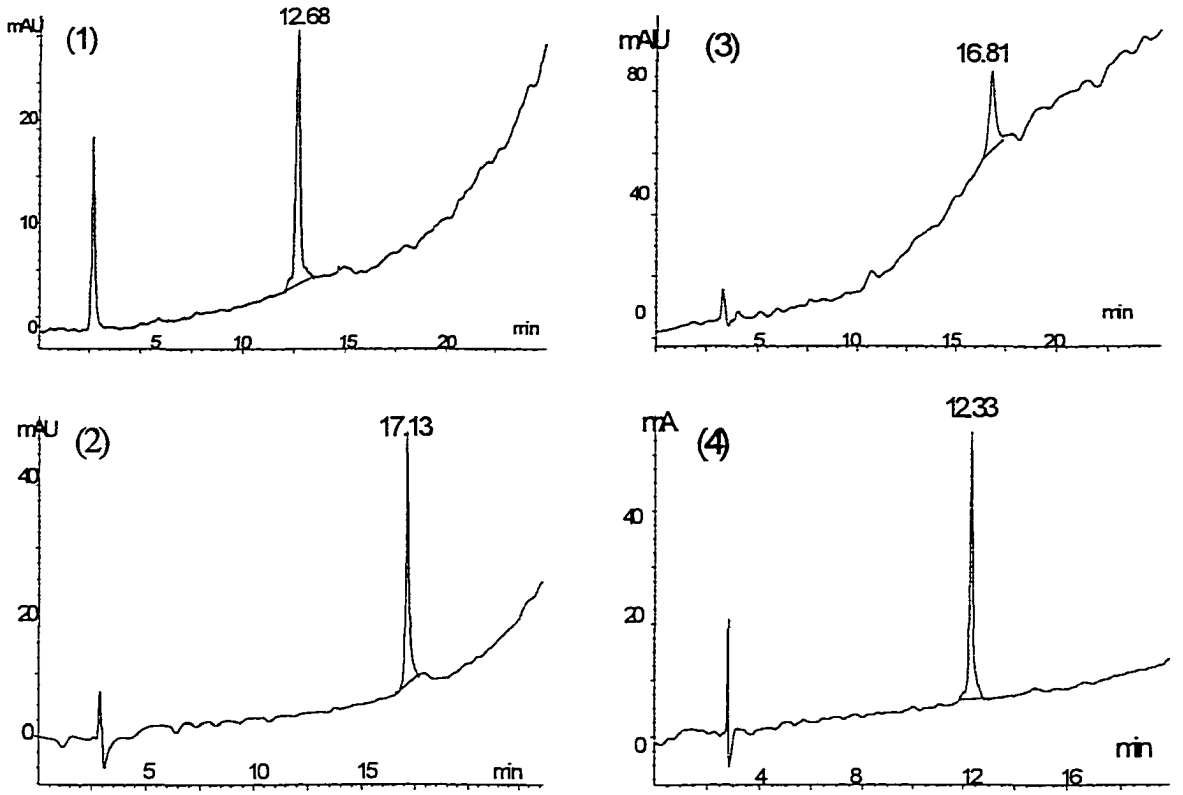

Figure 19. HPLC spectra of purified membrane peptides. (1) M1-33; Gradient: 20%-80% B in 20 min. A: water (0.1% TFA) B: acetonitrile (0.1% TFA); (2) M2-35. Gradient: 10%-100% B in 20 min. A: water (0.1% TFA) B: acetonitrile (0.1% TFA); (3) M3-35. Gradient: 40%-100% B in 30 min. A: 5% MeOH (0.1% TFA) B: MeOH (0.1% TFA); (4) M4-36. Gradient: 20%-80% B in 20 min. A: water (0.1% TFA) B: acetonitrile (0.1% TFA). Vydac 259VHP54 polymer column (4.6×250 mm); λ=220 nm, Temperature = 80 ^{0}C.

Table 14 Chemical Characterization of Transmembrane Domains of Ste2p

Name	Primary Sequence[a]	MS[b]	Amino Acid analysis
M1-33	VNSTVTQAIMFGVR**A**GAAALTLIV	3567.58	A(5)4.99,R(3)3.27,N(1)0.93, Q(1)1.06,G(2)2.04,I(2)1.93, L(2)2.30,
	MWMTSRSRK	(3565.90)	Lys(1) ,M(3)2.63, P(1)1.09, S(3)0.96,T(5)2.18, V(4)3.74, W(1)*ND*[c]
M2-35	RSRKTPIFIINQVSLFLIILHSALYFK	4146.97	A(1)1.20,R(2)1.82,N(2)2.03,Q(1)1.14,H(1) 1.17, I(5)4.41, L(6)6.67,
	YLLSNYSS	(4144.32)	K(2)2.19, P(1)0.97,F(3)3.11, S(6)1.05,T(1)0.45, Y(3)2.32,V(1)1.02
M3-35	**KKK**NIIQVLLVASIETSLVFQIKVIFT	3948.47	A(1)1.09,D&N(3)3.02,E&Q(3)3.38, G(2)2.24,I(5)4.22, L(3)3.05,
	GDNFK**KKG**	(3946.34)	K(7)6.79,F(3)3.15, S(2)0.45,T(2)1.09,V(4)4.06
M4-36	**KKK**GLMLTSISFTLGIATVTMYFVS	3907.08	A(2)2.33, G(4)4.15, I(3)2.88, L(3)2.67, M(3)2.79 K(8)7.79, F(2)2.02,
	AVKGMIK**KKKG**	(3904.25)	S(3)0.75,T(4)2.14, Y(1)1.00,V(3)3.36
M6-35P	**KKK**FDSFHILLIMS**A**QSLLVPSIIFIL	4007.6	A(2)2.46, D(1)0.85, H(1)0.88, I(5)4.64, L(6)6.47, K(6)5.45, M(1)0.89,
	AYSLK**KKS**	(4006.35)	Q(1)1.14, F(3)2.84, P(1)1.21, S(6)1.32, Y(1)0.95, V(1)1.21
M6-35L	**KKK**FDSFHILLIMS**A**QSLLV**L**SIIFIL	4024.5	A(2)2.46, D(1)1.05, H(1)0.99, I(5)4.54, L(7)7.70, K(6)5.53, M(1)0.86,
	AYSLK**KKS**	(4022.38)	Q(1)1.22,F(3)2.38, S(6)1.43,Y(1)0.97, V(1)1.18, W(1) *ND*[c]

a. The bold and underlined residues are additional or mutated residues.

b. Values in parentheses are calculated ones. Experimental values were from electrospray mass spectroscopy.

c. ND: Not determined

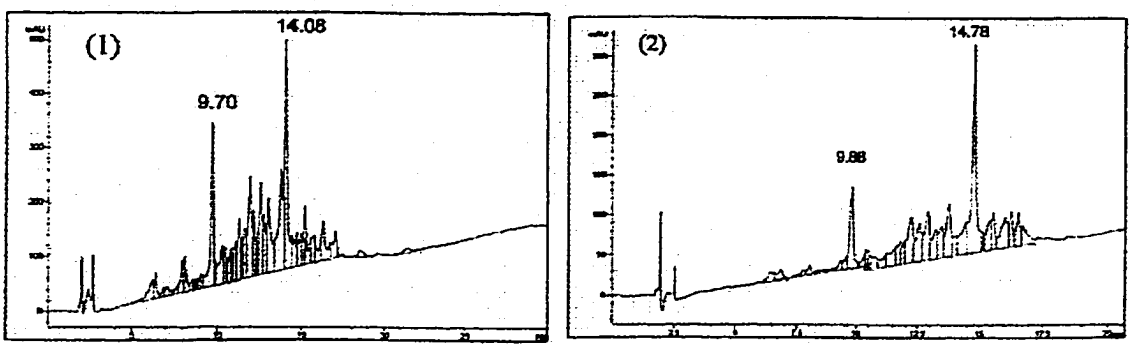

Figure 20 The effect of temperature on the purification of M1-33 (1) at 25 ^{0}C and (2) at 80 ^{0}C. Gradient: 90%A-100% B in 30 min. A: water (0.1% TFA) B: acetonitrile (0.1% TFA).259VHP54 polymer column (4.6×250 mm); λ=220 nm.

Figure 21 illustrates the effect of elution solvent on the purification of M3-35: a poor separation observed using an acetonitrile/water gradient was significantly improved in a methanol/water gradient. Other more denaturing systems including the use of inorganic or organic salts have also been shown to reduce aggregation and lead to marked improvements in the HPLC profile of the crude peptide (Chen *et al.*, 1999). However, I did not wish to have to desalt the peptides and were concerned about the effect of the salts on the HPLC column and equipment at the elevated temperatures I used. Therefore, this issue was not explored in detail. Figure 22 illustrates the effect of flow rate on the purification of M4-36: a higher yield indicated by a higher intensity of the major peak was obtained by a lower flow rate.

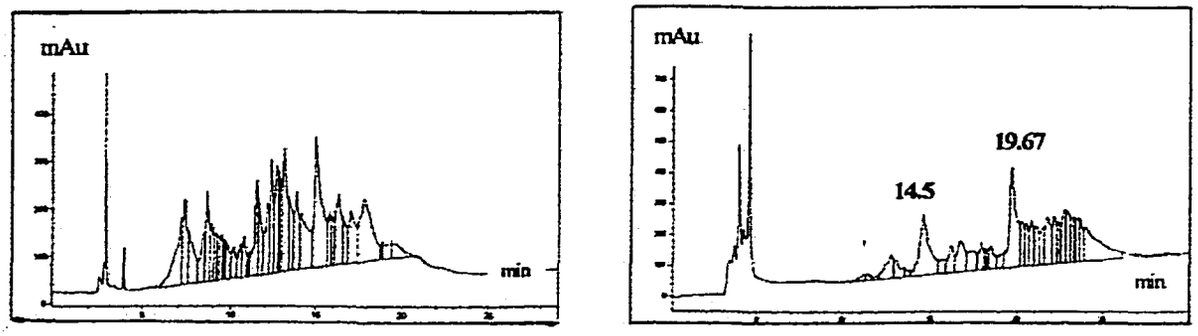

Figure 21 Effect of gradient composition on HPLC profiles of crude M3-35. Vydac 259VHP54 polymer column (4.6×250 mm). **Left**: 90%A-0% A in 30 min. A: Water (0.1% TFA) B: CH_3CN (0.1% TFA); **Right**: 70% A-0% A in 30 min. A: 5% CH_3OH/ 95% water (0.1% TFA) B: CH_3OH (0.1% TFA).

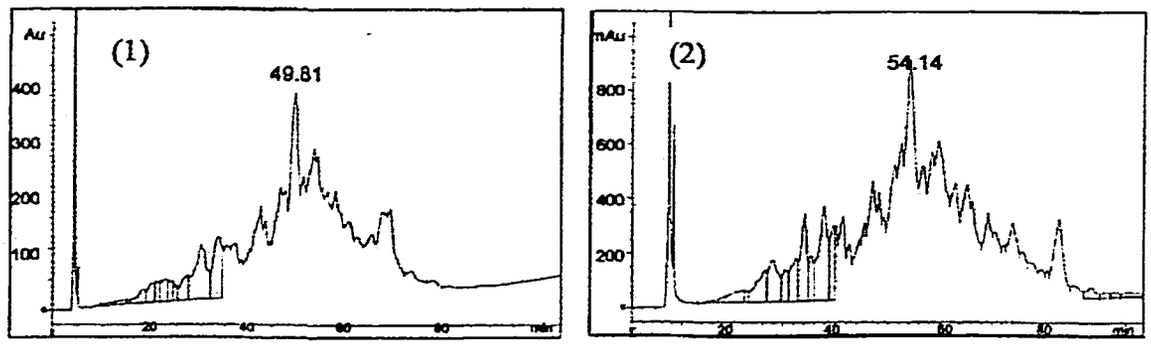

Figure 22 The effect of flow rate on the purification of M4-36: (1) **4 ml/min;** (2) **2.5 ml/min.** Gradient; 90%A-80% B in 120 min. A: H_2O (0.1% TFA) B: MeCN (0.1% TFA), λ=220 nm; 259VHP54 polymer column (10×250 mm) at 65 ^{0}C. Sample preparation: 8.0 mg crude dissolved in 0.5 ml TFE.

Secondary structures determined from CD spectroscopy

The shape and intensity of the CD spectrum between 180 and 240 nm is extremely sensitive to protein secondary structure. As the Ste2p receptor protein is localized to the plasma membrane in *Saccharomyces cerevisiae*, the seven TM peptides were analyzed by CD in membrane mimetic solvents including aqueous TFE, SDS buffer, and DMPC vesicles.

Quantitative analysis of the α-helicities in these CD spectra were carried out using Equation A and B as described in chapter II. Although more sophisticated algorithms for deconvoluting CD spectra are available, most of these have not been optimized for membrane proteins. Attempts to apply several algorithms such as Contin and PROSEC to deconvolute the CD spectra of the transmembrane peptides failed to give meaningful results in that negative percentages were calculated for certain secondary structures. Others have noted difficulty in the application of these algorithms to membrane peptides (Hunt *et al.*, 1997). I believe that $[\theta]_{222}$ approximation is sufficient for the comparative purpose of this study, and the results on the seven transmembrane domains of Ste2p are summarized in Table 15. It should be noted that calculations based on the mean residue ellipticity at 222 nm will not be significantly affected by the presence of His residue (e.g. in M2-35), since the contribution of the imidazole chromophores to the CD spectrum at 222 nm is negligible (Grebow and Hooker, 1975; Zieglar and Bush, 1971).

Table 15 Summarized data of helical contents for the seven Ste2p fragments

Peptides	TFE/water				0.5%	3.6 mM
	100%	75%	50%	25%	SDS	DMPC
M1 A[a]	73%	70%	64%	54%	78%	67%
B[a]	81%	76%	70%	58%	82%	63%
M2 A[a]	84%	77%	72%	64%	54%	46%
B[a]	84%	77%	72%	66%	46%	43%
M3 A[a]	77%	78%	82%	68%	/[b]	/[b]
B[a]	84%	85%	90%	74%	/[b]	/[b]
M4 A[a]	92%	91%	86%	80%	85%	77%
B[a]	96%	92%	87%	81%	84%	59%
M5 A[a]	73%	66%	64%	60%	52%	45%
B[a]	74%	66%	64%	59%	43%	/(16%)
M6 A[a]	61%	47%	48%	29%	/[b]	/[b]
B[a]	68%	51%	52%	31%	/[b]	/[b]
M7 A[a]	80%	62%	58%	48%	39%	41%
B[a]	91%	72%	67%	56%	43%	42%

a. A: calculation based on ellipticities at 222 nm; B: calculation based on equation ellipticities at 208 nm. (see chapter II for details).

b. /: Not determined due to low α-helicity.

(1) CD spectra of M1 through M7 in TFE/water

The CD spectra of the seven transmembrane peptides in TFE/water from 100% TFE to 50% TFE are all characterized by double minima at 222 nm and 208 nm and a ratio of the magnitude of the molar ellipticity at 195 *vs* 222 nm greater than or equal to 2:1 (Figure 23). These characteristics are expected for peptide chains in primarily α-helical conformations (Johnson 1988). Despite the similarities the different transmembrane peptides in TFE exhibit

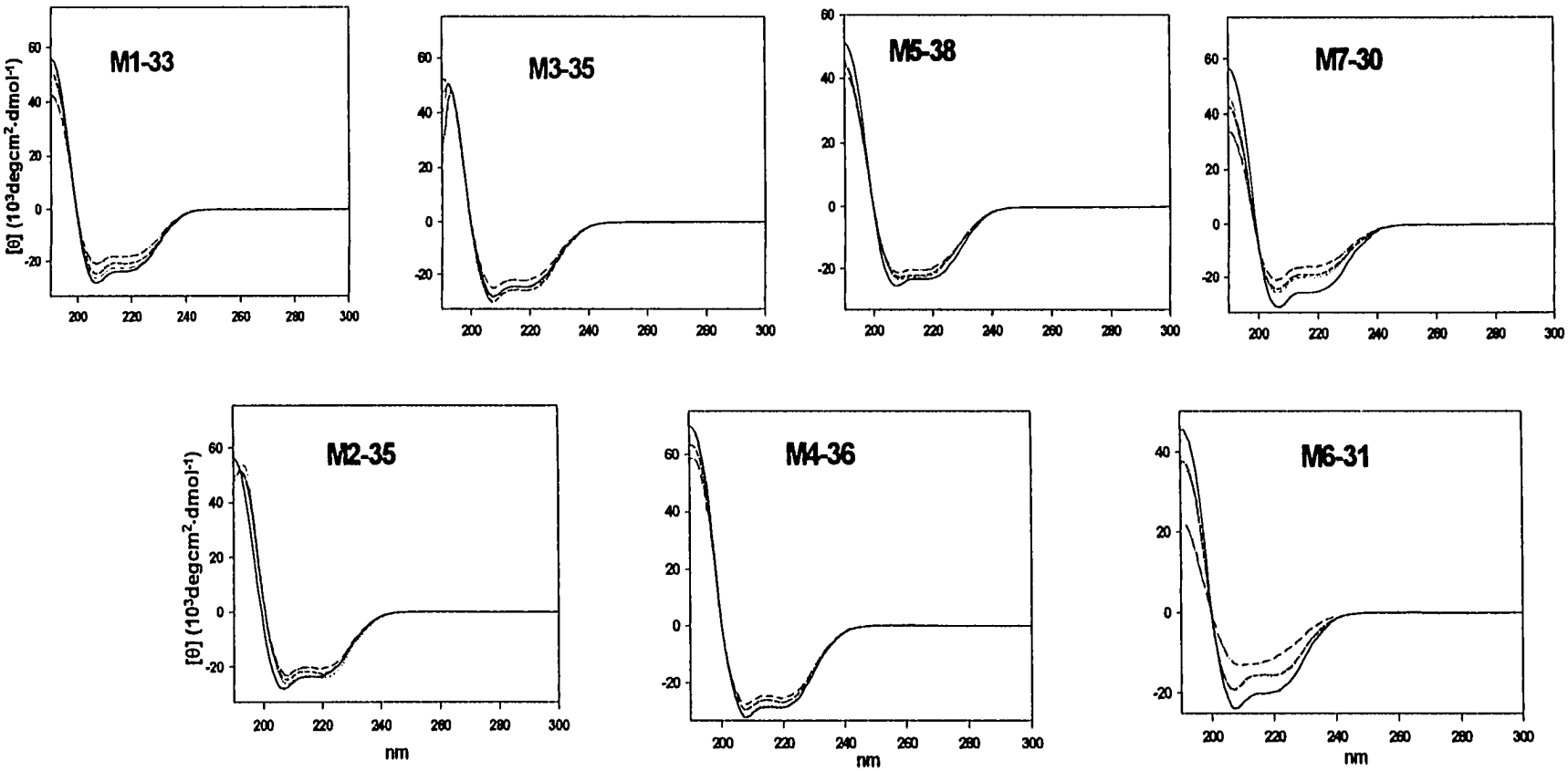

Figure 23 CD spectra of synthetic membrane peptides in TFE/water. Samples were dissolved in TFE and incubated at 50-60 ^{0}C for several hours. The resultant stock solutions were then diluted with TFE and/or water. In each panel, the solid line represents peptide in 100% TFE, dotted line 75% TFE, dashed line 50% TFE, and dots and dashes 25% TFE. The final peptide concentrations ranged from 20-70 μM.

individual responses to water titration. For example M4-36 remains highly helical even in 25% TFE/ 75% water whereas the helicity of M6-31 falls to 29% and the shape of the CD curve changes significantly under these conditions (Figure 23, Table 15). As summarized in Table 15, the helicity was calculated to be 45% or greater for all the peptides in 50% TFE/water with a range between 48% and 86%. As expected none of the peptides was soluble in 100% water and CD analysis could not be undertaken in this solvent.

In addition, the monomeric states of M1, M2, M6, and M7 were verified from NMR experiments on the respective peptide in aqueous TFE (Personal communication with Dr. Boris Arshava), so I assumed that all the sample for CD analyses were monomeric under the experimental concentration.

(2) CD spectra of M1 through M7 in SDS micelles and DMPC vesicles

The secondary structures of the transmembrane domains were also examined in media which contained micelles and lipid bilayers. In the detergent SDS, M1-33, M2-35, M4-36, M5-38 and M7-30 were helical as judged by the split π-π^* transition and the significant n-π^* transition at 222 nm (Figure 24). Similar results were obtained for these peptides in DMPC bilayers (Figure 24). Helicity was calculated to vary from ~40% to ~ 85% (Table 15). In contrast to spectra for these peptides, CD patterns for M3-35 and M6-31 in both SDS and DMPC exhibited a broad minimum centered near 215 nm and a maximum near 200 nm (Figure 24). These patterns are similar to standard spectra for peptides in a β conformation.

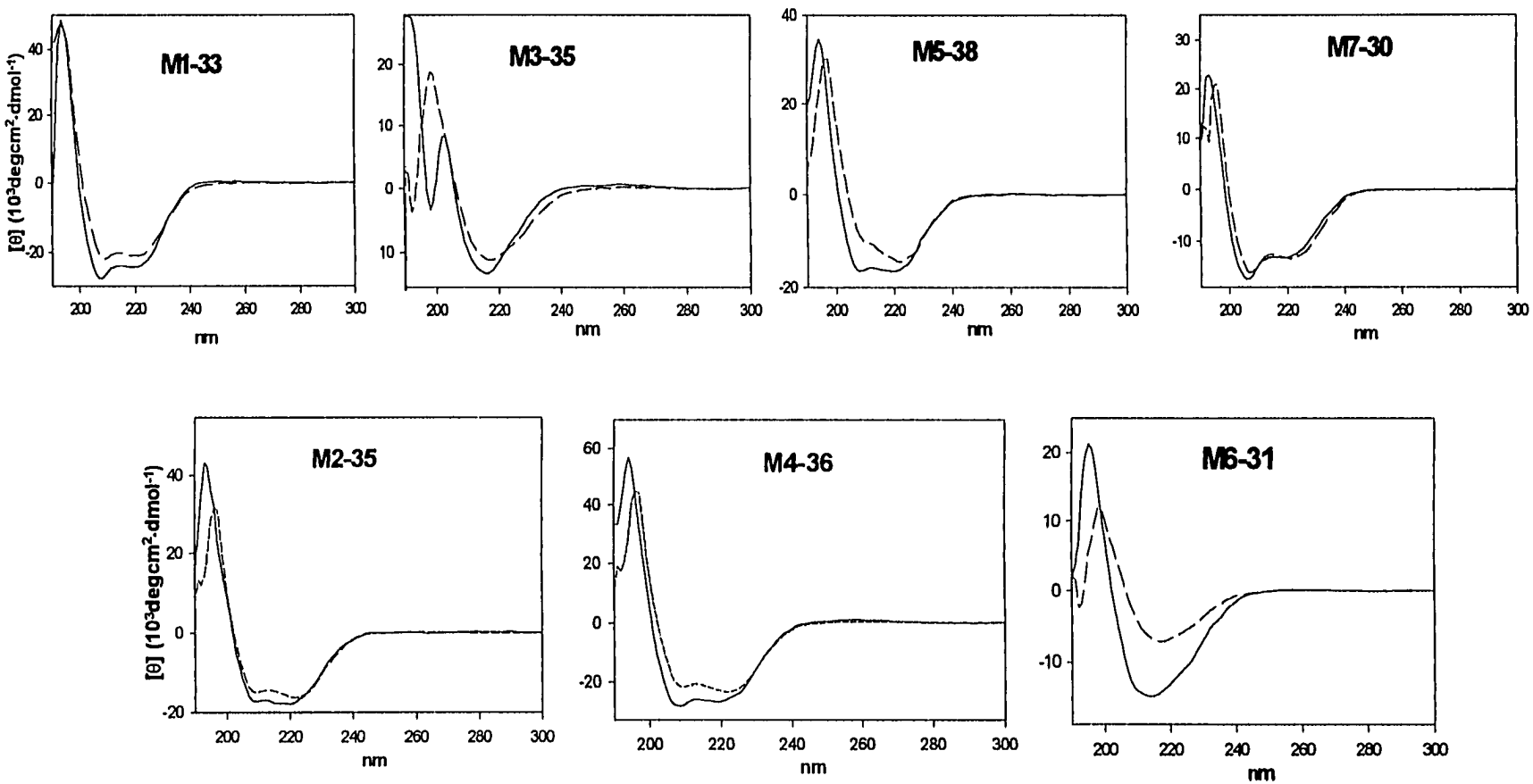

Figure 24 CD spectra of synthetic membrane peptides in SDS micelles and DMPC vesicles. In each panel, the solid line represents the indicated peptide dissolved in 0.5% SDS buffer, and the dashed line represents the peptide prepared in the presence of 3.6 mM DMPC. The final peptide concentrations ranged from 10-30 μM.

To investigate whether the β structures would revert to helices Icarried out CD measurements of M6-31 at different concentrations. Figure 25 shows that lowering concentration from 150 μM to 18 μM did not result in significant changes in ellipticity (<1%) or peak position. The major variation was observed upon dilution from 18 μM to 6 μM with the mean residue ellipticity at 214 nm changing by 30%. Nevertheless, even at 6 μM the CD pattern for M6-31 was totally different from that of a helical peptide.

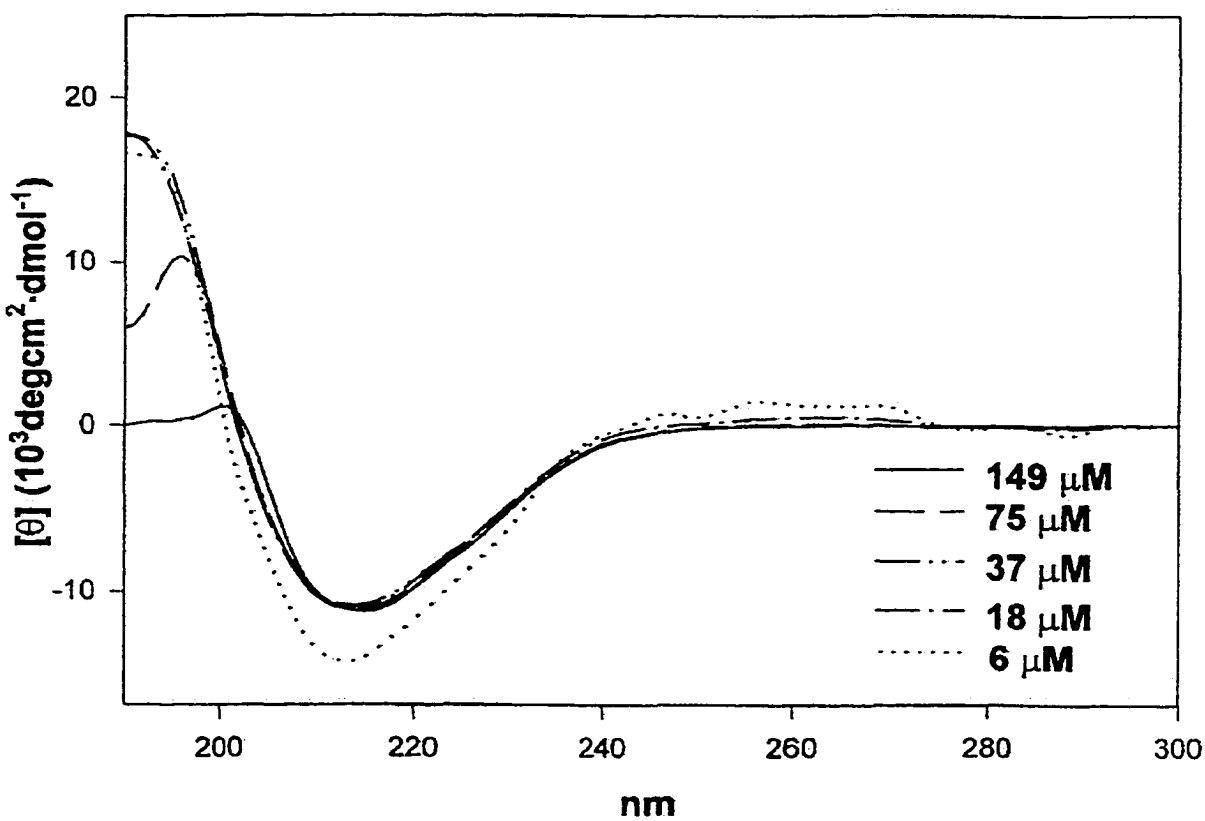

Figure 25 CD spectra of M6-31 at different concentrations in SDS micelles.

(3) Comparative CD spectra of M2 fragments

CD spectra of four M2 fragments with increasing chain length: M2-16 (93-108), M2-20 (89-108), M2-25 (84-108), and M2-35 (74-108; RSRKTPIFIINQVS-LFLIILHSALYFKYLLSNYSS, where the R at the N terminus =74 and the S at the C terminus =108) were run to study the effect of chain length on the secondary structure of membrane peptides in TFE/water mixtures (Figure 26). Under all conditions every peptide was at least partially helical. Quantitative analysis on the spectra indicated that M2-25 was the most helical in all solvent mixtures whereas M2-16 had the lowest percent helicity. M2-35 and M2-20 had similar helicities (Table 16). As in TFE/water mixtures the chain length dependence for helix formation in both SDS and DMPC environments revealed that M2-25 was the most helical followed by M2-20≈M2-35>M2-16 (Figure 27, Table 16).

Table 16 Calculated helicities for M2 fragments[a]

Peptides	TFE/water				0.5%	3.6 mM
	100%	75%	50%	25%	SDS	DMPC
M2-16	50%	36%	36%	32%	35%	29%
M2-20	76%	67%	72%	59%	57%	49%
M2-25	88%	86%	83%	74%	66%	71%
M2-35	84%	77%	72%	64%	54%	46%

a. Calculated using $[\theta]_{222}$ values (see Experimental Procedures)

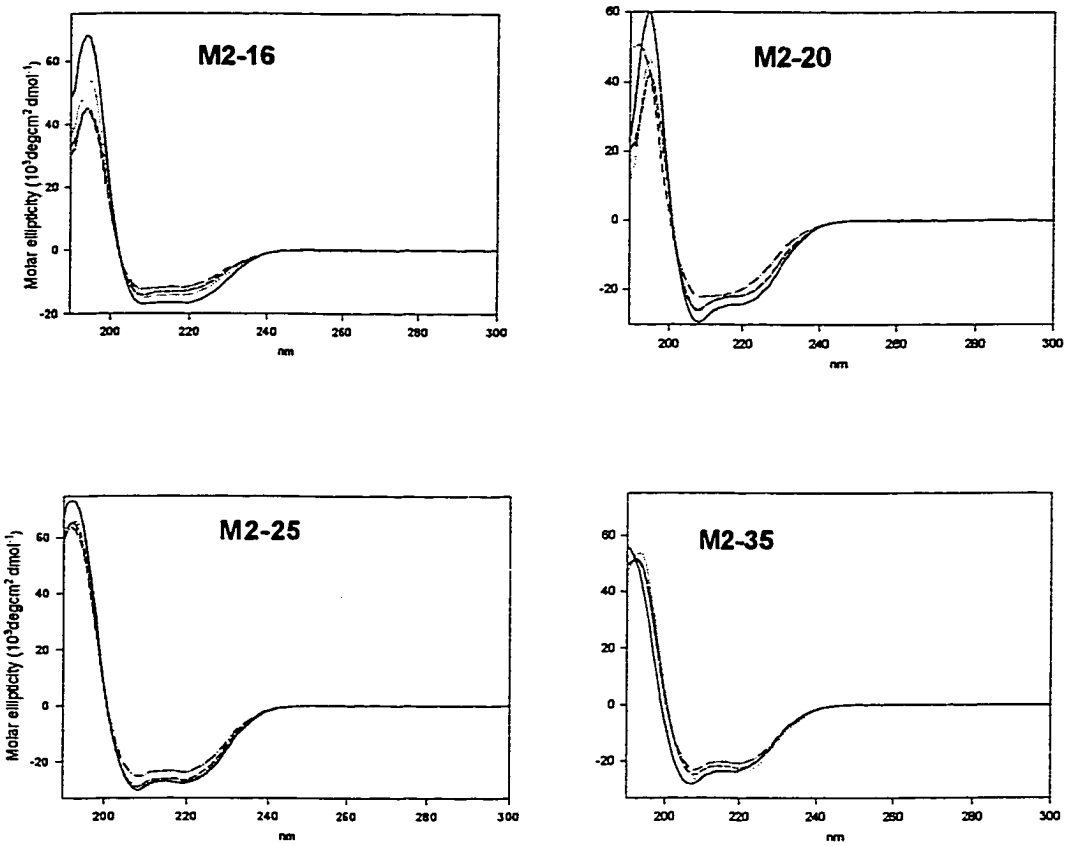

Figure 11 CD spectra of M2 fragments in TFE/water. See Figure legend 5 for sample preparation. In each panel, the solid line represents peptide in 100% TFE, dotted line 75% TFE, dashed line 50% TFE, and dots and dashes 25% TFE. The final peptide concentrations ranged from 30-70 μM.

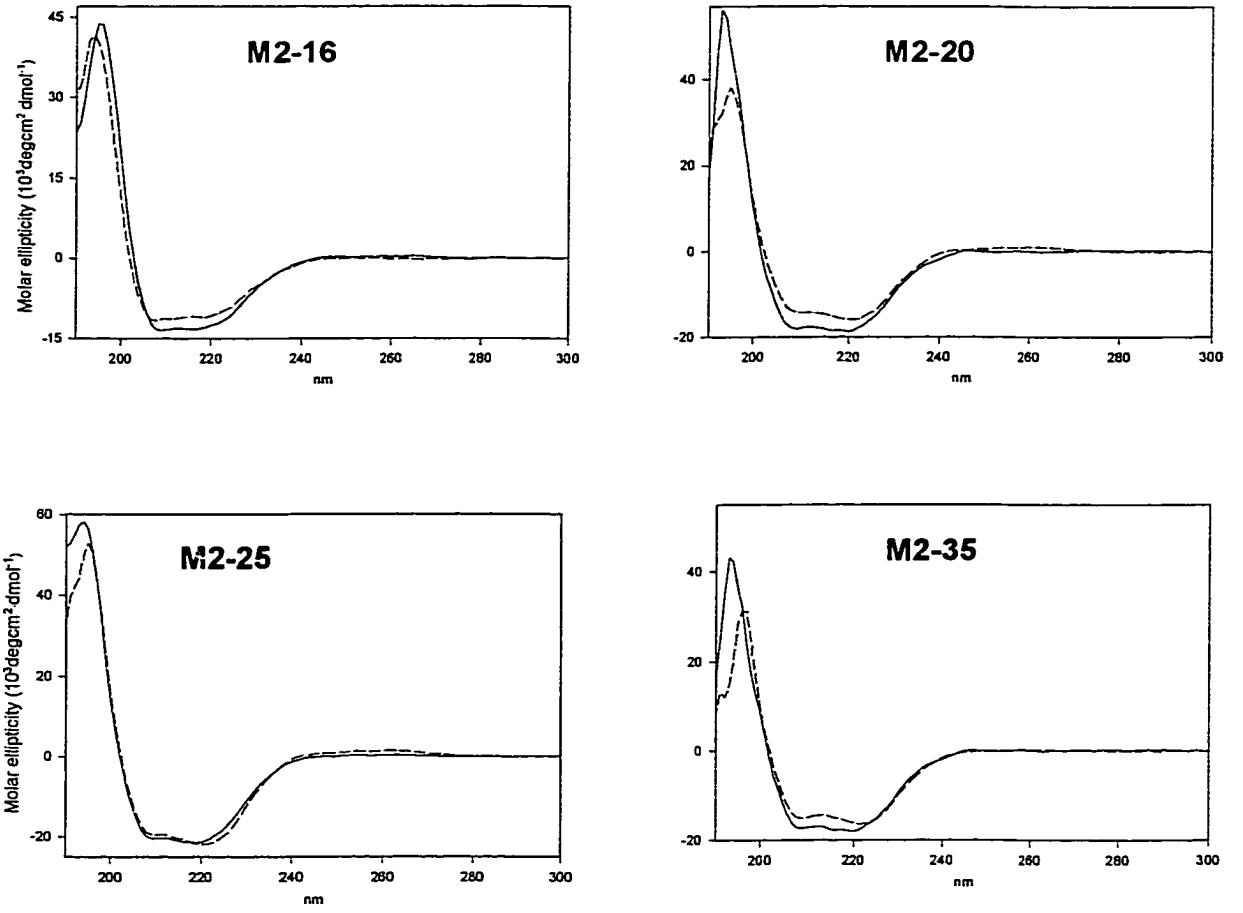

Figure 27 CD spectra of M2 fragments in SDS micelles and DMPC vesicles. In each panel, the solid line represents the indicated peptide dissolved in 0.5% SDS buffer, and the dashed line represents the peptide prepared in the presence of 3.6 mM DMPC. The final peptide concentrations ranged from 10-30 μM.

(4) Thermal stability

The thermal stability of these membrane peptides in SDS micelles was examined by raising the temperature in steps, allowing equilibrium to be obtained, and then measuring the CD spectrum (see Experimental Procedures). The helicity of M4-36 decreased gradually as the temperature was raised to 85 ^{0}C (Figure 28: top panel). The best indicator of decreased helicity is the change in the π-π^* component located below 200 nm. Upon cooling, the original spectra

were recovered indicating that the process was reversible. Similar trends were observed for the other helical transmembrane peptides in SDS micelles (data not shown). The β-like CD pattern of M6-31 varied very little on raising the temperature to 85 ^{0}C (Figure 28: bottom panel). The negative ellipticity at 215 nm is almost identical at all temperatures. However, the ellipticity near 200 nm shifts and decreases as the temperature was raised. Again the CD spectra were reversible on cooling (data not shown). Similar results were found for M3-35 (data not shown). These observations indicated the high thermostability of the conformations assumed by all of the transmembrane peptides in a variety of membrane mimetic solvents.

(5) Comparative CD data of 3 M6 fragments

In a previous investigation we studied the influence of a mutation of Pro258 to Leu on the structure of M6-18 because this mutation in native Ste2p results in a constitutively active receptor possibly due to a conformational change that activates the receptor without the necessity of ligand binding (Konopka *et al.,* 1996). However all attempts to investigate this same mutation in M6-31 failed because we could not purify the peptide due to its extremely poor solubility (Arshava *et al.,* 1998). To circumvent this problem I added Lys residues to both the extracellular and cytosolic sides of the sixth transmembrane domain (Table 16). The CD patterns of M6-35L and M6-35P in SDS and DMPC environments differ significantly from those of M6-31 (Figure 29). Both of the

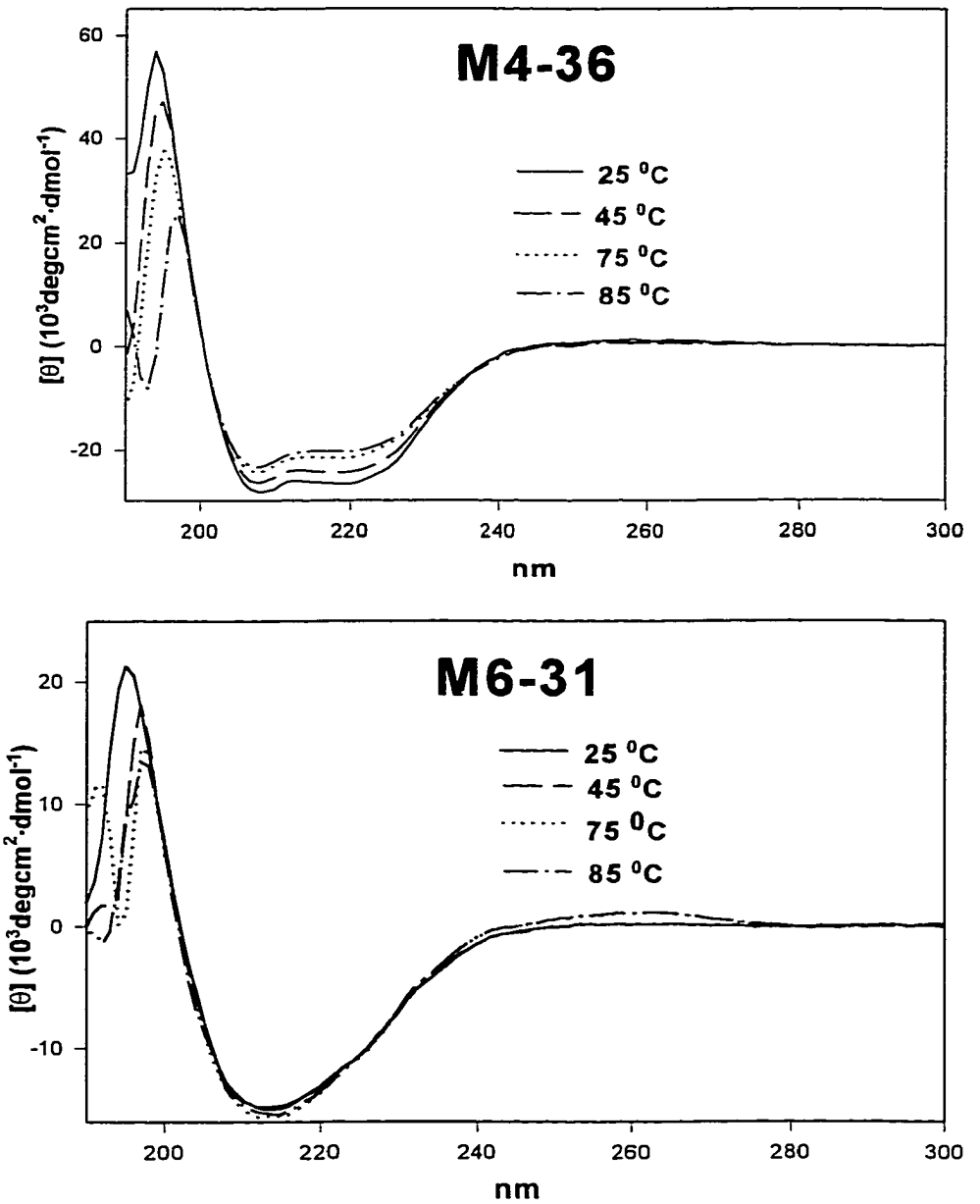

Figure 28 Thermal stability of 2^0 structures of synthetic membrane peptides in SDS micelles. Top panel: A representative α-helical peptide, M4-36; concentration 12 μM. Bottom panel: A representative β-like peptide, M6-31; concentration 36 μM.

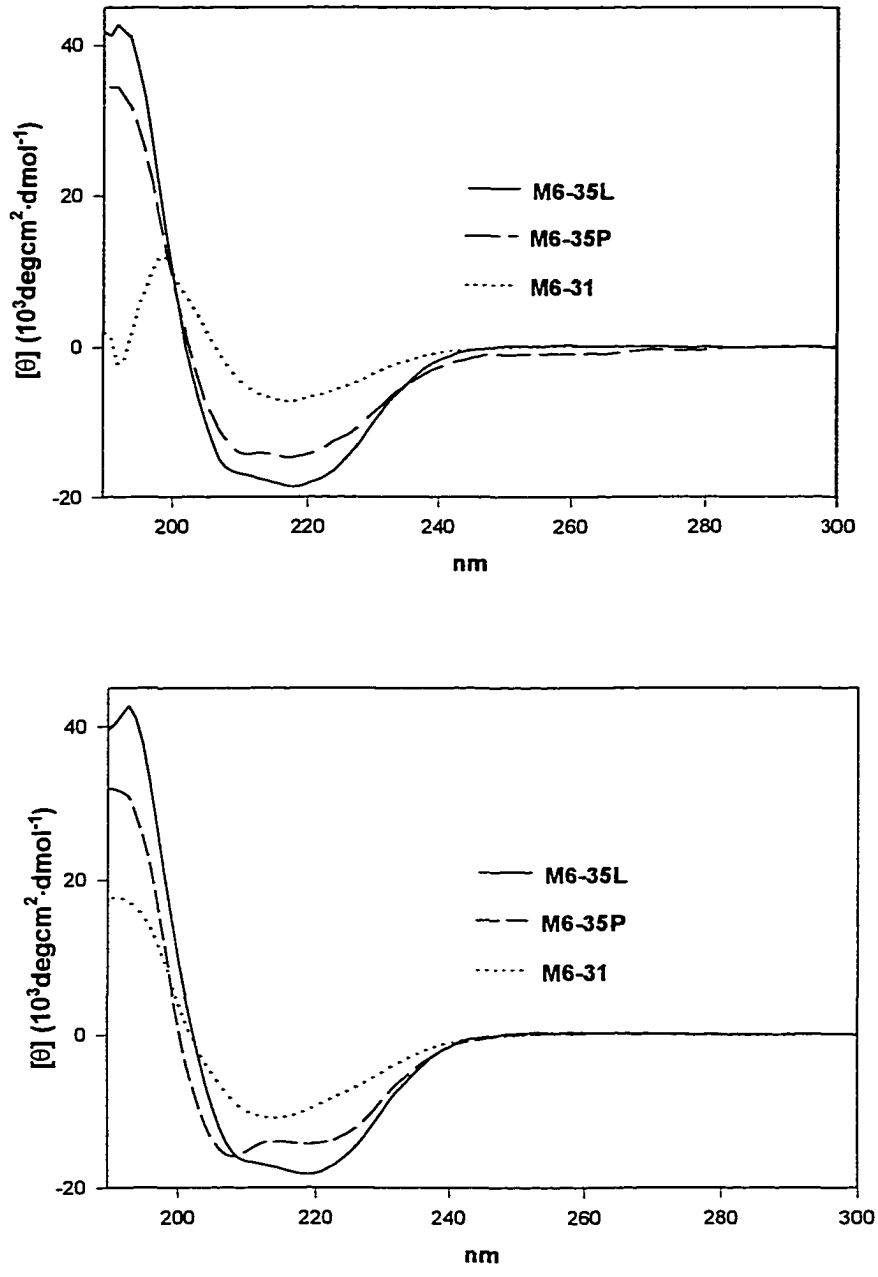

Figure 29 CD spectra of M6 fragments. **Top:** DMPC vesicles; **Bottom:** SDS micelles. In each panel, the solid line represents M6-35L, the dashed line M6-35P and dotted line M6-31. The final peptide concentrations ranged from 10-40 μM.

peptides with the lysine extensions show significantly more helicity. As judged by the magnitude of the ellipticity at 222 nm and the splitting of the π-π^* transition, M6-35P is intermediate in helicity as compared to M6-35L and M6-31. Quantitative calculations show that the helicity of M6-35L varies from 90% to 74% as the water content in trifluoroethanol is changed from 0 to 75%. M6-35P exhibits helicities from 73% to 52% in the same solvent mixtures. The leucine containing peptide is 55% and 46% helical in SDS micelles and DMPC bilayers, respectively, whereas M6-35P is 43% and 35% helical under these conditions (Table 17).

Table 17 Calculated Helicities of Various M6 Peptides[a]

Peptide	TFE/water				0.5%	3.6 mM
	100%	75%	50%	25%	SDS	DMPC
M6-35L	90%	82%	80%	74%	55%	46%
M6-35P	73%	67%	61%	52%	43%	35%
M6-31	61%	46%	47%	29%	/[b]	/[b]

a. Calculated using $[\theta]_{222}$ values (see Experimental Procedures)

b. Not calculated due to low α-helicity.

NMR Analysis of M2-25 in TFE/Water

To gain insights into the detailed secondary structures of the membrane segments of Ste2p, I chose M2-25(84-108) as a representative peptide to conduct detailed NMR analysis because it has a very good solubility, and CD studies have shown that this 25-residue peptide assumes a highly helical structure in TFE and/or TFE/water mixture. Because of the concentration limit, I could not obtain reliable NOE signals of this peptide in SDS micelles. Complete assignments of proton signals were made using TOCSY spectrum to define spin systems (Figure 30) and NOESY spectra (Figure 31) to provide intra- and inter-residue connectivities. The assignments are presented in Table 18. From the NOESY spectrum, numerous medium and long-range connectivities were observed between amide NHs and αCHs and between amide NHs (Figure 31). In particular, many $d_{\alpha N}$ (*i* to *i*+3 and *i* to *i*+4, Figure 31A) and d_{NN} (*i* to *i*+2 and *i* to *i*+3, Figure 31B) connectivities were observed for residues Gln^{85} to Asn^{105}. In addition, coupling constant analysis showed residues Gln^{85} through Ser^{104} had $J_{NH\text{-}\alpha CH}$ values between 3 and 5 Hz, and residue Gln^{105} had a coupling constant of 6.0 Hz, whereas residues Tyr^{106} through Ser^{108} had *J* values more than 6 Hz (Table 18). Comparison of chemical shifts with random coil values (Wishart 1992) suggests that residues 84-106 have an Hα chemical shift index of –1 (Table 18). All of these results are qualitatively consistent with formation of a tight α-helix for residues from N-terminus to Gln^{105}, and the residues 106-108 at the carboxyl terminus are more flexible. These results are also consistent with the structure of

Table 18 ^{1}H Assignments for M2-25 in TFE/H_2O (4:1)at 25 ^{0}C

Residue	$J_{NH-\alpha CH}$	αCH Index	NH	αCH	βCH	γCH	δCH	εCH	Other
Asn[1]		-1	-----	4.29	3.35/3.20	----	----	----	βNH_2: 7.52/6.53
Gln[2]	3.4	-1	9.31	4.17	2.14	2.49	----	----	γNH_2: 7.04/6.41
Val[3]	3.3	-1	7.48	3.91	2.19	1.06	----	----	---
Ser[4]	/[b]	-1	7.88	4.21	4.03/3.98	----	----	----	----
Leu[5]	3.6	-1	7.57	4.23	1.82/1.68	1.72	0.94/0.99	----	----
Phe[6]	/[b]	-1	7.87	4.32	3.34	----	----	----	ArH: 7.22
Leu[7]	/[b]	-1	8.21	4.06	2.13/2.07	1.67	0.99	----	----
Ile[8]	3.0	-1	8.17	3.81	2.21	1.88/1.14/0.97	0.87	----	----
Ile[9]	3.0	-1	8.53	3.68	2.05	1.85/1.20/0.94	0.94	----	----
Leu[10]	3.6	-1	8.73	4.02	1.56/1.45	1.46	0.82	----	---
His[11]	2.9	-1	8.28	4.20	3.38	----	----	----	C_2H: 8.33, C_4H: 7.28
Ser[12]	/[b]	-1	8.34	4.32	4.26/4.02	----	----	----	----
Ala[13]	2.9	-1	8.49	4.27	1.60	----	----	----	----
Leu[14]	3.6	-1	8.15	4.15	1.88/1.57	1.47	0.89	----	----
Tyr[15]	3.1	-1	8.09	4.35	3.12/3.09	----	----	----	ArH: 6.95/6.75
Phe[16]	2.9	-1	8.37	4.29	3.27	----	----	----	ArH: 7.31
Lys[17]	/[b]	-1	8.20	3.96	2.06	1.45/1.60	1.71/1.74	2.99	ε-NH_2: 7.47
Tyr[18]	/[b]	-1	8.33	4.13	3.33/3.16	----	----	----	
Leu[19]	/[b]	-1	8.45	3.82	1.79/1.47	1.58	0.87/0.84	----	----
Leu[20]	/[b]	-1	8.46	4.05	1.67/1.50	1.50	0.82	----	----
Ser[21]	4.2	-1	8.07	4.20	3.88/3.97	----	----	----	----
Asn[22]	6.0	-1	7.68	4.47	2.46/2.38	----	----	----	βNH_2: 6.75/5.66
Tyr[23]	6.6	-1	8.12	4.49	3.18/3.01	----	----	----	ArH: 7.12/6.80
Ser[24]	7.2	0	7.73	4.47	4.00/3.91	----	----	----	----
Ser[25]	7.2	0	7.74	4.46	3.99/3.90	----	----	----	----

a Chemical shifts are given in parts per million relative to the residual proton resonance of TFE at 3.88 ppm.

b Not determined due to overlapping.

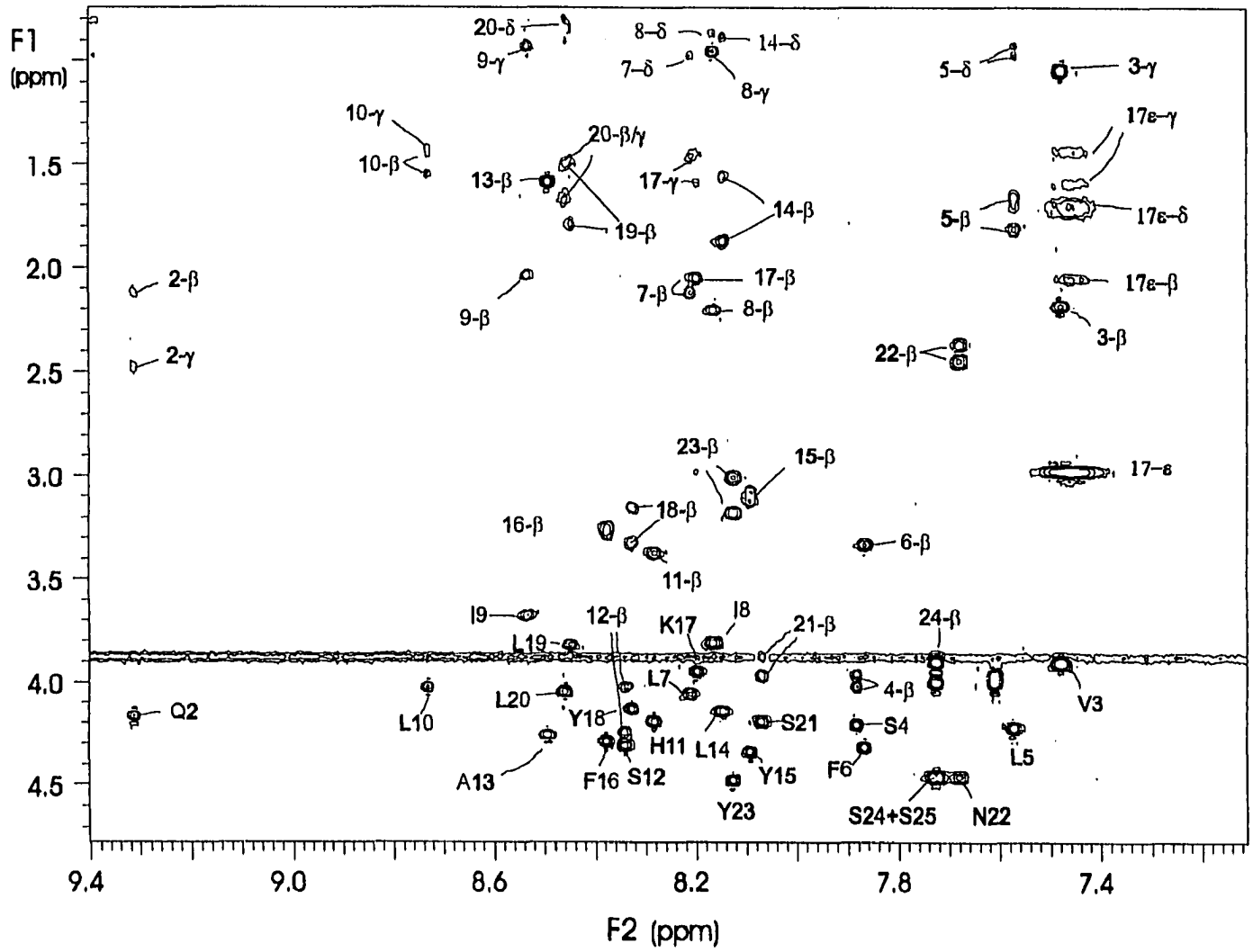

Figure 30 TOCSY spectrum of TM2 (84-108) in TFE/H2O (4:1 v/v) at ambient temperature. Connectivities from the NH of each residue through the side chain appear along the F1 axis. The numbering system used in the figure for this 25-mer peptide assigns the amine terminal residue (Asn^{84}) as position 1 and the carboxyl terminal residue (Ser^{108}) as position 25.

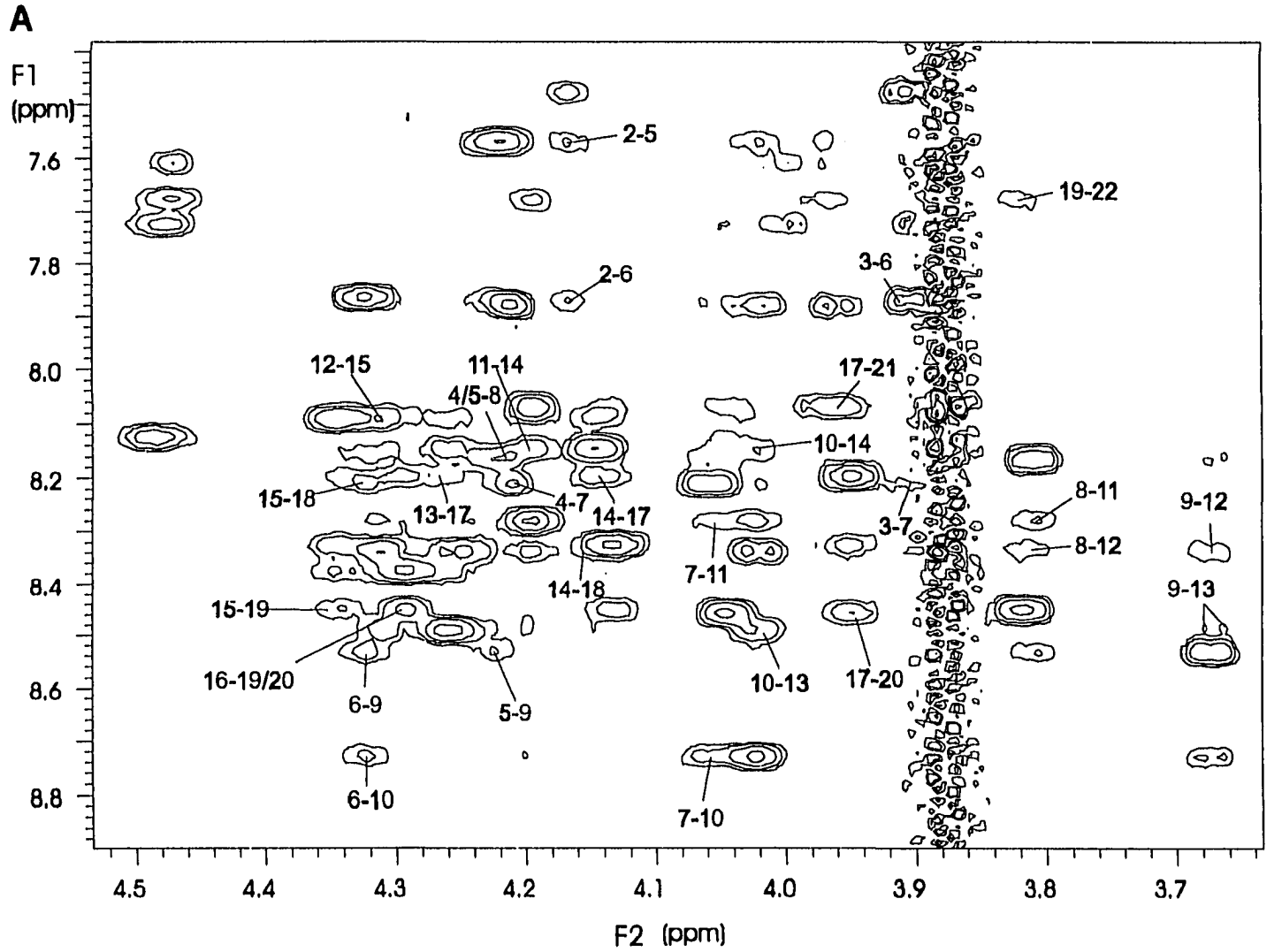

Figure 31 NOESY spectrum of M2(84-108) in TFE/H2O (4:1) at ambient temperature. The mixing time was 300 ms. (A) NH to αCH connectivities; (B) NH to NH connectivities. See Figure 15 for explanation of numbering system. For clarity, the intra-residue and sequential NOEs are not numbered in the figure.

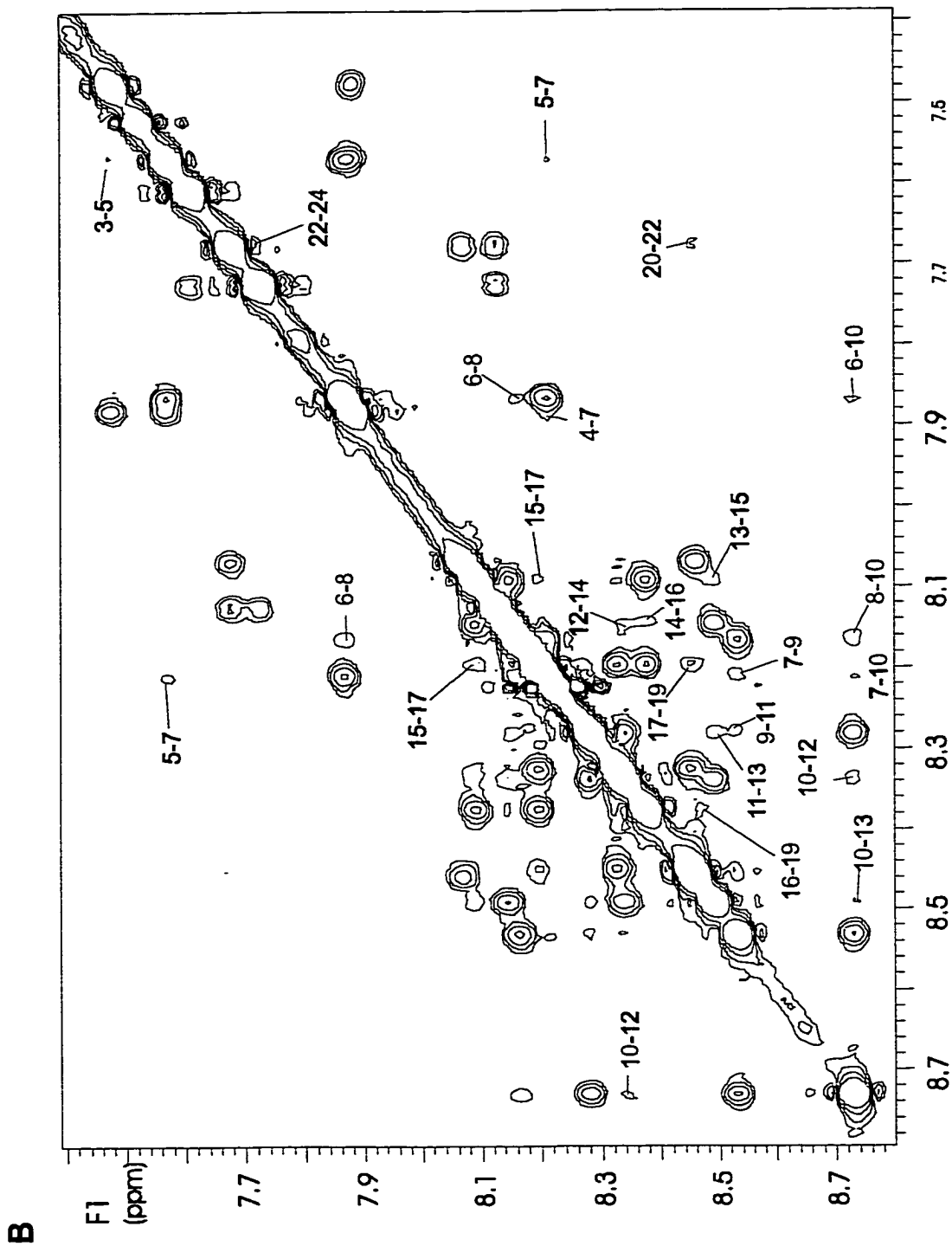

Figure 31 (Continued).

Ste2p from gene fusion and protein reporter methodologies (Figure 16, Cartwright and Tipper 1991; Harley and Tipper, 1996).

Fluorescence Quenching

The analysis of the environment of the transmembrane peptides was further assessed using fluorescence spectroscopy. Both M1-33 and M7-30 contain Trp residues that are predicted to be in the lipid interior of the membrane (Figure 16). Trp fluorescence of M1-33 in MeOH solution and in the presence of DMPC vesicles showed emission maxima of 350 nm and 344 nm respectively (Figure 32A). Thus the environment of the Trp residue of M1-33 in the DMPC vesicles is slightly less polar than methanol. A water-soluble quencher such as iodide can effectively quench the fluorescence of tryptophan upon collision if the tryptophan is exposed to the solvent. As shown in Figure 32A, the fluorescence intensity of M1-33 dissolved in methanol was reduced by 28% upon addition of KI. In contrast, the fluorescence intensity of M1-33 in vesicles was reduced only by 8%. These results are similar to those observed for M7-30 (Personal communications with Dr. Ding).

Iodide quenching was further analyzed in a quantitative way using the Stern-Volmer equation, which relates fluorescence quenching to the concentration of quencher (Figure 32B). The Stern-Volmer plot illustrated that M1 in vesicles had a smaller slope (K_{sv} = 2.11 M^{-1}) than in methanol [K_{sv} = 5.88 (M^{-1})], indicating successful incorporation of the peptides into vesicles. The quenching constants are also similar to those of M7-30 previously measured in the laboratory: 1.67 M^{-1} and 5.67 M^{-1} in vesicles and MeOH, respectively. These results suggest that the lipids effectively shield the Trp from collision with iodide.

A

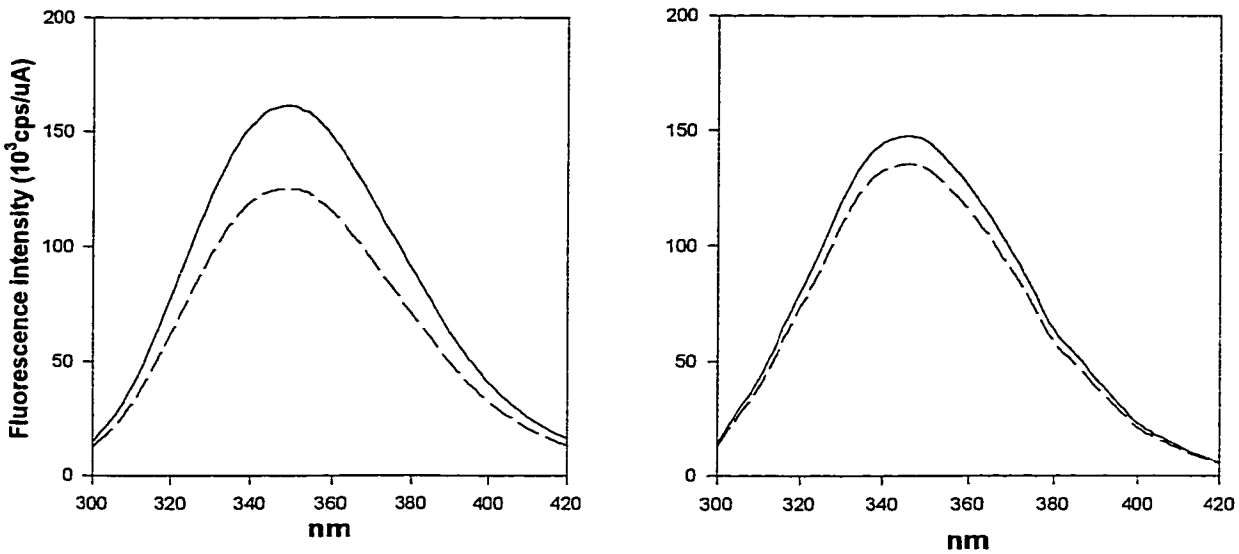

B

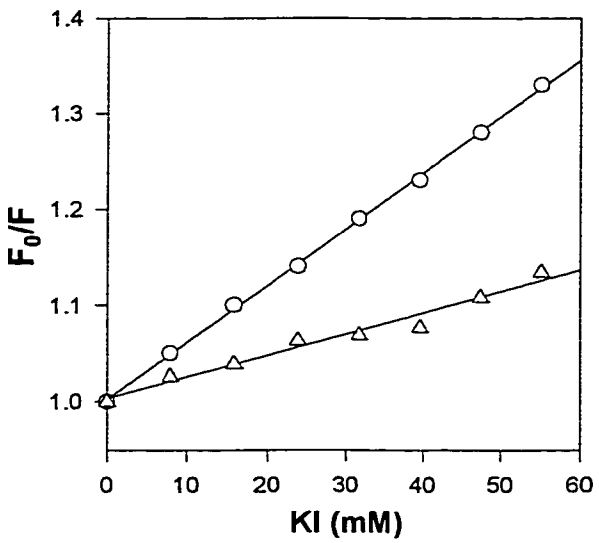

Figure 32. Panel A: Fluorescence emission of M1-33 in the presence of KCl (50 mM, solid line) or KI (50 mM, dashed line). Left: in MeOH; Right: in DMPC vesicles. Both peptide concentrations are 2.5μM.; Panel B: Stern-Volmer Plot for M1-33 in DMPC vesicles (Δ) and MeOH (O).

Tricine SDS-PAGE of Membrane Peptides

SDS-polyacrylamide gel electrophoresis (SDS-PAGE) was used to assess the molecular size of the peptides in the presence of detergent micelles. The seven transmembrane peptides ran as bands of various breadth when the peptides were subjected to electrophoresis on 27.7% gels in a Tricine-SDS buffer (Figure 33). Attempts were made to apply similar amounts of peptide to the gel. Nevertheless bands of very different size resulted, and the staining efficiencies with silver stain varied from peptide to peptide (compare gel B lane h with gel A M4). In fact, several of the peptides did not stain at all using Coomassie Blue (data not shown). Nevertheless except for M6-31 the monomeric form of each peptide is visible near the bottom of their corresponding lanes (Figure 33A). M6-31 mainly self-associates (a faint band is seen near the monomer molecular weight) and forms a higher molecular species containing 7-8 molecules. Lowering concentration of M6-31 to 6 μM did not significantly affect its multimeric state (Figure 33B). In M3, a significant band was observed at the stacking gel along with a broad band with a slight split moving as a monomer (Figure 33A; M3).

Comparison of M6-31, M6-35P and M6-35L using SDS/PAGE revealed that the leucine mutant peptide moved predominantly as a monomer whereas at similar concentrations M6-35P was a mixture of low and high molecular weight species. At very high concentrations both M6-31 and M6-35P showed a number of different high molecular weight forms. However as stated above even at very

low concentrations M6-31 would not form a monomer in the gel (Figure 33B lanes f & g).

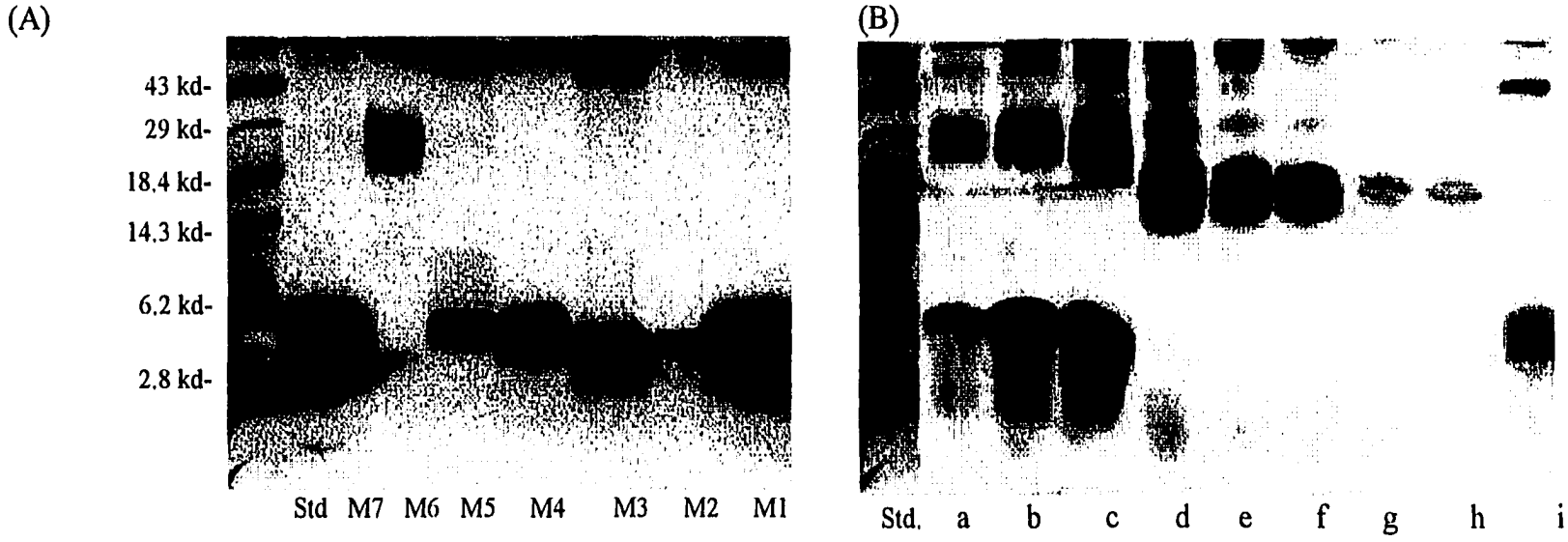

Figure 33 Tricine SDS-PAGE of synthetic membrane peptides. 20 μl of each peptide sample was loaded to its respective lane. (A) M1 through M7. Peptide concentrations: [M1]=10 μM, [M2]=5.3 μM, [M3]=11.1 μM, [M4]= 6.3 μM, [M5]=8 μM, [M6]=18.0 μM, [M7]= 19 μM; (B) M6-35P (Path a through c), M6-31 (Path d through h), and M6-35L (Path I). Peptide concentration: a: 18 μM; b: 36 μM; c: 72μM; d: 75 μM; e: 37 μM; f: 18 μM, g: 9 μM; h: 6 μM; i: 14 μM

CHAPTER IV DISCUSSION

The lower resolution structure deduced for the transmembrane core of rhodopsin has served as a model system with which to compare other conformational data for *GPCRs*. However, the way in which these hydrophobic domains pack together in the membrane is poorly understood because the inherent problems associated with purifying, solubilizing and crystallizing integral membrane proteins (IMP's) have hindered the application of X-ray crystallography and NMR to *GPCRs*. Therefore conformational insights into these receptors has relied on more novel approaches. Specifically, rather than study the entire protein individual transmembrane domains are examined to learn about the intact protein.

Hydropathy algorithms are believed to be quite reliable and have proven to be correct for the small set of α-helical IMP's where structure has been characterized at high resolution (Engelman *et al.,* 1986); these algorithms identify putative TM α-helices in the primary sequence of an IMP by scanning it for regions that are long enough and hydrophobic enough to span a phospholipid bilayer in an α-helical conformation (von Heijne 1980; Kyte & Doolittle 1982; Engelman *et al.,* 1986); A Hydropathy algorithm estimates the free energy of transferring each 20-residue segment of the protein from water to a phospholipid bilayer in an α-helical conformation (Engelman *et al.,* 1986). The magnitude of the free energy of insertion estimated in this way is very large, with values≤ -15 kcal/mol calculated for the experimentally observed structures. Because this

estimate is made for a single, isolated TM α-helix, it suggests that these helices should be thermodynamically stable in the TM configuration, even in the absence of any other structural interactions. On this basis, the folding of polytopic α-helical IMP's could proceed by a simple, two-step pathway in which all of the individual α-helices are stably inserted into the phospholipid bilayer in the first step followed by the association within the plane of the bilayer to form the final tertiary structure in a second, mechanistically independent step (Popot & Engelman 1990). This model infers spontaneous folding of the integral membrane protein and suggests that both intact receptors and fragments of receptors would refold to biologically active species. *In vitro* evidence supporting this hypothesis has been presented for bacteriorhodopsin (Huang *et al* 1981; London and Khorana, 1982) and for fragments of this protein (Kahn and Engelman 1992; Marti 1998). In addition, co-expressed polypeptide fragments of rhodopsin were demonstrated to spontaneously assemble into functional receptor in COS-1 cells (Ridge *et al.,* 1995). These analyses indicated that study of segments of transmembrane proteins could allow important insights into the overall structures of these molecules.

It is valid to inquire as to the biological relevance of studies on relatively short peptides conforming to regions of large integral membrane proteins. One might argue that despite the individual conformational tendencies of these peptides the structures of all regions of the receptor are influenced by long-range interactions between various domains. However, as indicated by the above studies on rhodopsin and bacteriorhodopsin, it is clear that regions of receptors

do maintain functional relevance. Specifically, in the case of rhodopsin, 3 fragments representing transmembrane helices 1-3, 4-5, and 6-7 re-formed a functional pigment in the membrane of COS-1 cells (Ridge *et al.,* 1995). Recently, a similar analysis was made on the G protein coupled hepta-helical receptor (Ste2p) for the mating factor of yeast. Co-expressed fragments representing splits in every loop of the receptor reformed a protein which signaled in response to the peptide pheromone (Martin *et al.,* 1999). This study supports the notion that biophysical analysis of receptor fragments should provide structural information that is relevant to the assembly and stability of the intact Ste2p.

Previous investigations of synthetic peptide model compounds to study the biophysical properties of *GPCRs* have been very limited. To our knowledge in only one case has the synthesis and characterization of all the transmembrane domains of a hepta-helical protein, bacteriorhodopsin, been reported (Hunt *et al.*, 1997). This photoreceptor is not coupled to G proteins. In another elegant study six of the putative twelve transmembrane peptides of the cystic fibrosis chloride transporter were synthesized and characterized (Wigley *et al.,* 1998).

I herein report results from the biophysical experiments on all seven synthetic TM fragments of the α-factor receptor (M1 through M7) and two variants of the M6 (M6-35P and M6-35L). Although these sequences are predicted to be α-helical, no direct structural evidence has been presented except for M6-31 and M7-30. All peptides studied in this investigation have similar chain length (30-38 amino acid residues). We found the synthesis and

purification of several of the Ste2p transmembrane peptides to be extremely challenging. All of the crude peptides give very complex patterns on HPLC analysis, despite long coupling times, driving coupling conditions, and use of highly solvating solvents during coupling reactions. In M3 even after extensive efforts we found it impossible to obtain a peptide that was soluble enough for HPLC characterization and purification. Using the approach of Kyte and Doolittle (Kyte and Doolittle 1982) to calculate the average hydrophobicity of the wild-type sequence of the portions of the synthetic peptides that are in the interior of the membrane (excluding the hydrophilic loops in M1-M7) values from 1.46 to 2.36 were obtained (Table 19). Among the Ste2p transmembrane peptides, the two most difficult domains to synthesize, M3 and M4, had relatively low hydrophobicities. Thus, it is clear that the average hydrophobicity does not

Table 19 Hydrophobicities of Transmembrane Regions of M1-M7

Domain[a]	Sequence	Φ[b]
M1(52-71)	AIMFGVRCGAAALTLIVMWM	1.82
M2(80-99)	IFIINQVSLFLIILHSALYF	1.95
M3(135-154)	QVLLVASIETSLVFQIKVIF	1.66
M4(166-185)	LTSISFTLGIATVTMYFVSA	1.46
M5(209-228)	ILLASSINFMSFVLVVKLIL	2.23
M6(246-265)	ILLIMSCQSLLVPSIIFILA	2.36
M7(278-297)	TTVATLLAVLSLPLSSMWAT	1.47

a. Residues predicted to be in the membrane (see Figure 16)

b. Average hydrophobicity

account for the difficulties encountered during synthesis of M3 and M4 and that specific sequence dependent effects must be important.

The addition of several lysine residues at the carboxyl and amino ends of M3 resulted in a dissolvable peptide. Notwithstanding these additional residues the normal acetonitrile-based solvent gradient gave a broad envelope without resolvable peaks. It is likely that membrane peptides form a variety of aggregated species in HPLC solvents and that the very broad bands observed reflect the state of aggregation and not the success of the synthesis. We found significant improvement in the HPLC pattern using a methanol (Figure 21) based gradient and at elevated temperatures (Figure 20). Others have reported that the aggregated states of peptides can be disrupted using strong denaturants such as guanidine hydrochloride (Chen *et al.,* 1999) or mixtures of solvents such as formic acid/glacial acetic acid/chloroform/ethanol (Jones *et al.,* 2000). It is essential that careful attention be paid to such detail when assessing peptide purity and developing purification systems. Applying the above approaches we were able to obtain 10-20 mg quantities of the seven transmembrane peptides of Ste2p.

Biophysical experiments were carried out on the putative seven synthetic transmembrane fragments of Ste2p (M1-M7) and two variants of M6 (M6-35P and M6-35L). All peptides studied in this investigation have similar chain length of 30-38 amino acid residues. Based on CD results in TFE/water mixtures the seven transmembrane domains have a high proclivity to assume α-helical structures (Figure 23, Table 15). Indeed in 100% TFE the percent helicity ranges

from 61% to 92%. However, titration with water begins to reveal the conformational differences in the various regions of this *GPCR*. M6-31 is only 29% helical in 25% TFE/ 75% water and exhibits a CD pattern which is not characteristic of an α-helix whereas M4-36 is still 80% helical in the identical solvent.

In contrast to the helicity found for all peptides in aqueous TFE, the membrane peptides exhibited significant structural diversity in SDS and DMPC environments. Several peptides (*e.g.* M4-36) retained high helicity in both micelles and bilayers. Others such as M3-35 and M6-31 formed β-structures. Fluorescence studies in DMPC on both M1-33 and M7-30, the two transmembrane domains that contained Trp residues, showed that the aromatic residue is in the lipid environment and protected from quenching by a hydrophilic iodide anion. Thus, it is reasonable to conclude that these peptides do insert into the lipid bilayers. We observed that the method of sample preparation was very important in determining the conformational state of the peptides in SDS and DMPC. It was critical to allow the peptide to reach equilibrium with the lipid environment of either the micelle or the bilayer. Direct attempts to sonicate several of the peptides in the presence of either SDS or DMPC resulted in either very poor spectra (no incorporation) or β-like CD patterns. In contrast when the peptide was equilibrated by dialysis with these membrane mimetic environments, helical structures sometimes resulted. The conclusions with CD have been verified using ATR/FTIR analysis (Ding, personal communication). Similar observations concerning sample preparation were reported for the

bacteriorhodopsin transmembrane domains (Arshava *et al.,* 1998). Given the care taken to prepare all samples under identical conditions, the conformational tendencies of M3-35 and M6-31 are especially significant. The β-structure formed by M6-31 is very stable. It existed over a 30-fold range of concentration (Figure 25) and was stable up to 85° C (Figure 28 bottom). As the helix formed by peptides such as M4-36 was also stable to relatively high temperatures (Figure 28 top) and as the CD spectra were reversible on heating, it is reasonable to conclude that the CD patterns represent the thermodynamically stable forms of these peptides in the lipid-like media.

Quantitative analyses on representative series of M2 supported the structure of this domain from gene fusion and protein reporter methodologies (Figure 16) (Cartwright and Tipper 1991; Harley and Tipper, 1996): the 25-mer fragment exhibits a higher helicity than the 35-mer, indicating the extended residues at the N terminus of the 35-mer are located in the loop I1 and therefore, tend to form more disordered structures. Detailed NMR analysis concluded that in TFE/water the 25 residue peptide M2(84-108) of the second transmembrane domain is highly helical from the carboxyl terminus to the Asn^{105} residue, which also supports the structure of this domain predicted by hydropathy. Compared to about 86% helicity from CD spectra, the NMR result that 21 out of total 25 residues are in the helical region indicates that the method we used in calculating helicity from CD spectra is rather reliable for highly helical peptides.

Gel electrophoresis of the transmembrane domains gave support to the conclusions from CD analysis in SDS micelles. At similar concentrations helical

peptides M1-33, M2-35, M4-36, M5-38 and M7-30 all ran as monomers (Figure 33A). In contrast the two peptides, which gave β-like CD patterns, ran as either an oligomeric species (M6-31) or as a monomer plus a higher MW band (M3-35). The oligomer of M6-31 (~7-8 peptide chains) exists over at least a 10-fold concentration range. One can conclude that M3 and M6 have a much greater tendency to self-associate than the other transmembrane peptides of Ste2p.

The observation of β-sheet structures for M3 and M6 in detergent and lipids is to some extent unexpected. A β structure was also reported for a transmembrane fragment (domain G) from bacteriorhodopsin (Hunt *et al.,* 1997). These observations support the conclusion that the conformation of the transmembrane domains of intact receptors is not determined simply by the secondary structural propensity of the isolated fragments, but is further influenced by long-range interactions within the protein. This conclusion suggests that the two-step model (Popot, J.L. and Engelman, D.M. 1990) would not account for all features of the folding of Ste2p.

Recently, a high-resolution crystal structure of rhodopsin revealed intramolecular interactions between various transmembrane regions (Palczewski *et al., 2000*). These regions are stabilized by a number of interhelical hydrogen bonds and hydrophobic interactions, most of which are mediated by highly conserved residues. Interestingly, Arg^{135} in helix H-III interacts with Glu^{247} and Thr^{251} in helix H-VI. It is tempting to conclude that such interactions are a general feature in all *GPCRs*, and domains III and VI in Ste2p are similarly in contact. Indeed, several studies have demonstrated that helix-helix interactions

are necessary for receptor activation (Dube and Konopka, 1998; Tarasava *et al.,* 1999; Feng *et al.,* 1999). This perspective would allow us to propose that lack of domain-domain interactions for the isolated M3 and M6 fragments could account for the failure of these peptides to form stable helices in micelles and lipids. We note that Ste2p lacks the conserved Glu^{134}-Arg^{135}-Tyr^{136} tripeptide of helix III of rhodopsin and does not have corresponding residues in helix VI. It also belongs to a distinct subfamily of *GPCRs* that only includes fungal receptors (Horn *et al.,* 1998). Therefore, definitive information on the interaction between M3 and M6 in Ste2p will require high resolution studies on the intact receptor.

As an α-helix→β-sheet transition was observed for M6-31 when the solvent is changed from TFE/water to either DMPC vesicles or SDS micelles, this receptor domain also manifests significant conformational flexibility. The tendency of domain six to be conformationally flexible may be biologically significant. Greater than 90% of all *GPCRs* contain a proline residue at similar positions in transmembrane domain 6. Mutation of these proline residues often has biological consequences. For Ste2p mutation of Pro258 to Leu resulted in constitutive activity with 45% of the saturable wild-type signaling in the absence of pheromone (Konopka *et al.,* 1996; Sommers *et al.,* 2000). The current model of signal transduction by G protein-coupled receptors involves the isomerization of the receptor from an inactive to an active form. Using mutational analysis the sixth transmembrane domain and the third cytoplasmic loop were implicated in receptor activation (Clark *et al.,* 1994; Stefan *et al.,* 1994; Weiner *et al.,*1993) and polar residues in transmembrane domain 6 of Ste2p were suggested to interact

with other domains of the receptor (Dube *et al.,* 1998). Previously we reported that an 18-residue homolog, M6-18L(252-269, C252A, P258L) corresponding to the constitutively active receptor Ste2p-P258L, was highly α-helical structure in SDS micelles, but was a β-structure in HFA/water (Arshava *et al.,* 1998). However, the synthesis of the 31 residue homologue M6-31L(239-269, C252A, P258L) failed because of extreme aggregation. In this study CD analyses indicated that a soluble variant of M6 (M6-35L, Table 12) is highly helical in the three membrane mimetic environments examined (Table 17 and Figure 30). The wild-type homolog M6-35P is decidedly less helical. Moreover, FTIR analysis indicates that in DMPC/DMPG (4:1) M6-35L is predominantly α-helical whereas M6-35P is predominantly a β-sheet structure (Dr. Ding, personal communications). Interestingly, in SDS/PAGE studies M6-35P forms a mixture of monomer and aggregated forms whereas M6-35L forms mostly monomer (Figure 33B). Thus, if one hypothesizes that the activated receptor involves stabilizing a state wherein the sixth transmembrane domain forms a helical structure, then the CD, IR and the gel studies suggest that the Pro258Leu mutation would favor this helical structure. Although Pro has often been considered to be a potent α-helix breaker, studies in membrane mimetic solvents concluded its conformational tendencies are highly environment sensitive (Li *et al.,* 1996). Moreover, we have recently shown that after extensive mutagenesis only a limited spectrum of mutations in Ste2p lead to a constitutively-activated receptor and that a number of these mutations are in the sixth transmembrane domain (Sommers *et al.,*

2000). Thus, it is not unreasonable to conclude that the Pro258 serves as a conformational switch for Ste2p.

The idea of oligomerization of *GPCRs* is gaining credence from a variety of investigations (Herbert *et al.,* 1998) including one report where transmembrane peptides inhibited dimerization of β-adrenergic receptor (Herbert *et al.,* 1996). In our gel studies, M6 was found to self-aggregate and M3 also forms high molecular weight species (Figure 33A). In preliminary studies we found that M6 also tends to interact with other domains as judged by gel electrophoresis analysis (Xie and Arevalo unpublished results). Since a recent study demonstrated that Ste2p is oligomeric in intact cells and membranes of *S. cerevisiae* (Overton *et al.,* 2000), our results suggest that Ste2p might form dimers through a direct interaction of specific transmembrane domains having a tendency to aggregate due to their biophysical properties.

It should be noted that most of the hydrophobic amino acids commonly found in transmembrane domains (i.e. Tyr, Val, Ile, Trp, Phe, and Leu) have a higher propensity to form β-sheets than α-helices according to the scale of Chou and Fasman derived from the statistical analysis of observed secondary structure in soluble proteins (Chou and Fasman, 1978). However, an experimental study of α-helix in SDS micelles has shown that α-helical propensity in a hydrophobic environment scales with the hydrophobicity of the amino acid side chain and not according to the structural propensity of the residue in soluble proteins (Li and Deber, 1994). Recently, an investigation of the six transmembrane peptides of the first membrane spanning region of the cystic fibrosis conductance regulator

(Wigley *et al.,* 1998) concluded that the Chou-Fasman algorithm incorrectly predicted β-sheets for these peptides and that there were significant differences in the secondary predictions from the five algorithms they utilized. Our results give additional experimental evidence that the Chou-Fasman calculation cannot be used for transmembrane peptides. In particular, it should be noted that proline 290 in the center of M7-30 was found to "stabilize" the α-helical conformation in all environments, which also argues against the doctrine that Pro is the most potent α-helix breaker as established in aqueous media. This phenomenon was also observed by Li *et al.*, and they proposed that α-helical, but not β-sheet, propensity of proline is determined by peptide environment. (Li *et al.,* 1996).

An aspect of this study that requires consideration is the influence of the additional lysine residues on the structure of the central core in the transmembrane peptides. It was our belief that placing several lysines on both sides of the domain would prevent aggregation due to hydrophobic stacking of the central core. Other scientists working with membrane peptides have used lysine residues to solubilize these molecules (Bianchi *et al.,* 1999; Chen *et al.*, 1999) and this approach was used many years ago to solubilize poly-L-alanine (Ingwall *et al.,* 1968). Our data support the conclusion that the hydrophilic chain ends do not significantly affect the helix formation by residues in the center of the peptide. Study of the series of peptides representing different lengths of M2 showed that M2-25 was the most helical whereas M2-20 and M2-35 had similar percent helicities. Assuming the model in Figure 16, 19/25 = 76% of the residues of M2-25 should be helical. For M2-35 23/35 = 66% should be helical. This

calculation is in excellent agreement with the CD results in 25% aqueous TFE. One would conclude then that the extra-membranous portions of the model peptides assume random structures. A comparison of the CD profiles and the SDS gels and the IR spectra of M6-31 and M6-35P indicates that the peptide without the lysine residues does have a greater tendency to aggregate. Nevertheless the comparison of the same data for M6-35P and the mutant peptide M6-35L shows that the lysine extensions do not conceal the different conformational tendencies of these molecules. Finally both M3-35 and M4-36 contain similar extensions on the carboxyl and amine terminus yet one of these peptides is highly helical in SDS and DMPC environments whereas the other is a β-aggregate. We conclude that useful information on the inherent conformational tendencies of a transmembrane domain can be obtained using oligolysine substitutions in the hydrophilic loops of the receptor, however, one should be careful in the interpretation of the results. Conjugation with polyethylene glycol has also been suggested as an approach to enhance the solubility of transmembrane domains in aqueous media (Pomroy *et al.*, 1999). The generality of this solubilizing group needs to be systematically explored with different domains.

As stated above the seven transmembrane peptides of bacteriorhodopsin were previously subjected to detailed analysis using CD, FTIR, and proteolysis experiments (Hunt *et al.*, 1997a). The authors found that the first 5 transmembrane domains formed stable α-helical structures in detergent and lipids whereas the sixth domain did not have a stable structure and the seventh

domain formed a hyperstable β-sheet structure. More recently five of the first six transmembrane peptides of the CFTR receptor were found to be helical whereas the sixth domain underwent a shift from an α-helix to a β-structure in 20% methanol (Wigley *et al.,* 1998). Our results on Ste2p show that most of the domains of this receptor were helical but that two of the domains, M3 and M6, could form β-structures. Finally, a recent solution NMR study on the sixth transmembrane peptide of rhodopsin in DMSO-d_6 concluded that this domain was helical throughout most of its length and that the Pro residue induced only a small distortion in the helix (Chopra *et al.,* 2000). Our NMR studies on the sixth transmembrane peptide of Ste2p in TFE/water indicated that the helix formed by this peptide is kinked (Arshava *et al.,* 1998) and that this domain may be conformationally diverse (*vida supra*). The high resolution structure of rhodopsin showed that there was a significant bend at Pro 267 of the sixth transmembrane helix (Palczewski *et al.,* 2000). It seems clear that transmembrane peptides of integral membrane proteins will have individual biophysical tendencies and that they will not all simply behave as rigid helical rods.

Chapter V Conclusion

In conclusion, we successfully synthesized 4 transmembrane domains (TMs) of a model *GPCR*, Ste2p. The synthesis and purification strategies were optimized and will serve as a guide for the synthesis of other transmembrane peptides. Then we measured the secondary structures of all seven TMs by CD, in TFE/water, DMPC vesicles and SDS micelles. The results indicated that all synthetic peptides corresponding to the individual α-helices from the integral membrane protein are stable in isolation from the remainder of the tertiary structure of the protein, with the exception that M3, M6-31 and M6-35P showed a significant β-sheet structure in both DMPC vesicles and SDS micelles. In addition, we studied their oligomeric state and domain-domain interactions in SDS by Tricine-SDS-PAGE. The results presented herein represent the first complete analysis of all membrane segments of one *GPCR*. The analysis shows that despite the helical proclivity of the transmembrane regions of Ste2p each domain is unique in its biophysical properties. In particular two domains M3 and M6 showed a higher tendency than the other peptides to aggregate and form β-structures and domain six may be a conformationally flexible region of the receptor. These findings lead us to suggest that domain six may be involved in a conformational transition during receptor activation and that this domain and domain three may be involved in domain-domain interactions which result in isomerization and/or receptor.

The work outlined in this part of my thesis has resulted in the following publications:

1. Xie, H., Ding, F.-X., Schreiber, D., Eng., G., Liu, S.-F., Arshava, B., Arevalo, E., Becker, J.M. and Naider, F. (2000) Synthesis and Biophysical Analysis of Transmembrane Domains of a *Sacchromyces cerevisiae* G Protein-coupled Receptor. *Biochemistry,* in press.
2. Naider, F. Arshava, B., Xie, H., Liu, S.-F., Eng, W.Y., Wang, S.-H., Valentine, K., Veglia, G., Marassi, F., Opella, S.J. and Becker, J.M. (2000) Biophysical Studies on A Transmembrane Domain of the *Sacchromyces cerevisiae* α-Factor Receptor. *Peptides: Proceedings of the 16th American Peptide Symposium,* 376-378.

FUTURE WORK

The association of transmembrane helices in the plane of the membrane plays a crucial role in the folding and oligomerization of integral membrane proteins. An understanding of the forces that drive membranous helix-helix interactions may reveal the mechanism of the *GPCRs'* assembly and function. Recent studies have suggested that TMs of *GPCRs* interact in a specific way in the assembly of receptor molecules. Specifically, Feng *et al.* (1999) reported that a single-residue deletion in transmembrane helix IV led the angiotensin II type 1 (AT_1) receptor chimera CR17 to retain GTP-sensitive high affinity for the agonist angiotensin II but resulted in complete inactivation of intracellular inositol phosphate production. The results emphasized that the contacts within the membrane-embedded portion in the receptor is important for specific G-protein selection. (Feng *et al* 1999). Tarasova *et al's* (1999) study has demonstrated that structural analogs of individual TMs of *GPCRs* can serve as potent and specific receptor antagonists. Peptides derived from the TMs of CXCR4 and CCR5 chemokine receptors specifically inhibited receptor signaling and the *in vitro* replication of human immunodeficiency virus-1 (HIV-1) at concentrations as low as 0.2 μM. Similarly, peptides mimicking the TMs of cholecystokinin receptor A, were found to abolish ligand binding and signaling through the receptor (Tarasova, N. I. *et al.* 1999). A similar approach was used to inhibit coupling of *GPCRs* to intracellular signaling molecules, adenylate cyclase (Anand-Srivastava *et al.,* 1996) and G-proteins (Merkouris *et a.,* 1996) by peptides corresponding to the intracellular loops of the receptors. A peptide

from the 6th TM of 2-adrenergic receptor was found to inhibit receptor activation and dimerization (Hebert, T.E. *et al.,* 1996). These studies led to the hypothesis that an externally added peptide corresponding to one of the putative transmembrane domains of a *GPCR* is able to disrupt the function of the receptor by interfering with the proper association of the TM domains.

The essential objective of our project is to understand *GPCRs'* structure and function using Ste2p as a model system. An unanswered question is how the binding of α-factor molecule results in the conformational transition of the sixth TM. Mutational analysis of Ste2p indicated that residues near the extracellular ends of the TMs are involved in binding (Dosil *et al.,* 1998), while the third intracellular loop (I3) plays a key role in G protein activation (Clark *et al.,* 1994; Schandel and Jenness 1994; Stefan and Blumer, 1994; Martin *et al.,* 1999). Very recently, scanning mutagenesis studies by Dube *et al.* (2000) identified an important region of interaction between M5 and M6 that bracket the I3 loop. Based on X-ray and electron crystallography study of rhodopsin and bacteriorhodopsin, TMs of *GPCRs* are believed to be arranged in a barrel-like structure with a tightly packed core (Urger and Schertler, 1995; Palczewski *et al.* 2000; Pebay-Peyroula *et al.,* 1997; Kimura *et al.* 1997;). Therefore it appears highly probable that TMs play important role in receptor activation by propagating a conformational change from the binding domain to the intracellular domain.

In this report, gel studies showed that M3 and M6 of Ste2p tend to self-associate, suggesting they may play an important role of propagating conformational change by helix-helix interaction. For future work, targeting intramembrane interactions of Ste2p with designed TM fragments may allow for understanding on specific regulation of receptor activation. To this end, we will test the ability of all seven TMs and two variants of M6, i.e. M6-35P and M6-35L, to inhibit signaling through the Ste2p receptor. Because flexibility is required to allow for conformational changes during signaling from the cell surface to the intracellular domains, the helix-helix interactions are unlikely to lead to rigid structure. Considering the conformational flexibility of M6, this fragment is very likely to be an antagonist.

Second we will conduct structure-activity studies on the TMs which result in significant inhibition of Ste2p bioactivity. Using M6 as the example, we can design and synthesize shorter and modified analogs of M6-31 as follows:

M6(243-269, C252A): SFHILLIMSAQSLLVPSIIFILAYSLK

M6(246-269, C252A): ILLIMSAQSLLVPSIIFILAYSLK

M6(249-269, C252A): IMSAQSLLVPSIIFILAYSLK

M6(252-269, C252A): AQSLLVPSIIFILAYSLK

M6(243-268, C252A): SFHILLIMSAQSLLVPSIIFILAYSLDD

M6(246-268, C252A): ILLIMSAQSLLVPSIIFILAYSLDD

M6(249-268, C252A): IMSAQSLLVPSIIFILAYSLDD

M6(252-268, C252A): AQSLLVPSIIFILAYSLDD

The shorter peptides 2-4 are designed based on Dube *et al.*'s (2000) results: the region around 247-251 of M6 is responsible for the interaction with M5. For each peptide, the extracellular terminus is modified by adding two negative-charged Asp, because it has been reported that anionic terminus increased the antagonist potency (Tarasova *et al.,* 1999). In addition to bioassay studies, gel studies on these analogs will be carried out to relate the antagonist activity to their tendency of self-association. Finally, the results on these analogs can be applied to other TMs and allow the identification of antagonists derived from other domains.

Considering the entropy factor, fragments linking two TMs may result in significantly increased affinity. Therefore appropriate pairs of TM analogs may produce very potent agonists. We have successfully biosynthesized M5-I3-M6 (personal communications, E. Arevalo), so it should be practical to biosynthesize longer fragments linking two TMs and test their antagonist potency.

In general, future work will focus on domain-domain interactions, synthetic TM analogs will be good candidates for this study.

References

Anand-Srivastava, M.B., Sehl, P.D. and Lowe, D.G. (1996) Cytoplasmic domain of natriuretic peptide receptor-C inhibits adenylyl cyclase. Involvement of a pertussis toxin-sensitive G protein. *J. Biol. Chem. 271,* 19324-19329.

Anderegg, R.J., Betz, R., Carr, S.A., Crabb, J.W. and Duntze, W. (1988) Structure of *Saccharomyces cerevisiae* mating hormone **a**-factor: Identification of S-farnesyl cysteine as a structural component. *J. Biol. Chem. 263,* 18236-18240.

Arshava, B., Liu, S.F., Jiang, H., Breslav, M., Becker, J.F. and Naider, F. (1998) Structure of segments of a G protein-coupled receptor: CD and NMR analysis of the *Saccharomyces cerevisiae* tridecapeptide pheromone receptor. *Biopolymers 46,* 343-357.

Balaram, P. (1985) *Proc. Indian Acad. Sci. (Chem. Sci.) 95*, 21-38.
Baldwin, J. M. (1993) The probable arrangement of helices in G protein-coupled receptors. *EMBO J. 12*, 1693-1703

Bardwell, L., Cook, J.G. and Inouye, C.J. and Thorner, J. (1994) Signal propagation and regulation in the mating pheromone response pathway of the yeast *Saccharomyces cerevisiae. Dev. Biol .166,* 363-379.

Bechinger, B., Kinder, R., Helmle, M., Vogt, T.C., Harzer, U. and Schinzel, S. (1999) Peptide structural analysis by solid-state NMR spectroscopy. *Biopolymers 51,*174-190.

Bender, A. and Sprague, G.F. (1986) Yeast peptide pheromones, **a**-factor and α-factor, activate a common response mechanism in their target cells. *Cell 47,* 929-937.

Bhattacharya, S., Chen, L., Broach, J.R. and Powers, S. (1995) Ras membrane targeting is essential for glucose signaling but not for viability in yeast *Proc. Acad. Sci. USA 92,* 2984-2988.

Bianchi, E., Ingenito, R., Simon, R.J. and Pessi, A. (1999) Engineering and chemical synthesis of a transmembrane protein: The HCV protease cofactor protein NS4A. *J. Am. Chem. Soc. 121,* 7698-7699.

Blumer, K. J., Reneke, J. E. and Thorner, J. (1988) The *STE2* gene product is the ligand-binding component of the α-factor receptor of *Saccharomyces cerevisiae. J. Biol. Chem. 263*, 10836-10842.

Bradley, E.K., Ng, S.C., Simon, R.J. and Spellmeyer, D.C. (1994) Synthesis, molecular modeling and NMR structure determination of four cyclic peptide antagonists of endothelia. *Bioorg. Med. Chem. 2,* 279-296.

Burkholder, A.C. and Hartwell, L. H. (1985) The yeast α-factor receptor: structural properties deduced from the sequence of the *STE2* gene. *Nucleic Acids Res. 13*, 8463-8475.

Burrell, J. W. K., Garwood, R.F., Jackman, L.M.; Oskay, E. and Weedon, B.C. L. (1966) Carotenoids and Related Compounds. Part XIV. Stereochemistry and synthesis of geraniol, nerol, farnesol and phytol. *J. Chem. Soc. (C)* 2144-2154.

Caldwell, G.A., Wang, S.-H., Naider, F. and Becker, J.M. (1994a) Consequence of altered isoprenylation targets on **a**-factor export and bioactivity. *Proc. Natl. Acad. Sci. USA. 91,*1275-1279.

Caldwell, G. A., Wang, S.-H., Xue, C.-B., Jiang, Y., Lu, H.-F., Naider, F. and Becker, J.M. (1994b) Molecular determinatants of bioactivity of the *Saccharomyces cerevisiae* lipopetide mating pheromone. *J. Biol. Chem. 269(31),* 19817-19826.

Caldwell, G.A., Wang, S.-H., Dawe, A.L., Naider, F. and Becker, J.M. (1993) Identification of a hyperactive mating pheromone of *Saccharomyces cerevisiae. Biochem. Biophys. Res. Commun. 172*, 1310-1318.

Cartwright, C.P. and Tipper, D.J. (1991) *In vivo* topological analysis of Ste2, a yeast plasma membrane protein, by using beta-lactamase fusions. *Mol. Cell. Biol. 11*, 2620-2628.

Casey, P.J., Solski, P.A., Der, C.J. and Buss, J.E. (1989) p21ras is modified by a farnesyl isoprenoid. *Proc. Natl. Acad. Sci. USA 86*, 8323-8327.

Chen, C.C., Kao, J. and Marshall G.R. (1999) *Peptides: Proceedings of the 16th American Peptide Symposium. Minneapolis, MN.* Poster 681.

Chen, Y. H., Yang, J. T., Chau, K. H., (1974) Determination of the helix and β-form of proteins in aqueous solution by circular dichroism. *Biochemistry 13*, 3350-3359.

Chiou, A.J., Ong, G.T., Wang, K.T., Chiou S.H. and Wu, S.H. (1996) Conformational study of two linear hexapeptides by two-dimensional NMR and computer-simulated modeling: implication for peptide cyclization in solution. *Biochem. Biophys. Res. Commun. 219,* 572-579.

Chopra, A., Yeagle, P.L., Alderfer, J.A. and Albert, A.D. (2000) Solution structure of the sixth transmembrane helix of the G-protein-coupled receptor, rhodopsin. *Biochim. Biophys. Acta 1463*, 1-5.

Chou, P.Y. and Fasman, G.D. (1978) Prediction of the secondary structure of proteins from their amino acid sequence. *Adv. Enzymol. 474,* 45-148.

Clark, C. D., Palzkill, T. and Botstein, D. (1994) Systematic mutagenesis of the yeast mating pheromone receptor third intracelilular loop. *J. Biol. Chem. 269*, 8831-8841

Dawe, A.L., Becker, J.M., Jiang, Y., Naider, F., Eummer, J.T., Mu, Y.-Q. and Gibbs, R.A. (1997) Novel modifications to the farnesyl moiety of the **a**-factor lipopetide pheromone from *Saccharomyces cerevisiae*: A role for isoprene modifications in ligand presentation. *Biochemistry 37,* 12036-12044.

Dohlman, H.G., Thorner, J., Caron, M.G. and Lefkowitz, R.J. (1991) Model systems for the study of seven transmembrane segment receptors. *Ann. Rev. Biochem. 60,* 653-688.

Dorey, M., Hargrave P.A., McDowell, J.H., Arendt, A., Vogt, T., Bhawsar, N., Albert, A.D. and Yeagle, P.L. (1999) Effects of phosphorylation on the structure of the G-protein receptor rhodopsin. *Biochim. Biophys. Acta. 1416*, 217-224.

Dosil, M., Giot, L., Davis, C., and Konopka, J.B. (1998) Dominant-negative mutations in the G protein-coupled α-factor receptor map to the extracellular ends of the transmembrane segments. *Mol. Cell Biol. 18,* 5981-5991.

Du, W., Lebowitz, P. F. and Prendergast, G. C. (1999) Cell growth inhibition by farnesyltransferase inhibitors is mediated by gain of geranylgeranylated RhoB. *Mol. Cell. Biol. 19*, 1831-1840.

Dube, P. and Konopka, J.B. (1998) Identification of a polar region in transmembrane domain 6 that regulates the function of the G protein-coupled α-factor receptor. *Mol. Cell. Biol. 18,* 7205-7215.

Dube, P., DeCostanzo, A. and Konopka, J.B. (2000) Interaction between transmembrane domains five and six of the α-factor receptor. *J. Biol. Chem. 275,* 26492-26499.

Dyson, J.H., Rance, M., Houghten, R.A., Lerner, R.A. and Wright, P.E. (1988) Folding of immunogenic peptide fragments of proteins in water solution. I. Sequence requirements for the formation of a reverse turn. *J. Mo., Biol. 201,* 161-200.

Elwell, M.I. and Schellman, J.A. (1977) Stability of phase T4 lysozymes. I. Native properties and thermal stability of wild type and two mutant lysozymes. *Biochim. Biophys. Acta. 494,* 367-383.

Engelman, D.M., Steitz, T.A. and Goldman, A. (1986) Identifying nonpolar transbilayer helices in amino acid sequences of membrane proteins. *Annu. Rev. Biophys. Biophys. Chem. 15,* 321-53.
Engelman, D.M. and Steitz, T.A. (1981) The spontaneous insertion of proteins into and across membranes: the helical hairpin hypothesis. *Cell 23,* 411-422.

Epand, R.F., Xue, C.-B., Wang, S.-H., Naider, F., Becher, J. M. and Epand, R. M. (1993) Role of prenylation in the interaction of the **a**-factor mating pheromone with phospholipid bilayers. *Biochemistry* 32, 8368-8373.

Feng, Y.H. and Karnik, S.S. (1999) Role of transmembrane helix IV in G-protein specificity of the Angiotensin II type 1 receptor. *J. Biol. Chem. 274,* 34546-34552.

Freidinger, R.M., Veber, D.F., Perlow, D.S., Brooks, J.R. and Saperstein, R. (1980) Bioactive conformation of luteinizing hormone-releasing hormone: evidence from a conformationally constrained analog. *Science 210:*656-658.

Fujino, M., Kitada, C., Sakagami, Y., Isogai, A., Tamura, S. and Suzuki, A. (1980) Biological activity of synthetic analogs of Tremerogen A-10: A mating hormone of heterobasidiomycetous yeast, *Tremella mesenterica. Nature 67,* 406-408.

Gelb, M.G. (1997) Protein prenylation *et cetera*: signal transduction in two dimensions. *Science 275,* 1750-1751

Gibbs, J.B. and Oliff, A. (1997) The potential of farnesyltransferase inhibitors as cancer chemotherapeutics. *Annu. Rep. Pharmacol. Toxicol. 37,*143-166.

Gounarides, J.S., Broido, M.S., Xue, C.-B., Becker, J.M. and Naider, F. (1991) The conformation of *Saccharomyces cerevisiae* **a**-factor is not influenced by the S-prenylation of Cys^{12}. *Biochem. Biophys. Res. Commun. 183,* 1125-1130.

Gosser, Y. Q., Nomambhoy, T. K., Aghazadeh, B., Manor, D., Combs, C., Cerione, R. A. and Rosen, M.K. (1997) C-terminal binding domain of Rho GDP-dissociation inhibitor directs N-terminal inhibitory peptide to GTPases. *Nature 387,* 814-819.

Greenfield, N. and Fasman, G. D. (1969) Computed circular dichroism spectra for the evaluation of protein conformation. *Biochemistry 8,* 4108-4116.

Grewbow, P.E. and Hooker, T.M., Jr. (1975) Conformation of histidine model peptides. II Spectroscopic properties of the imidazole chromophores. *Biopolymers 14,* 871-881.

Grigorieff, N., Ceska, T.A., Downing, K.H., Baldwin J.M., and Henderson, R. (1996) Electron-crystallographic refinement of the structure of bacteriorhodopsin. *J. Mol. Biol. 259,* 393-421.

Gudermann, T., Schoneberg, T. and Schultz, G. (1997) Functional and structural complexity of signal transduction via G-protein-coupled receptors *Annu. Rev. Neurosci. 20,* 399-427

Hagen, D.C and Sprague, G.F. (1984) Induction of the yeast α-specific STE3 gene by the peptide pheromones **a**-factor *J.Mol.Biol. 178,* 835-852.

Harley, C. A. and Tipper, D. J. (1996) The role of charged residues in determining transmembrane protein insertion orientation in yeast. *J. Biol. Chem. 271*, 24625-24633.

Herbert, T.E. and Bouvier, M. (1998) Structural and functional aspects of G protein-coupled receptor oligomerization. *Biochem. Cell. Biol. 76,* 1-11.

Hebert, T.E., Moffett, S., Morello, J.P., Loisel, T.P., Bichet, D.G., Barret, C. and Bouvier, M. (1996) A peptide derived from a β2-adrenergic receptor transmembrane domain inhibits both receptor dimerization and activation. *J. Biol. Chem. 271,* 16384-16392.

Hibert, M.F., Trumpp-Kallmeyer, S., Hoflack, J. and Bruinvels, A. (1993) This is not a G protein-coupled receptor. *Trends Pharmacol. Sci. 14,* 7-12.

Horn, F., Weare, J., Beukers, M.W., Horsch, S., Bairoch, A., Chen, W., Envardsen, O., Campagne, F. and Vriend G. (1998) Effects of chronic dietary creatine feeding on cardiac energy metabolism and on creatine content in heart, skeletal muscle, brain, liver and kidney. *Nucleic Acids Res. 26,* 277-281.

Hruby, V.J. (1982) Conformational restrictions of biologically active peptides via amino acid side chain groups. *Life Sci. 31,* 189-199.

Huang, K.S., Bayley, H., Liao, M.J., London, E., Khorana, H.G. (1981) Refolding of an integral membrane protein. Denaturation, renaturation and reconstitution of intact bacteriorhodopsin and two proteolytic fragments. *J. Biol. Chem. 256,* 3802-3809;

Hunt, J.F., Earnest, T.N., Boushe, O., Kalghatgi, K., Reilly, K., Horvath, C., Rothschild, K.J. and Engelman, D.M. (1997a) *Biochemistry 36*, 15156-15176.

Hunt, J.F., Rath, P., Rothschild, K.J. and Engelman, D.M. (1997b) *Biochemistry 36*, 15177-15192.

Ingwall, R.T., Scheraga, H.A., Lotan, N., Berger, A. and Katchalski, E. (1968) Conformational studies of poly-*L*-alanine in water. *Biopolymers 6,* 331-368.

Jenness, D.D., Burkholder, A.C. and Hartwell, L.H. (1983) Binding of α-factor pheromone to yeast cells: chemical and genetic evidence for an α-factor receptor. *Cell 35,* 521-529.

Johnson, W.C. (1988) Secondary structure of proteins through circular dichroism spectroscopy. *Anun. Rev. Biophys. Chem. 17*, 145-166.

Jones, D.H., Ball, E.H., Sharpe, S., Barber, KR and Brant, C.W. (2000) Expression and membrane assembly of a transmembrane region from Neu. *Biochemistry 39,* 1870-1878.

Josefsson, L.G. (1999) Evidence for kinship between diverse G protein-coupled receptor. *Gene 239,* 333-340.

Kahn, T.W. and Engelman, D.M. (1992) Bacteriorhodopsin can be refolded from two independently stable transmembrane helices and the complementary five-helix. *Biochemistry 31*, 6144-6151.

Keep, N.H., Barns, M., Barsukov, I., Baddi, R., Lian, L.Y., Segal, A.W., Moody, P.C.E. and Roberts, G.C.K. (1997) A modulator of the family G proteins, rhoGDI, binds their G proteins via an immunoglobulin-like domain and a flexible N-terminal arm *Structure 5,* 623-633.

Kent, S.B. (1988) Chemical synthesis of peptides and proteins. *Annu. Rev. Biochem. 57,* 957-989.

Kent, S.B., et al in "*Innovations and Perspectives in Solid Phase Synthesis*", Epton, R. (ed.), Intercept Ltd. andover, UK, 1992, pp 1.

Khouri, O., Sherrill, C. and Roise, D. (1996) Partitioning of **a**-factor analogs into membranes: Analysis of binding and importance for biological activity. *Biochemistry 35,* 14553-14560.

Kimura, Y., Vassylyev, D.G., Miyazawa, A., Kidera, A., Matsushima, M., Mitsuoka, K., Murata, K., Hirai, T. and Fujiyoshi, Y. (1997) Surface of bacteriorhodopsin revealed by high-resolution electron crystallography. *Nature 389,* 206-211.

Konopka, J. B., Margarit, S. M. and Dube, P. (1996) Mutation of Pro-258 in transmembrane domain 6 constitutively activates the G-protein-coupled α-factor receptor. *Proc. Natl. Acad. Sci. USA 93*, 6764-6769.

Koppitz, M., Spellig, T., Kahmann, R. and Kessler, H. (1996) Lipoconjugates: structure-activity studies for pheromone analogues of Ustilago maydis with varied lipophilicity. *Int. J. Pept. Protein Res. 48*, 377-390.

Kyte, J. and Doolittle, R.F. (1982) A simple method for displaying the hydrophobic character of a protein. *J. Mol. Biol. 157,* 105-132.

Lehninger, L.A., Nelson, L.D. and Cox, M.M. (1992) *Principles of Biochemistry* (2^{nd} edition) Worth Publishers, N.Y.

Lemmon, M.A. and Engelman D.M. (1994) Specificity and promiscuity in membrane helix interactions. *Q. Rev. Biophys. 27,* 157-218.

Li, S.C. and Deber C.M. (1994) A measure of helical propensity for amino acids in membrane environments. *Nat. Struct. Biol. 1,* 558.

Li, S.C., Goto, N.K., Williams, K.A. and Deber, C. M. (1996) α-helical, but not β-sheet, propensity of proline is determined by peptide environment. *Proc. Natl. Acad. Sci. USA 93*, 6676-6681.

London, E. and Khorana, H.G. (1982) Denaturation and renaturation of bacteriorhodopsin in detergents and lipid-detergent mixtures. *J. Biol. Chem. 257,* 7003-7011.

Lui, J., Schoneberg, T., Rhee, M. and Wess, J. (1995) Mutational analysis of the relative orientation of transmembrane helices I and VII in G-protein coupled receptors. *J. Biol. Chem. 270,* 19532-19539.

Ma, Y.T., Shi, Y.Q., Lim, Y.H., McGrail, S.H., Ware, J.A. and Rando, R.R. (1994) Mechanistic studies on human platelet isoprenylated protein methyltransferase: farnesylcysteine analogs block platelet aggregation without inhibiting the methyltransferase. *Biochemistry 33,* 5414-5420.

Marcus S., Caldwell G.A., Miler D., Xue C.-B., Naider F. and Becker J.M. (1991) Significance of C-terminal cysteine modifications to the biological activity of the *Saccharomyces cerevisiae* **a**-factor mating pheromone. *Mol. Cell. Biol. 13*, 3603-3612.

Marshall, C.J. (1993) Protein prenylation: a mediator of protein-protein interactions. *Science 259,* 1865-1866.

Marti T. (1998) Refolding of bacteriorhodopsin from expressed polypeptide fragments. *J. Biol. Chem. 273,* 9312-9322.

Martin, N.P., Leavitt, L.M., Sommers, C.M. and Dumont, M.E. (1999) Assembly of G protein-coupled receptors from fragments: identification of functional receptors with discontinuities in each of the loops connecting transmembrane segments. *Biochemistry 38*, 682-695.

McGeady, P., Kuroda, S., Shimizu, K., Takai, Y. and Gelb, M.H. (1995) The farnesyl group of H-Ras facilitates the activation of a soluble upstream activator of Mitogen-activated protein kinase. *J. Biol. Chem. 270,* 26347-26351.

Melkonian, K.A., Ostermeyer, A.G., Chen, J.Z., Roth, M.G. and Brown, D.A. (1999) Role of lipid modifications in targeting proteins to detergent-resistant membrane rafts. *J. Biol. Chem. 274*, 3910-3917.

Merkouris, M., Dragatsis, I., Megaritis, G., Konidakis, G., Zioudrou, C., Milligan, G. and Georgoussi, Z. (1996) Identification of the critical domains of the delta-opioid receptor involved in G protein coupling using site-specific synthetic peptides. *Mol. Pharmacol. 50,* 985-993.

Mizobe, T., Maze, M., Suryanarayana, S., Kobilka, B.K. (1996) Arrangement of transmembrane domains in adrenergic receptors: similarity to bacteriorhodopsin. *J. Biol. Chem. 271,* 2387-2389.

Moy, F.J., Desai, S.A., Wang, X., Noronha, E.J., Zhou, Q., Ferrone, S., Powers, R. (2000) Analysis by NMR spectroscopy of the structural homology between the linear and the cyclic peptide recognized by anti-human leukocyte antigen class I monoclonal antibody TP25.99*. *J. Biol. Chem. 275*, 24679-24685.

Nakayama N., Miyajima, A. and Arai, K. (1985) Nucleotide sequences of *STE2* and *STE3*, cell type-specific sterile genes from *Saccharomyces cerevisiae*. *EMBO J. 4*, 2643-2648.

Naider F. and Becker J.M. (1997) Synthesis of prenylated peptides and peptides esters. *Biopolymers 43,* 3-14.

Naider, F., Jelicks, L.A., Becker, J.M. and Broido, M.S. (1989) Biologically significant conformation of the *Saccharomyces cerevisiae* α-factor. *Biopolymers 28*, 487-497.

Niall, H.D. (1982) The evolution of peptide hormones. *Annu. Rev. Physiol. 44*, 615-616.

Niv, H., Gutman, O., Henis, Y.I. and Kloog, Y. (1999) Membrane interactions of a constitutively active GFP-Ki-Ras 4B and their role in signaling. *J. Biol. Chem.*

274, 1606-1613.

Oehlen, B., Cross, F.R. (1994) Signal transduction in the budding yeast *Saccharomyces cerevisiae. Curr. Opin. Cell. Biol. 6,* 836-841.

Overton, M.C. and Blumer, K.J. (2000) G protein-coupled receptors function as oligomers *in vivo. Curr. Biol. 10,* 341-344.

Palczewski, K., Kumasaka, T., Hori, T., Behnke, C.A., Motoshima, H., Fox, B.A., Trong, I.L., Teller, D.C., Okada, T., Stenkamp, R., Yamamoto, M. and Miyano, M. (2000) Crystal structure of rhodopsin: a G-protein-coupled receptor. *Science 289,* 739-745.

Parish, C. A. and Rando, R. R. (1996) Isoprenylation/methylation of proteins enhances membrane association by a hydrophobic mechanism. *Biochemistry, 35*, 8473-8477.

Pebay-Peyroula, E., Rummel, G., Rosenbusch, J.P., and Landau, E.M. (1997) X-ray structure of bacteriorhodopsin at 2.5 angstroms from microcrystals grown in lipidic cubic phases. *Science 277,* 1676-1681.

Perczel, A. and Hollosi, M. (1996) *Circular Dichroism and the Conformational Analysis of Biomolecules* pp 285-380; (Fasman, G.D., ed.) Plenum Press, New York and London.

Perczel, A., McAllister, M.A., Csazar, P. and Czizmadia, I.G. (1993) *J. Am. Chem. Soc.* 115, 4849-4858.

Pomroy, N.C. and Deber, C.M. (1999) Conjugation of polyethylene glycol *via* a disulfide bond confers water solubility upon a peptide model of a protein transmembrane segment. *Anal. Biochem. 275,* 224-230.

Popot, J.L. and Engelman, D.M. (1990) Membrane protein folding and oligomerization: the two-stage model. *Biochemistry 29*,4031-4037.

Reddy, A.P., Tallon, M.A., Becker, J.M. and Naider, F. (1994) Biophysical studies on fragments of the α–factor receptor protein. *Biopolymers 34*, 679-689.

Ridge, K.D., Lee, S.S.J. and Yao, L.L. (1995) *In vivo* assembly of rhodopsin from expressed polypeptide fragments. *Proc. Natl. Acad. Sci. USA 92*, 3204-3208.

Ridge, K.D., Lee, S.S.J. and Abdulaev, N.G. (1996) Examining rhodopsin folding and assembly through expression of polypeptide fragments. *J. Biol. Chem. 271,* 7860-7877.

Schafer, W.R., Kim, R., Sterne, R., Thorner, J., Kim, S.-H. and Rine, J. (1989) Genetic and pharmacological suppression of oncogenic mutations in ras genes of yeast and humans. *Science 245*, 379-385.

Schafer, W.R. and Rine, J. (1992) Protein Prenylation: Genes, Enzymes, Targets and Functions. *Annu. Rev. Genet. 30*, 209-237.

Schafer, W.R., Trueblood, C.E., Yang, C.-C., Mayer, M.P., Rosenberg, S., Poulter, C.D., Kim, S.-H. and Rine, J. (1989) Enzymatic coupling of cholesterol intermediates to a mating pheromone precursor and to the ras protein. *Science 249,* 1133-1139.

Schandel, K.A. and Jenness, D.D. (1994) Direct evidence for ligand-induced internalization of the yeast α-factor pheromone receptor. *Mol. Cell Biol. 14,* 7245-7255.

Scheer, A. and Gierschik, P. (1995) S-prenylated cysteine analogues inhibit receptor-mediated G protein activation in native human granulocyte and reconstituted bovine retinal rod outer segment membranes. *Biochemistry 34,* 4952-4961.

Schertler, G.F.X., Villa, C., Henderson, R. (1993) Projection structure of rhodopsin. *Nature 362,* 770-772.

Schagger, H. and von Jagow, G. (1987) Tricine-sodium dodecyl sulfate-polyacrylamide gel electrophoresis for the separation of proteins in the range from 1 to 100 kDa. *Anal. Biochem.* 166, 368-379.

Schoneberg, T, Liu, J. and Wess, J. (1995) Plasma membrane localization and functional rescue of truncated forms of a G-protein-coupled receptor. *J. Biol. Chem. 270,* 18000-18006.

Siddiqui, A. A., Garland, J.R., Dalton, M.B. and Sinensky, M. (1998) Evidence for a high affinity, saturable, prenylation-dependent $p21^{Ha\text{-}ras}$ binding site in plasma membrane. *J. Biol. Chem. 273*, 3712-3717.

Sommers, C.M., Martin, N.P., Akal-Strander, A., Becker, J.M., Naider, F. and Dumont, M.E. (2000) A limited spectrum of mutations causes constitutive activation of the yeast α- factor receptor. *Biochemistry 39,* 6898-6909.

Stefan, C. J. and Blumer, K. J. (1994) The third cytoplasmic loop of a yeast G-protein α-coupled receptor controls pathway activation, ligand discrimination and receptor internalization. *Mol. Cell. Biol. 14*, 3339-3349.

Stotzler, D. and Duntze, W. (1976) Isolation and characterization of four related peptides exhibiting α factor activity from *Saccharomyces cerevisiae*. *Eur. J. Biochem. 65,* 257-262.

Suryanarayana, S., Zastrow, M. and Kobilka, B.K. (1992) Identification of intramolecular interactions in adrenergic receptors. *J. Biol. Chem. 267,* 21991-21994.

Tarasava, N.I., Rice, W.G. and Michejda, C.J. (1999) Inhibition of G-Protein-coupled receptor function by disruption of transmembrane domain interactions. *J. Biol. Chem. 274,* 34911-34915.

Tocimil, J.M., Carson, I.W., Kanes, K.J., Vogelaar, N.J., Emerling, M.R. and Richard, J.H. (1988) Prevention of aggregation of synthetic membrane-spanning peptides by addition of detergent. *Anal. Biochem. 174,* 197-203.
Urger, V.M. and Schertler, G.F.X. (1995) Low resolution structure of bovine rhodopsin determined by electron cryo-microscopy. *Biophys. J. 68,* 1776-1786.

Von Heijne, G. (1980) Trans-membrane translocation of proteins. A detailed physico-chemical analysis. *Eur. J. Biochem. 103,* 431-438.
Wess, J. (1997) G-protein-coupled receptors: molecular mechanisms involved in receptor activation and selectivity of G-protein recognition. *FASEB J. 11*, 346-354.

Weiner, J.L., Guttierez-Steil, C. and Blumer, K. J. 1993. Disruption of receptor-G protein coupling in yeast promotes the function of an *SST2*-dependent adaptation pathway. *J. Biol. Chem. 268*, 8070-8077.

Wigley, W., Vijayakumar, S., Jones, J.D., Slaughter, C. and Thomas, P.J. (1998) Transmembrane domain of cystic fibrosis transmembrane conductance regulator: design, characterization and secondary structure of synthetic peptides m1-m6. *Biochemistry 37*, 844-853

Wishart, D.S., Sykes, B.D. and Richards, F.M. (1992) The chemical shift index: A fast and simple method for the assignment of protein secondary structure through NMR spectroscopy. *Biochemistry* 31, 1647-1651.

Woody, R. W. (1974) *Peptides, Polypeptides and proteins* (Blout, E.R., Bovey, F.A., Lotan N. and Goodman, M. eds.), pp 338-350, Wiley, New York.

Wu, C. S. C., Ikeda, K., Yang, J. T. (1981) Ordered conformation of polypeptides and proteins in acidic dodecyl sulfate solution. *Biochemistry 20*, 566-570.

Wüthrich, K. (1986) in *NMR of Proteins and Nucleic Acids,* Wiley, New York.

Xie, H., Ding, F.-X., Schreiber, D., Eng., G., Liu, S.-F., Arshava, B., Arevalo, E., Becker, J.M. and Naider, F. (2000) Synthesis and biophysical analysis of transmembrane domains of a *Sacchromyces cerevisiae* G Protein-coupled receptor. *Biochemistry 39,* 15462-15474.

Xue, C.-B., Becker, J.M. and Naider, F. (1991) Synthesis of S-alkyl and C-terminal analogs of the *Saccharomyces cerevisiae* **a**-factor. *Int. J. Peptide Protein Res. 37*, 476- 486.

Xue, C.-B., Becker, J.M. and Naider, F. (1992) Efficient regioselective isoprenylation of peptides in acidic aqueous solution using zinc acetates as catalyst. *Tetrahedron Lett. 33,* 1435-1438.

Xue, C.-B., Caldwell, G.A., Becker, J.M. and Naider, F. (1989) Total synthesis of the lipopeptide **a**-mating factor of *Saccharomyces cerevisiae. Biochem. Biophys. Res. Commun. 162*, 253-257.

Xue, C.-B., Ewenson, A., Becker, J.M. and Naider, F. (1990) Solution phase synthesis of *Saccharomyces cerevisiae* **a**-mating factor and its analogs. *Int. J. Peptide Protein Res. 36,* 362-373.

Yan, Y., Erickson, B.W., and Tropsha, A. (1995) Free energies for folding and refolding of four types of β turns: simulation of the role of D/L chirality. *J. Am. Chem. Soc. 117,* 7592-7599.

Yeagle, P.L., Alderfer, J.L., and Albert, A.D. (1995) Structure of the carboxy-terminal domain of bovine rhodopsin. *Nat. Struct. Biol. 2,* 832-834.

Yeagle, P.L., Alderfer, J.L. Salloum AC, Ali L, and Albert, A.D. (1997) The first and second cytoplasmic loops of the G-protein receptor, rhodopsin, independently form beta-turns. *Biochemistry 36,* 3864-3869.

Zhang, D. and Weinstein, H. (1993) Signal transduction by a 5-HT2 receptor: a mechanistic hypothesis from molecular dynamics simulations of the three-dimensional model of the receptor complexed to ligands. *J. Med. Chem. 36,* 934-938.

Zhang, F. L. and Casey, P. J. (1996) Protein prenylation: molecular mechanisms and functional consequences. *Annu. Rev. Biochem. 65*, 241-269.

Zhang, Y.L., Dawe, A.L., Jiang, Y., Becker, J.M. and Naider, F. (1996) A superactive peptidomimetic analog of a farnesylated dodecapeptide yeast pheromone. *Biochem. Biophys. Res. Comm. 224,* 327-331.

Zieglar, S.M. and Bush, C.A. (1971) Circular dichroism of cyclic hexapeptides with one and two side chains. *Biochemistry 10,* 1330-1335.